ANALYTICAL AND EXPERIMENTAL DYNAMIC ANALYSIS OF A FOUR WHEELER VEHICLE WITH SEMI ACTIVE SUSPENSION SYSTEM

Thesis

Submitted in partial fulfillment of the requirements for the degree of

DOCTOR OF PHILOSOPHY

by

PUNEET N P

DEPARTMENT OF MECHANICAL ENGINEERING

NATIONAL INSTITUTE OF TECHNOLOGY KARNATAKA,

SURATHKAL, MANGALORE – 575025

APRIL 2023

ANALYTICAL AND EXPERIMENTAL DYNAMIC ANALYSIS OF A FOUR WHEELER VEHICLE WITH SEMI ACTIVE SUSPENSION SYSTEM

Thesis

Submitted in partial fulfillment of the requirements for the degree of

DOCTOR OF PHILOSOPHY

by

PUNEET N P

Under the guidance of

Dr. Hemantha Kumar   **Dr. K V Gangadharan**

Associate Professor   Professor

DEPARTMENT OF MECHANICAL ENGINEERING

NATIONAL INSTITUTE OF TECHNOLOGY KARNATAKA,

SURATHKAL, MANGALORE – 575025

APRIL 2023

DECLARATION

I hereby *declare* that the Research Thesis entitled **"ANALYTICAL AND EXPERIMENTAL DYNAMIC ANALYSIS OF A FOUR WHEELER VEHICLE WITH SEMI ACTIVE SUSPENSION SYSTEM"** which is being submitted to the **National Institute of Technology Karnataka, Surathkal** in partial fulfillment of the requirements for the award of the Degree of **Doctor of Philosophy** in **Department of Mechanical Engineering** is a *bonafide report of the research work carried out by me*. The material contained in this Research Thesis has not been submitted to any University or Institution for the award of any degree.

RegisterNumber   **:177156ME505**

Name of the Research Scholar   : **Puneet N P**

Signature of the Research Scholar   :

Department of Mechanical Engineering

Place   : **NITK, Surathkal**

Date   : **12th April, 2023**

CERTIFICATE

This is to *certify* that the Research Thesis entitled "ANALYTICAL AND EXPERIMENTAL DYNAMIC ANALYSIS OF A FOUR WHEELER VEHICLE WITH SEMI ACTIVE SUSPENSION SYSTEM" submitted by **Mr. Puneet N P (Register Number: 177156ME505** as the record of the research work carried out by him, is *accepted as the Research Thesis submission* in partial fulfillment of the requirements for the award of degree of **Doctor of Philosophy.**

Research Guides

Dr. Hemantha Kumar

Associate Professor

Dr. K V Gangadharan

Professor

Department of Mechanical Engineering

NITK, Surathkal

Chairman-DRPC

19. 4. 2023

Department of Mechanical Engineering

Dedicated to my beloved parents and my dearest ones…

ACKNOWLEDGEMENTS

ABSTRACT

Advances in the automobile industries in several engineering aspects have opened up never ending challenges and scopes. One such interesting challenge is to achieve better ride quality which intends to provide more comfort to the passengers. The road profile randomness is not uniform around the globe. Therefore, achieving a good ride comfort has always been a task for researchers over the years. A key component responsible for ride quality is the suspension system of the vehicle, a major combination of spring and damper. The nature and magnitude of energy dissipation from the damper provides suitable ride quality to the vehicle. Passive dampers provide constant response against any kind of road disturbances since the fluid properties cannot be altered with any external input. Hence, replacing passive damping medium with semi-active medium will provide added advantage to the suspension system in providing greater ride comfort. Magneto-rheological (MR) fluid is one such smart fluid which is known for its semi-active nature when the external magnetic field is varied. This research study deals with synthesis of magneto-rheological fluid and its application in damper of a light motor vehicle.

In the primary part of this study, a passive damper was extracted from the suspension system of the commercially available light motor vehicle. This passive damper was characterized in the dynamic testing machine (DTM) to understand the dynamic response of the damper towards varying cyclic input. The damping force response from the passive damper was considered as the benchmark for development of MR fluid damper particular for the test vehicle. A quarter car model was developed using the MATLAB/ Simulink and the response of the passive damper characterization was employed in the damping element of the model.

As a preliminary study of the MR fluid damper, a small stroke MR damper was designed and developed. For this purpose, an MR fluid was prepared in-house and used as the damping medium in the MR damper. This prototype was then characterized using dynamic testing machine subjected to different amplitude, frequency and DC current inputs. A mathematical model was established which could

relate the damping force and the current which was then used in quarter car simulation.

Based on the above preliminary works, a prototype MR damper with actual scale was then designed using optimization technique under certain geometrical constraints. The designed MR damper piston was analyzed by using finite element magnetic methods (FEMM) to verify the magnetic flux development in the fluid flow gap. MR fluid as the damper fluid was synthesized in-house using electrolytic iron particle (EIP) and paraffin oil. Rheological study of the synthesized MR fluid was conducted to analyze the shear stress as well as viscosity variation against the shear rate and the current inputs. The developed MR damper was then characterized under various dynamic and DC current inputs to study the force versus displacement nature. The hysteresis of the damper was mathematically represented using parametric modeling technique called Kwok model. The parameters of the model were determined for each condition by using optimization method. This model was then used in quarter car simulation to analyze the effect of suspension under off-state, constant current and through skyhook control. The validation of this simulation was carried out by using the suspension with MR damper in a quarter car test rig and the deviation in the results was analyzed.

As an important part of this research work, the suspension with the developed MR damper was tested on-road by using a test vehicle. The passive damper in the front suspension of the test vehicle was replaced with MR damper and the suspension was tested at two different velocities. Also, the ride comfort at different conditions was analyzed. As an extended part of the study, a control logic involving single sensor technique was developed. The performance of developed control was tested using the quarter car set up and the comparison of the responses through different current inputs was also presented.

Keywords: MR Fluid, MR damper, Passive damper, Quarter Car Testing, Quarter Car model, Kwok Model, Skyhook Control, On-road testing, Single Sensor Control Technique

CONTENTS

LIST OF FIGURES

LIST OF TABLES

CHAPTER 1

INTRODUCTION

Vehicles over the years have seen many transformations according to the requirements for ride comfort, road holding and technology implementation. One of the methods to provide ride comfort is by reducing the vehicular vibrations by using a suspension system, which includes spring, damper and other essential components. The damper being an energy dissipating device is responsible for reduction in amplitude of vehicular sprung mass vibrations. Passive dampers consist of hydraulic oil for damping the vibrations due to road disturbances. It is said that soft suspensions provide better ride comfort, whereas hard suspension is meant for good road handling performance. But satisfying these conflicting requirements by using a passive damper is a difficult task, since its damping coefficient is fixed and road conditions are variable.

Due to the above mentioned constraint, researchers are working on smart materials as damping media instead of conventional fluid. Smart materials invented for this purpose include some of the well known class of fluids like Electro-rheological (ER) fluids and Magneto-rheological (MR) fluids. These fluids change their properties according to the applied environment. Due to better rheology of MR fluids over ER fluids in most of the aspects, they are given major importance, when its application is mentioned to vehicles.

MR fluid was first discovered and applied to an engineering application (magneto-rheological clutch) by Rabinow (1948). Advantage of having MR fluid in damping application is that the damping media is controllable and the response is quicker. The response time of the MR fluid towards a variable magnetic field is less than 10 μs (Acharya et al. (2019)). Hence, it is possible to vary the damping coefficient of the damper according to the variable road conditions. Considering the ride comfort for the passenger, it is always preferable to have a controlled damping and hence, MR fluid dampers are better options for vehicles. The suspension systems with MR dampers are

one of the semi-active suspension systems. The technology implementation of MR fluids made a significant soar after the year 2002, when General Motors along with Delphi automotive systems launched a car with a semi-active suspension system using MR damper. Later, Audi, Ferrari and Porsche made an attempt with this technology for a few car models (Gołdasz and Sapiński (2015)). Still researches are going on for the betterment of MR fluid damper technology even though the technology implementation has already been done for expensive four wheeler models which include racing applications also.

It is also important to develop or implement a suitable control strategy for MR fluid dampers since the magnetic field generated which changes the rheology of MR fluid varies with the electric current supplied (when the damper has electromagnetic piston). This helps to vary the damping coefficient of the MR damper with respect to time and varying road profile. Selection of control strategy depends on the application of MR damper.

The proposed research is mainly focusing on the implementation of a semi-active suspension system by using an MR damper suitable for a four wheeler vehicle. Along with the design and fabrication of MR damper for a four wheeler vehicle, a control strategy is aimed to be developed for the damper. In the next stage, the ride comfort for the proposed MR damper will be analyzed using standard road profiles with the help of a quarter car test rig. Further, the designed MR damper has to be incorporated in a four wheeler vehicle, tested, analyzed and to be compared with a passive suspension system.

1.1 TYPES OF SUSPENSION SYSTEM

Suspension systems being the main cause for ride comfort have been classified based on the way in which it produces the damping. Following are the classification of suspension systems.

1.1.1 Passive Suspension system

The passive suspension is one of the most generally used ones due to its simplicity, and economical price. Passive suspension has restricted performance because its

components can only store or dissipate energy and it cannot adjust its properties with the conditions, which cannot fulfill both the comfort and handling necessities under changeable road conditions. Passive damper consists of hydraulic oil whose oil grade varies with varying applications. The viscosity of the hydraulic oil remains constant and hence, delivers invariable performance irrespective of the input disturbances. The majority passive suspension systems utilize springs with hydraulic or pneumatic shock absorbers.

(a)   (b)

(c)
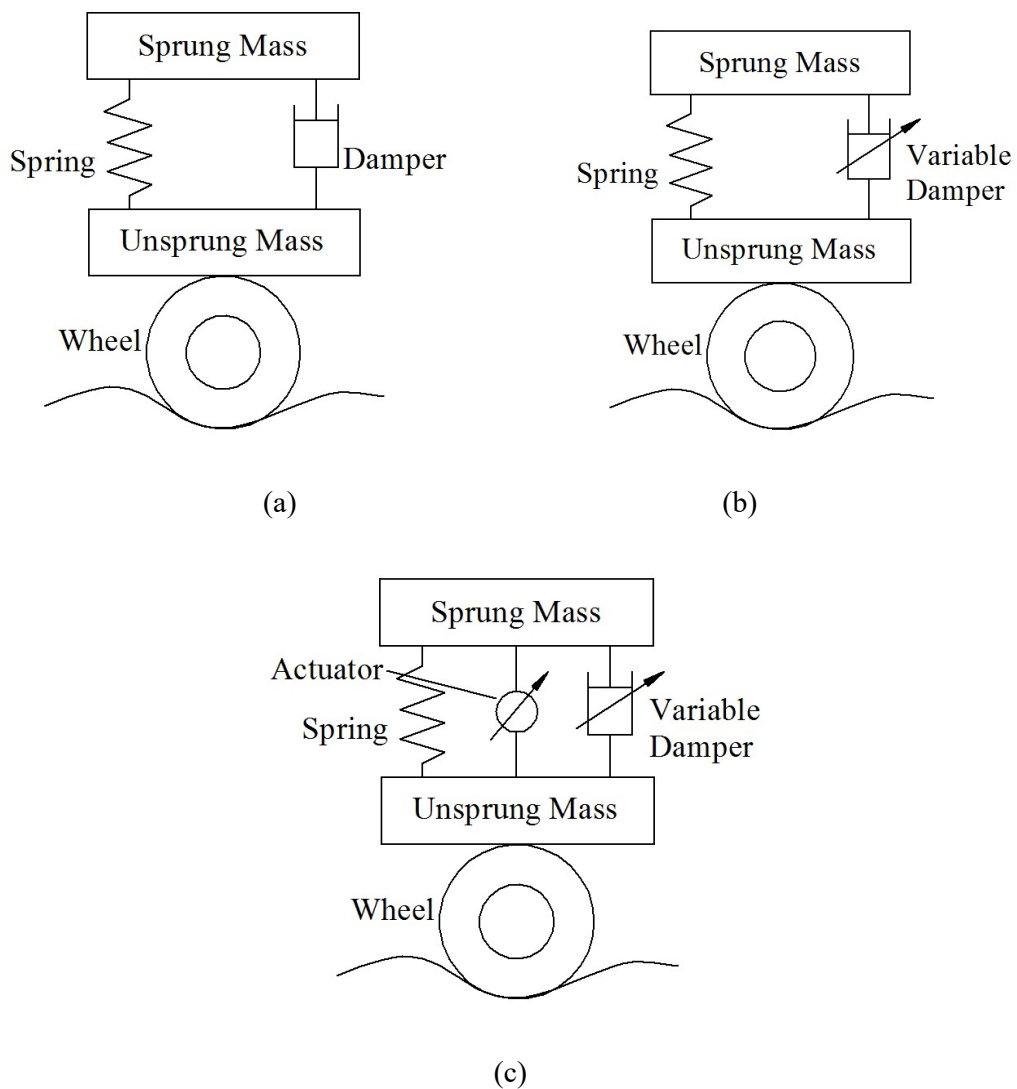
Figure 1.1 Suspension systems, (a) Passive suspension, (b) Semi-active suspension, (c) Active suspension system (*Courtesy: Omar et al. (2017)*)

1.1.2 Semi-active suspension system

The semi-activeness was initially brought in by Karnopp and Crosby in the beginning of 1970s, on the basis of a well-known skyhook control. The damping coefficient of the semi-active damper can be altered by a number of methods. The suspension system can only dissipate the road forces and cannot put in supplementary force to the system. The passive suspension's compromise can be condensed with the precise control system which results in making cars comfortable in any case of the road surface. Semi-active dampers may consist of smart fluid as the damping medium (eg: magneto-rheological fluid, electro-rheological fluid) or the ordinary hydraulic oil with varying operational flow (eg: variable orifice damper) to achieve semi-active nature. The semi-active suspension can be an optimized system between the passive and the active one by owning major advantages of active systems.

1.1.3 Active suspension system

Active suspension systems utilize a controllable actuator between the sprung and unsprung masses. This actuator is capable to both put in and dissipate energy to and from the system. A main advantage of such active suspensions is that these are capable of handling the conflict between ride comfort and road holding easily than passive suspension systems. The bandwidth of a fully active suspension is generally higher when compared to passive ones in order to damp the resonance of chassis mass as well as wheel hop. The actuator requires a high amount of external energy for operation and is expensive due to complexity of its operation.

1.2 DAMPER AND ITS CLASSIFICATION

Dampers are the energy dissipating devices and found themselves in the vibration control applications in vehicles, structures, washing machines, etc. In general, a damper comprises piston, piston rod and cylinder. The damping force developed by the damper depends on the flow of damping fluid in a specified path. Based on the cylinder and piston rod arrangements, the dampers are classified into following types.

1.2.1 Monotube damper

Monotube damper consists of a single cylinder and piston arrangement along with an accumulator. Working fluid is filled in the cylinder and the accumulator is charged with nitrogen gas. The working fluid and the gas are separated by floating piston. The function of the accumulator is to accommodate the volume change that occurs due to movement of the piston rod inside the cylinder. The arrangement is shown in figure 1.2 (a).

1.2.2 Twin tube damper

In this type, two cylinders can be seen out of which the inner cylinder guides the piston rod. The fluid flows from inner cylinder to outer cylinder through a base valve provided in the arrangement. This fluid flow between outer and inner cylinder accommodates for the volume changes due to motion of the piston rod. A schematic of the twin tube damper is shown in figure 1.2 (b).

(a)   (b)
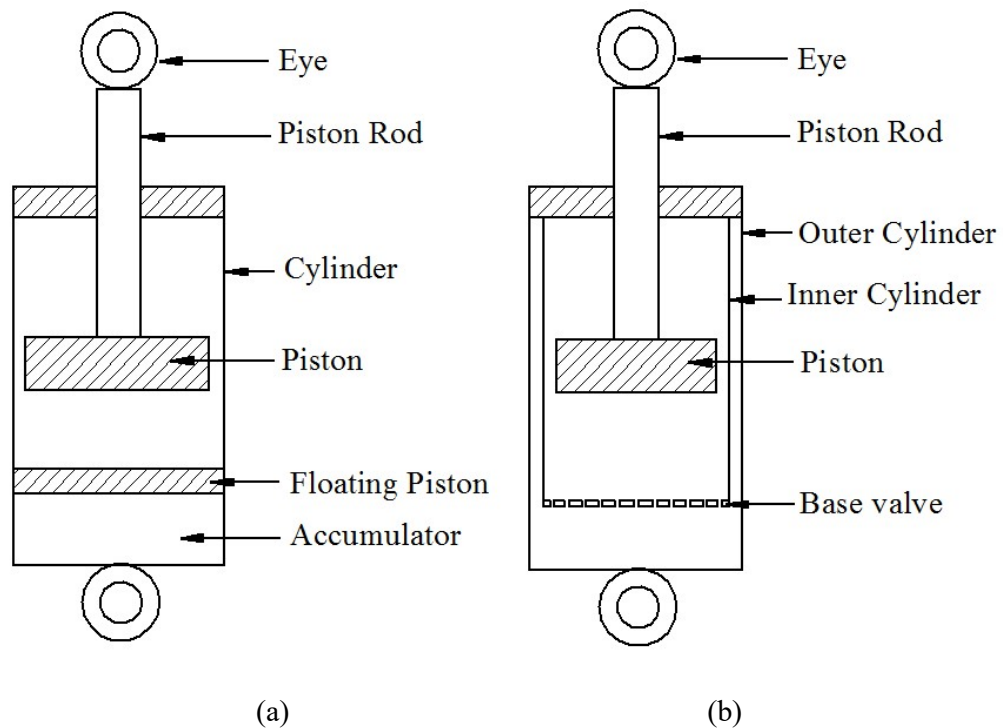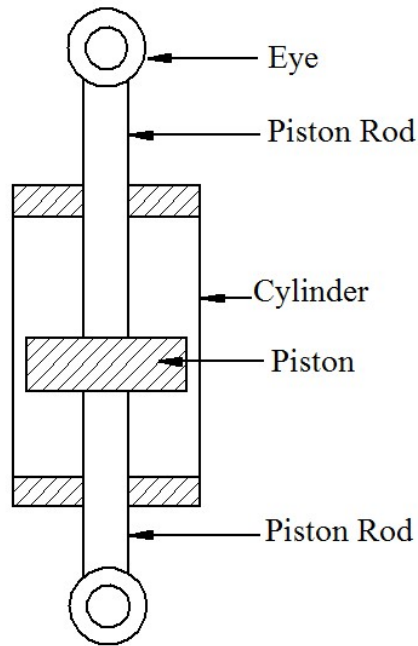
(c)

Figure 1.2 Different Dampers, (a) Monotube damper, (b) Twin tube damper, (c) Double ended type damper (Dezfouli (2014))

1.2.3 Double ended type damper

Double ended damper is an extended version of monotube damper where the piston is connected at both the ends by piston rod. Because of this design, inert gas type of accumulator is not essential. The design of double ended type considers the dimensions of piston rod and the stroke of the damper. General use of double ended damper can be seen in structural vibration control.

1.3 MAGNETO-RHEOLOGICAL (MR) FLUIDS

Magneto-rheological fluid (MRF) is a suspension of very fine, low coercive ferro-magnetic particles in a carrier fluid. These are generally referred under the category of controllable fluids, since the behavior of MR fluid changes from liquid state to semi solid state under the influence of externally applied magnetic field.
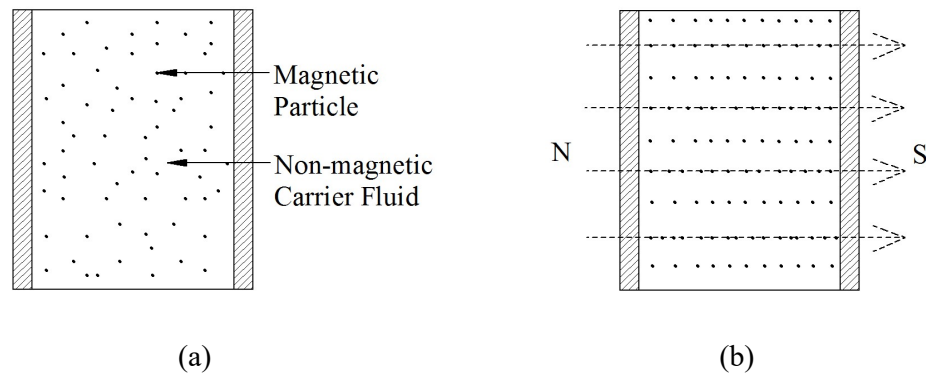
Figure 1.3 Nature of MR fluid (a) without magnetic field, (b) with Magnetic field
(Revabhai (2017))

The changes are quick and reversible. MR fluid is beneficial in terms of performance criteria such as low initial viscosity, higher shear stress upon application of magnetic field, low hysteresis, low power consumption, faster response and temperature stability. Such special characteristics have made it suitable for use in semi-active suspension devices.

An MR fluid mainly consists of magnetizable particles and carrier fluid in liquid phase. Along with these constituents, some additives are also added to improve the sedimentation characteristics and to reduce oxidation. Some of the commonly used carrier fluids are silicone oil, paraffin oil, mineral oil, hydrocarbon oil etc. An important requirement of a carrier fluid is that it must operate for a wide range of temperature range (typically from -40°C to 120°C). The range of suitable soft-magnetic, low coercivity materials for ferromagnetic particles includes pure iron, iron alloys (including cobalt, vanadium manganese, silicon etc.), carbonyl iron, atomized iron, water-atomized iron, iron oxides, silicon steel, low carbon steel grades, cobalt, nickel, ferritic stainless steel etc. In general, the solid phase should exhibit high saturation magnetization. The preferable size range for micron sized particle is 1 to 10 μm.

The operational modes of MR fluid have been classified into flow mode, shear mode, squeeze mode and pinch mode based on field and relative motion between the surfaces.

Flow mode (figure 1.4(a)) occurs when the fluid flows between two stationary surfaces due to pressure difference. A general application of flow mode of operation is found in damper. In shear mode (figure 1.4 (b)), the fluid flows between two surfaces that move relative to each other but requires large shear areas for generating the force. Engineering applications with shear mode of operation are dampers and brakes.
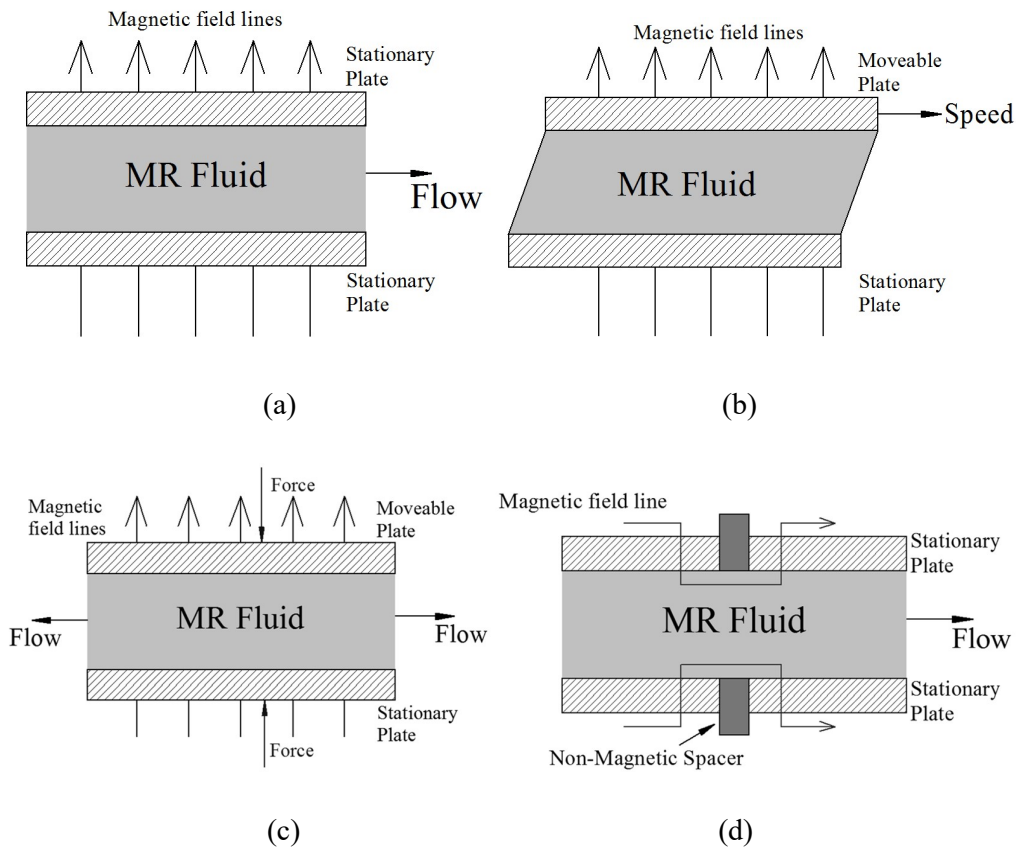
Figure 1.4 MRF operating modes: (a) Flow mode, (b) Shear mode, (c) Squeeze mode, (d) Pinch mode (Revabhai (2017))

In squeeze mode (figure 1.4 (c)), the fluid is sandwiched between two planar parallel surfaces. The distance between the poles changes with respect to the prescribed displacement or force input. Pinch mode (figure 1.4 (d)) features magnetic poles in an axial arrangement along the flow channel and this mode is useful in MR valves.

1.4 MAGNETO-RHEOLOGICAL DAMPER

Magneto-rheological dampers are similar to passive dampers with changes in damping fluid used and operational theory. MR dampers have found their application not only in vehicles, but in other domains also (Orečný et al. (2014), Spelta et al. (2009), Shixing et al. (2011), Hiemenz et al. (2008), Yildiz Sivrioglu (2016)). A major difference found between passive and MR dampers is the design of piston. A normal piston is used as per the operational mode in the passive damper whereas electromagnetic piston is designed and utilized in MR dampers. This is in accordance with the ease of operation and control of MR damper with application external power supply. The changing input may be in terms of current or voltage. Some studies have the demonstration in terms of permanent magnet too (Kim et al. (2017)).
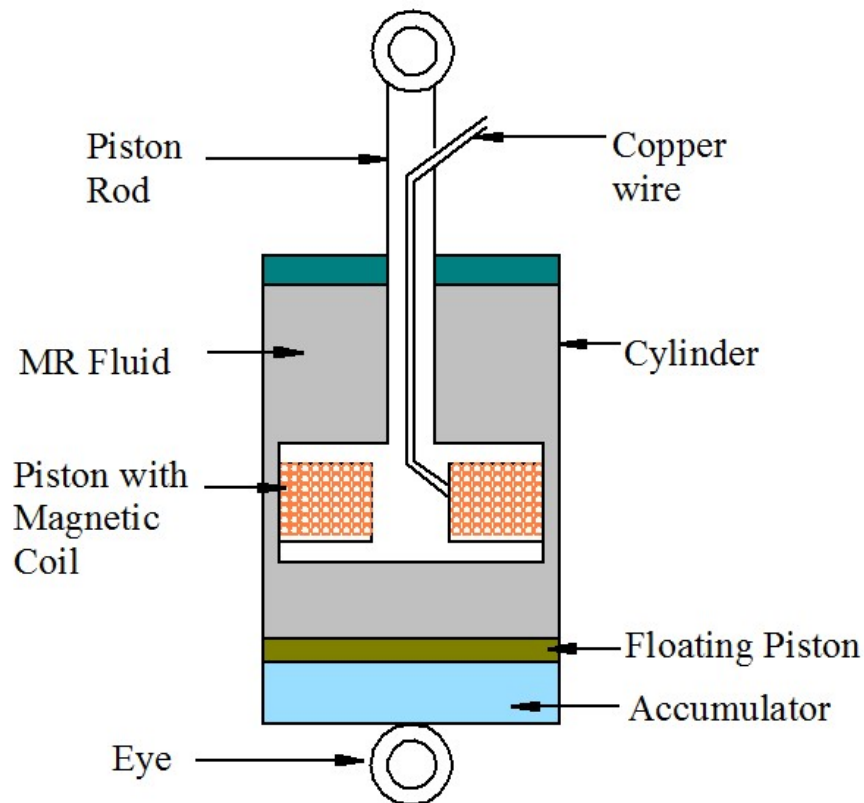
Figure 1.5 Schematic of MR damper (Revabhai (2017))

The MR dampers also classified as monotube, twin tube and double ended type MR dampers based on piston and cylinder arrangements. Along with this, MR dampers

work with flow mode, shear mode, squeeze mode and with combination of two modes together, it can operate in mixed mode too. A schematic of a monotube MR damper is shown in the figure 1.5.

1.5 MATHEMATICAL MODELING

Data obtained during experimentation must be converted into a mathematical equation form so that it is useful for further stages of analysis. The mathematical model of a damper behavior is an essential tool in the simulation process. Hydraulic fluids used in passive dampers generally behave in a linear manner since they obey Newtonian law. But it's not the same in case of Magneto rheological fluids and they behave in non-linear way with some amount of hysteresis. Representation of this non linear behavior using conventional mathematical models may result in a model with huge error and the validation of the simulation may not hold good. Hence it is always advisable to use non linear mathematical models such as Bingham model, Bouc -Wen model, Dahl model, etc for describing MR damper characteristics. The model representation is categorized into parametric and non-parametric models. Some of the parametric models are described in following subsections.

1.5.1 Bingham model

Bingham model is one of the simplest mathematical models used to represent non linear behavior. Bingham plastic model was proposed in 1985. Consider a system as shown in figure 1.6
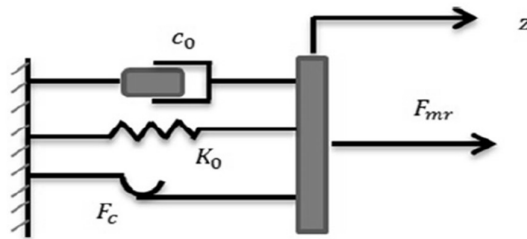
Figure 1.6 Bingham mechanical model *(Courtesy: Eshkabilov (2016))*

The Bingham model for the system shown can be represented as,

$$F_{mr} = F_c sgn\ (\dot{z}) + c_0 \dot{z} + K_0 z + F_0 \qquad (1.1)$$

Where, z is relative displacement of a piston that corresponds to the displacement (z_s) of a suspended mass (m_s) and $\dot{z}$ is its derivative that is velocity of a piston; F_c is frictional (control) force; c_0 is damping constant; K_0 is stiffness of the elastic element of the damper; F_0 is offset force (constant force value). The signum function $sgn\,(\dot{z})$ will take care of the direction of the frictional force, F_c with respect to the relative velocity $\dot{z}$ of the hysteresis (internal) variable z (Hong et al. (2005), Nguyen and Choi (2009)). The model represents the non-linearity in a simplest way whereas major hysteresis components are missing which may lead to a significant error between theoretical and experimental results.

1.5.2 Dahl model

Dahl model is another mathematical model to represent the non linearity of an MR damper. Dahl model considers quasi-static bonds in the origin of friction (Majdoub et al. (2013)). The Dahl model is formulated by the following expressions.

$$F_{mr} = k\dot{z} + (k_{wa} + k_{wb}u)w$$

$$\dot{w} = \rho(\dot{z} - |\dot{z}|w) \tag{1.2}$$

Where, F_{mr} is exerted force from the MR damper, u is the control voltage, w is the dynamic hysteresis coefficient, k, k_{wa}, k_{wb} and ρ are parameters that control the hysteresis loop shape.

1.5.3 Bouc-Wen model

Bouc-Wen model consists of a first-order nonlinear differential equation that relates the input displacement to the output restoring force in a rate-independent hysteretic way. The general Bouc-Wen expression for the system shown in figure 1.7 is,

$$\dot{y} = -\gamma |\dot{z}|y|y|^{n-1} - \beta z|y|^{n} + A\dot{z} \tag{1.3}$$
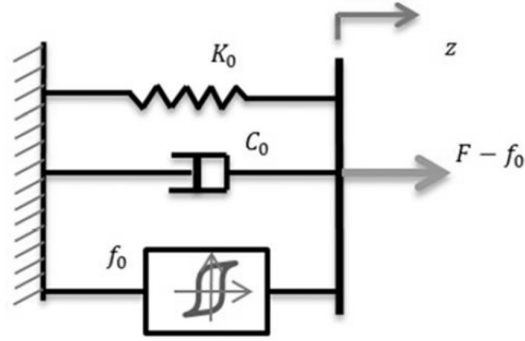
Figure 1.7 Bouc-Wen mechanical model *(Courtesy: Eshkabilov (2016))*

Where, y is the variable that can differ from a sinusoidal to a quasi-rectangular function on the parameters γ, β and A. Bouc-Wen model is very much suited to represent MR damper non-linear behavior (Yang et al. (2002), Yao et al. (2002), Prabakar et al. (2009), Graczykowski et al. (2017)).

To overcome some of the drawbacks of general Bouc-Wen model, a transformed model called modified Bouc-Wen model was proposed (Liu et al.(2011)). Characteristic model equations for modified Bouc-Wen model are,

$$F = c_1\dot{y} + k_1(x - x_0) \tag{1.4}$$

$$\dot{z} = -\gamma |\dot{x} - \dot{y}| z |z|^{n-1} - \beta(\dot{x} - \dot{y})|z|^n + A(\dot{x} - \dot{y}) \tag{1.5}$$

$$\dot{y} = \frac{1}{c_0 + c_1}[\alpha z + c_0\dot{x} + k_0(x - y)] \tag{1.6}$$

Where, x= damper displacement , x_0= is the initial deflection of spring with stiffness k_1, c_1= damping coefficient of dashpot, y= internal displacement of the MR damper, c_0= viscous damping observed at higher velocities, k_0= stiffness at high velocities, γ, β, α, A, n are the parameters related to shape of the hysteresis loop.

Table 1.1 Comparative table over modelling techniques

Name of the parameters	No. of. influencing parameters	Remark
Bingham model	4	Represents non-linearity in a simplest way but may lead to significant error.
Dahl model	6	Considers quasi-static bonds in the origin of friction
Bouc-Wen model	8	A very good tool for hysteresis representation and recommended for MR damper
Modified Bouc-Wen model	10	Can represent hysteresis even better than general Bouc-Wen model and may take more computational time.

1.6 DIFFERENT CONTROL STRATEGIES

Any mechanism or a system requires frequent input which may be a constant input or variable input. The complexity arises with a system when it has to be designed for a dynamically changing input. If it is planned with human interference, it will result in time delay as well as frequent errors. Hence, automatic control systems are gaining importance in recent days. In the sense, a feedback type of method needs to be adapted for continuous monitoring of the system which may result in better performance of the system as well as the possibility minimum deviation.
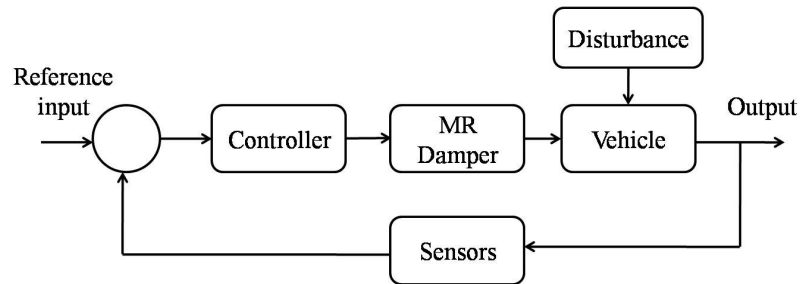
Figure 1.8 Block diagram of control system

Magneto-rheological dampers are subjected to change in rheology with variation in current supply and hence, they need a proper control strategy. The change in current supply changes the magnetic flux generated which in turn results in change in damping force. MR damper when implemented in a vehicle, undergoes different road input conditions. Because of this, generation of required damping force for varying road profile is a key to achieve good ride comfort. An instant change in the rheology of the MR fluid is very much essential towards varying road profile. This can be achieved with proper implementation of control strategy for MR damper. Some of the well known and effective control strategies are listed below.

1.6.1 Skyhook controller

The skyhook controller is one of the simplest yet very effective in a semi-active control systems associated with MR Fluid (Song (2009)). The control input of the skyhook controller (u) is defined as follows:

$$u = G_s \dot{x} \qquad\qquad (1.7)$$

where, G_s is called the control gain and $\dot{x}$ is the velocity of the system. The control gain of Gs for this controller is generally found out based on the trial-and-error method upon considering the amount of necessary damping force. This parameter is the key factor in attaining better performance of the control system. In general, this controller can offer favorable output in the lack of external disturbances and parameter deviations.

1.6.2 PID controller

The ideology of the PID controller is very simple and effective alike the skyhook controller (Choi et al. (2016)). This enables the PID controller to become a standard control means for industrial applications. The PID controller can be utilized in any configuration of control schemes due to its flexibility. Definition of PID control scheme can be expressed as,

$$u_{pid} = K_P e(t) + K_I \int_0^t e(t)dt + K_D \frac{de(t)}{dt} \qquad\qquad (1.8)$$

where, u_{pid} is the control variable, e is the error defined as $e = u_r - y$, where u_r is the reference value, and y is the process output. K_P, K_I, K_D are the control gains for the proportional, integral and derivative control actions, respectively. A general scheme of the PID controller is depicted in figure 1.9. The total control input of the PID controller is amplified and applied to the MR system. Its control performance usually depends greatly on the values of control gains.
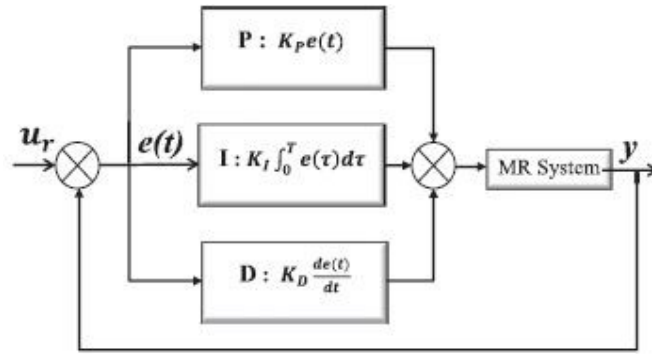
Figure 1.9 Scheme of PID controller *(Courtesy: Choi et al. (2016))*

1.6.3 Sliding mode controller (SMC)

There exist some system uncertainties related with MRF devices and systems in spite several merits of the PID controller. Furthermore, the dynamic performance of an MRF device is a function of magnetic field. There may also present nonlinear hysteresis of the damping force in the MRF damper. Hence, in order to assure robustness of the control system, a robust controller needs to be applied to take account of system uncertainties. An SMC is known as one of the most pretty candidates which guaranty control robustness in opposition to system uncertainties and external disturbances (Choi et al (2016)). The sliding mode control systems have invariance nature to the parameter dissimilarities and external disturbances under the sliding mode motion. A scheme of SMC is shown in figure 1.10.
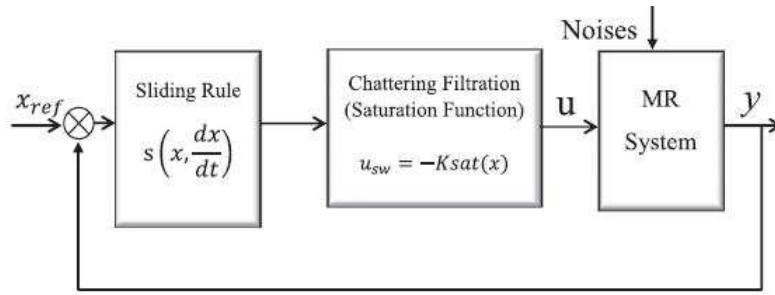
Figure 1.10 Scheme of Sliding Mode Controller *(Courtesy: Choi et al. (2016))*

1.6.4 Fuzzy controller

Fuzzy controller also known as fuzzy logic (FL) has the characteristics of inherent sturdiness, capability of handling nonlinearities and uncertainties and does not demand an accurate mathematical model (Nguyen et al. (2018)). Therefore, it has attracted the attention of engineers and researchers over the last decades. Fuzzy-set theory has been effectively implemented to a various range of applications, mostly towards control and intelligence systems. A general scheme of fuzzy controller is shown in figure 1.11.
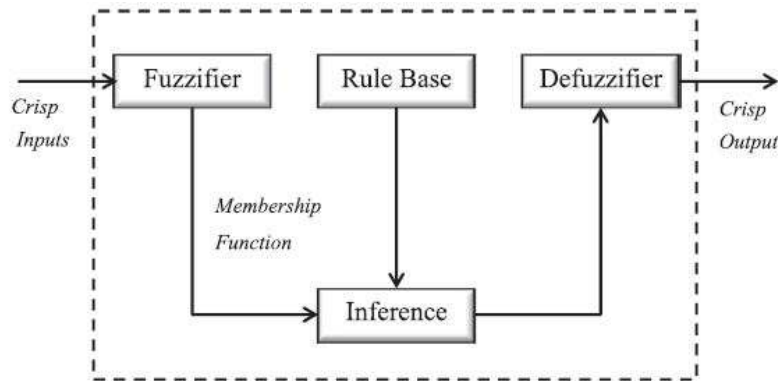
Figure 1.11 Schematic of Fuzzy control system *(Courtesy: Choi et al. (2016))*

1.7 VEHICLE SUSPENSION SYSTEM

There are several dependent and independent suspension systems available for four wheeler vehicles. Some of the well known suspension systems are Sliding pillar, MacPherson strut, Double wishbone system, Multi link suspension, Trailing arm

16

suspension, etc. All these suspension systems indicate various arrangements of spring, damper and the wheel components based on vehicle dimensions and the requirements. Illustration of few well known suspension systems are provided in the following subsections.

1.7.1 Sliding pillar suspension

A sliding pillar suspension is a type of self-sufficient front suspension for light cars. The stub axle and wheel assembly are attached to a vertical pillar or kingpin which slides up and down through a bush or bushes which are attached to the vehicle chassis, usually as part of transverse outrigger assemblies, sometimes resembling a traditional beam axle, although fixed rigidly to the chassis. Steering movement is provided by allowing this same sliding pillar to also have rotational movement.
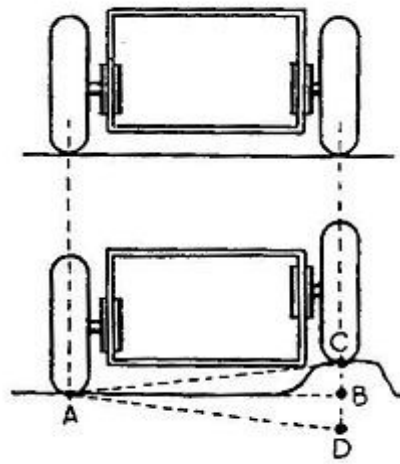
Figure 1.12 Sliding pillar suspension *(Courtesy: Abyzov (2014))*

1.7.2 Trailing arm suspension

Trailing arm suspension employs two trailing arms which are pivoted to the car body at the arm's front edge. The arm is relatively large compared with other suspensions' control arms because it is a single piece and the upper surface supports the coil spring. It is rigidly fixed to the wheel at the other end. Here, it only allows the wheel to move up and down to deal with bump. Any lateral movement and camber change (with respect to the car body) is not allowed.
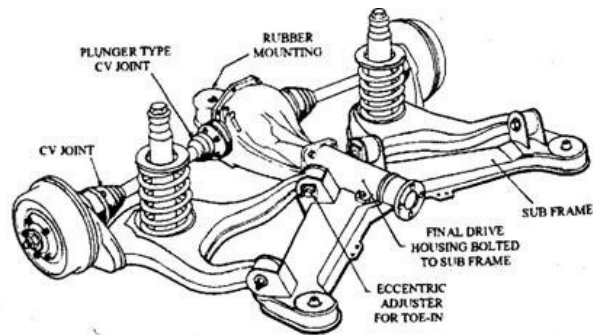
Figure 1.13 Trailing arm suspension *(Courtesy: Abyzov (2014))*

1.7.3 Double Wishbone suspension

Double wishbone suspension is an independent suspension which can be used for both front and rear suspension. The upper and lower arms of the suspensions are in the shape of the "Wishbone" and if a damper or coilover is linked then it would take the shape "A".
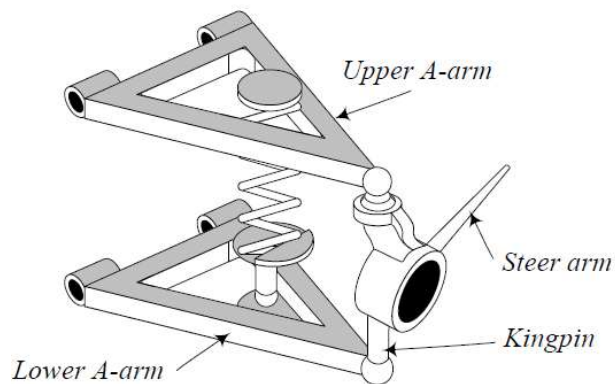
Figure 1.14 Double Wishbone suspension *(Courtesy: Abyzov (2014))*

These wishbones are connected to the vehicle chassis from the wheels and they use ball joint for the support and for the movement of the wheel for steering. The upper arm and the lower arm are usually of different sizes known as the short and long arm (SLA), which helps the wheel to gain proper camber angle during the wheel travel. The suspension spring is connected to the upper or lower arm and to the chassis of the vehicle.

1.7.4 Multilink Suspension

Derived from the double wishbone one, the multi-link suspension uses three or more lateral arms and one or more longitudinal arms, which don't have to be of equal length and can be angled away from their natural direction. Each of the arms has a spherical joint or rubber bushing at each end, causing them to work in tension and compression and not in bending.
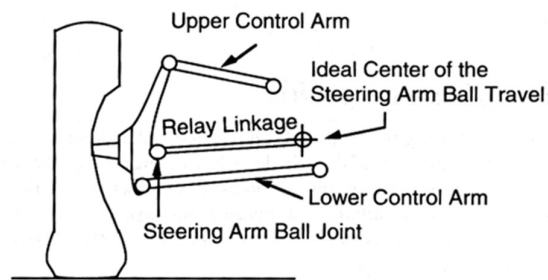
Figure 1.15 Multi link Suspension system *(Courtesy: Abyzov (2014))*

1.7.5 McPherson Suspension

A McPherson strut uses a wishbone, or a substantial compression link stabilized by a secondary link, which provides a bottom mounting point for the hub carrier or axle of the wheel as shown in figure 1.16. This lower arm system provides both lateral and longitudinal movement of the wheel.
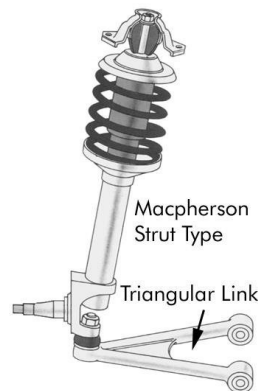
Figure 1.16 McPherson strut system *(Courtesy: Abyzov (2014))*

The upper part of the hub carrier is rigidly fixed to the bottom of the outer part of the strut proper; this slides up and down the inner part of it, which extends upwards directly to a mounting in the body shell of the vehicle. The line from the strut's top mount to the bottom ball joint on the control arm gives the steering axis inclination. The strut's axis may be angled inwards from the steering axis at the bottom, to clear the tire; this makes the bottom follow an arc when steering.

Table 1.2 Summary on different suspension system

Name of the suspension	Comments	Suitable for
Sliding pillar suspension	Self-sufficient front suspension, fixed rigidly to the chassis	Light cars
Trailing arm suspension	Pivoted to the car body, arm is relatively large, allows the wheel to move only up and down	Rear wheel of motorcycle, not suitable for heavy duty vehicles
Double wishbone suspension	Independent suspension, connected to the vehicle chassis from wheels, can gain proper camber angle	Luxury cars and even sports cars
Multi-link suspension	Uses three or more lateral arms, can work easily under tension and compression	Premium cars and even in off-road vehicles
McPherson suspension system	Uses compression link stabilized by secondary link, simpler design and more comfort, consume little space.	Widely used suspension system in cars

1.8 ROAD INPUT TO THE VEHICULAR TESTING

Literature studies explore the performance of the suspension systems when subjected to different kinds of road profiles. The road profiles are useful during the suspension analysis in theoretical or simulation studies. The road profiles generally used are harmonic profiles, bump input or random road profiles. Some of the road profiles are briefed below.

1.8.1 Random road roughness

Depending on the randomness of the road profile the roads are classified into different classes by International Standard Organization (ISO). The irregularities are measured in terms of power spectral density. The randomness for these road profiles are generated by using white noise signal. It can be noted that the amplitude or the severity of the road profile increases when the ranking approaches the badness in the road.
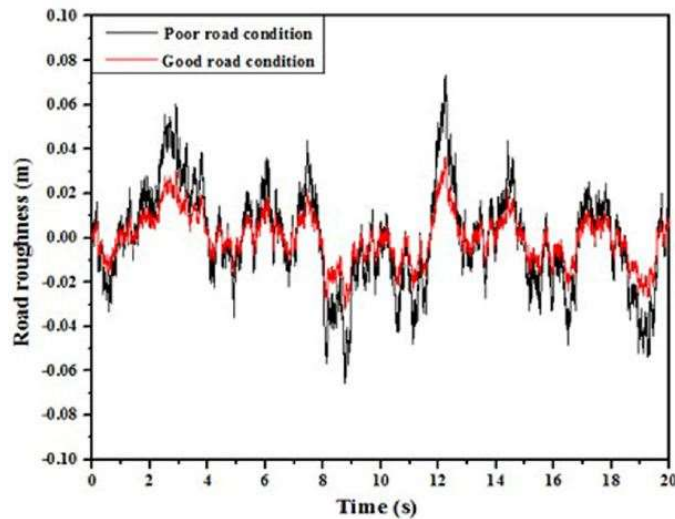
Figure 1.17 Random road profile (*Courtesy: Tharehallimata et al. (2019)*)

The random road profile can be expressed as (Tharehallimata et al. (2019)),

$$\dot{Z}_r(t) = -2\pi u n_0 Z_r(t) + \sqrt{G_q(\Omega_0)u}w(t)$$

(1.9)

Where,

$Z_r(t)$= Amplitude of road irregularity, $G_q(\Omega_0)$= Roughness coefficient of road, u= Vehicle velocity, $w(t)$= white noise signal, n_0= spatial frequency.

Table 1.3 Classification of random road as per ISO (Dixon (2008))

Degree of road roughness $G_q(\Omega_0)$ (10^{-6}m²/(cycle/min)) at Ω_0= 0.1 rad/min		
Rating	**Description**	**Spectral density(cm³/cycle)**
3	Very good road	8
4	Good road	16
5	Medium good road	32
6	Medium road	64
7	Medium bad road	128
8	Bad road	256
9	Very bad road	512

1.8.2 Harmonic road input

The harmonic road inputs in terms of sinusoidal or cosine expressions have been reported in several literature studies. Some studies have also implemented step inputs for the analysis (Desai et al. (2019)). Research studies have also reported suspension performance when the vehicle is run over the road bump (Jamadar et al. (2020)).
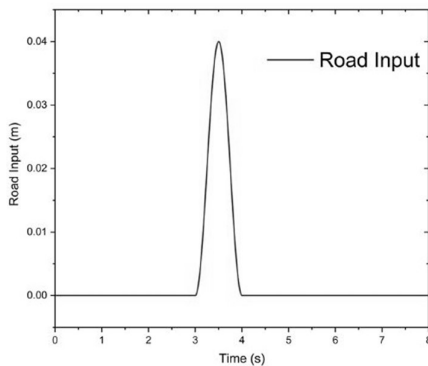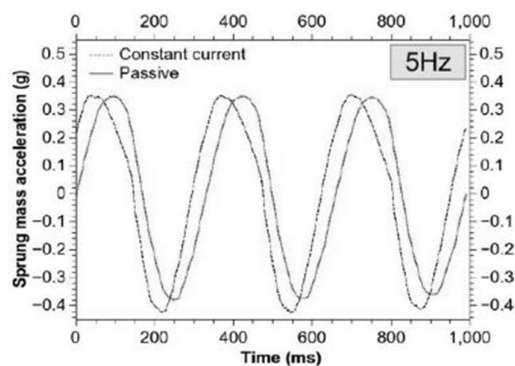
(a)   (b)
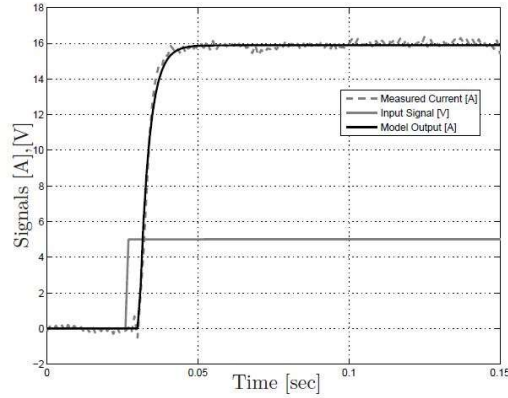
(c)

Figure 1.18 (a) Bump road input (*Courtesy: Jamadar et al. (2020)*), (b) sinusoidal input *(Courtesy: Desai et al. (2021))*, (c) step input (*Courtesy; Koch et al. (2010)*)

1.9 RIDE COMFORT AND ROAD HOLDING

The capability of the suspension to smooth down the road imperfections affects both the comfort and the road holding of the vehicle. Improving the comfort means, generally, limiting the vertical acceleration fluctuations of the vehicle body and hence of passengers. Improving road holding means, among other things, limiting the fluctuations of the vertical force that each tire exchanges with the road.

It is a well known fact that the ride comfort and road holding act in a contrary way. In the sense, an effort to make only the ride comfort better will reduce the road holding and vice versa. Therefore, improving both at once is a multi-objective and a crucial problem. As per ISO 2631 standard, the ride comfort is quantified based on root mean square of weighted acceleration.

$$a_w = \left[\frac{1}{T} \int_0^T (a_w(t))^2 dt \right] \qquad (1.9)$$

Where, a_w is the weighted RMS acceleration, $a_w(t)$ represents weighted acceleration in time domain, T is the time duration of the data measurement.

23

1.10 TEST RIGS FOR SUSPENSION EVALUATION

Evaluation of any new suspension logic directly in a vehicle may result in extra expenditure or damage to the vehicle during testing. To avoid all these adverse probabilities, researchers have used various kinds of test rigs for vehicular simulations the results of which could be used for suspension improvement.

1.10.1 Quarter car test rig

Quarter car testing is a simple way to analyze the performance of components of a suspension since it requires only $1/4^{th}$ of the full vehicle model.
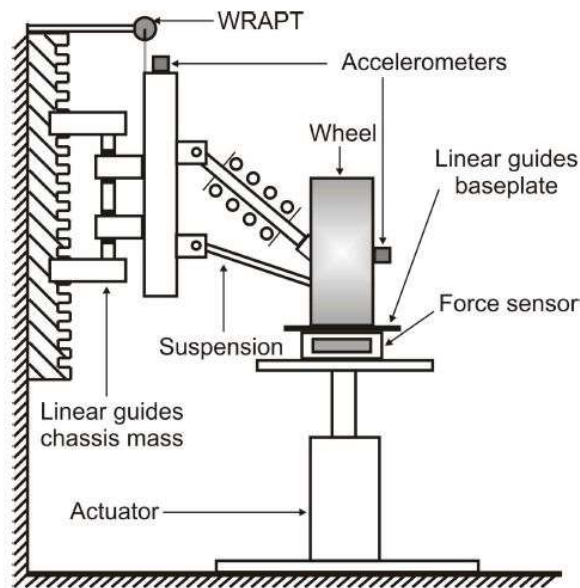
Figure 1.19 Scheme of quarter car test rig (*Courtesy: Koch et al. (2010)*)

A scheme of quarter car test rig is shown in figure 1.19 with a hydraulic actuator, a suspension system with a wheel and provision for application of loads. Along with these, it would have sensors for measurement of displacement or acceleration amplitude, load, etc. An actuator provides required input to the system which can be considered as the desired road profile on which the quarter car needs to be tested.

A suitable sensor with associated data acquisition system makes the analysis easier and the performance of the suspension can be quantified.

1.10.2 Two poster test rig

An advanced version of quarter car scheme known as two poster testing (or half car test) provides further dynamic results when compared to the former one. Along with translational movements, an analysis of rotational dynamics can be conducted by using this kind of scheme. The test scheme is better suited for analyzing two wheeler vehicle or the half portion of the four wheeler vehicle. A set up of two poster test rig is shown in figure 1.20.
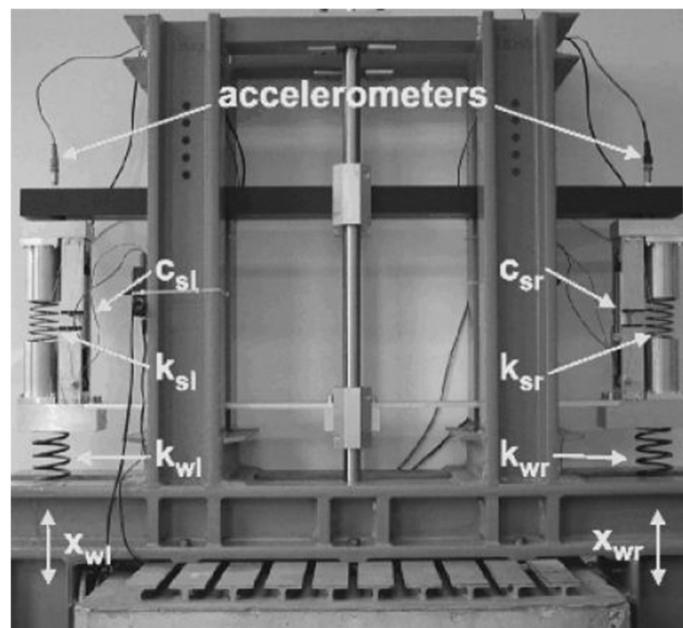
Figure 1.20 Half car test setup (*Courtesy: Vaes et al. (2005)*)

1.10.3 Four poster test rig

A four poster test rig is the one where the suspension or any other component evaluation is done which can simulate different road profiles. This kind of testing is very much useful for a four wheeler vehicle where the performance of the vehicle can be recorded and improved before on road running. A scheme of four poster test rig is shown in figure 1.21.
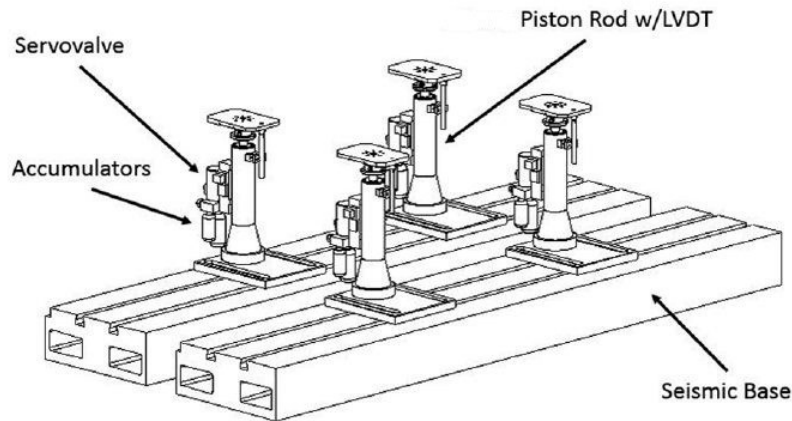
Figure 1.21 Scheme of a four poster test rig (*Courtesy: Chindamo et al. (2017)*)

1.11 VEHICLE MODELS

Vehicle models are the effective tools in analyzing the vehicle performance prior to the actual implementation or testing of vehicles. Proper utilization of these models results in cost effectiveness in the vehicle testing.

1.11. 1 Quarter car model

Mathematical modeling of vehicle is generally employed to understand and to simulate vehicle dynamic behavior. The most employed and useful model of a vehicle suspension system is a quarter car model.
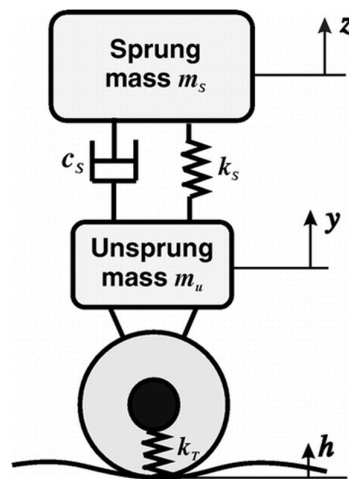
Figure 1.22 Quarter car representation *(Courtesy: Türkay et al. (2016))*

The quarter car model consists of one-fourth of the body mass, suspension components and one wheel. A typical quarter car model is schematically represented as shown in figure 1.22.

A quarter car model requires a numeric or the model of each essential component during the simulation process.

1.11.2 Half car and full car models

There are other two vehicle models are used in the vehicle dynamics are half car and full car models. Quarter car model is essentially used for its simplicity and mostly used to fetch the information on vertical vibrations in an effective way.
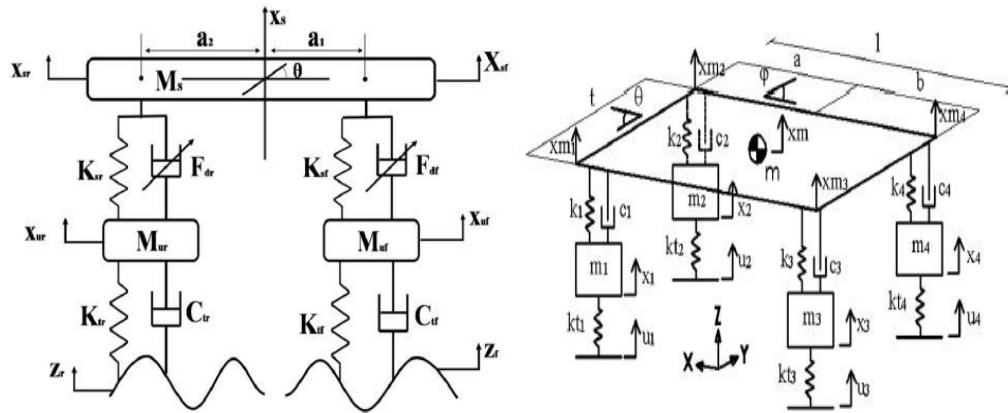
Figure 1.23 A scheme of half car model (*Courtesy: Devikiran et al. (2022)*) and full car model (*Chindamo et al. (2017)*)

On the other hand, half car and full car models provide additional information on other degree of freedom too. Typical half car and full car models are provided in figure 1.23.

In general, passive dampers are used in dominant number of passenger vehicles to reduce the cost as well as complexity of the vehicles. Even though active suspension systems reduce the contrast between ride comfort and road holding, the system demands precise and complex mechatronics circuit. This will automatically hike the budget of the overall package. Semi-active suspension is thus an effective

compromise between passive and active system to provide an added comfort in the passenger vehicles.

1.12 ORGANIZATION OF THE THESIS

The thesis consists of totally seven chapters namely Introduction, Literature review, Development of magneto-rheological damper (prototype-1), Design and development of MR damper for vehicle, Quarter car testing and analysis, On road testing of car with MR damper, Summary and conclusions of the research work.

In the chapter 1, brief introductions on the MR fluid, MR dampers, quarter car system, mathematical modeling of MR damper, control logics for MR fluid applications were discussed. Along with these, the standard methodologies as well as the quantification of the ride comfort are also discussed.

Chapter 2 provides literature review on MR fluids and its applications, quarter car modeling, control logics for MR dampers and Vehicular testing with MR dampers. Various standards discussed in the literature for ride comfort evaluation are also listed.

Chapter 3 discusses the characterization of the passive damper of the desired test vehicle, design of experiments with passive damper, quarter car simulation with passive damper. Along with these, the Chapter 3 also elaborates the design, development and characterization of MR damper prototype-1.

Chapter 4 discusses the synthesis of MR fluid, design and development of full scale MR damper, magnetostatic analysis of the MR piston, characterization of the developed MR damper. Also, this chapter explains about the mathematical modeling of MR damper using Kwok modeling technique.

Chapter 5 discusses the mathematical modeling and analysis using quarter car model, characterization of tire and spring, control logic to MR damper, implementation of MR damper into quarter car system with McPherson strut system and its deviation with analytical results. . Also, this chapter majorly narrates about the development of single-sensor method, experimental testing on quarter car and the comparative results.

Chapter 6 briefly discusses the implementation of MR damper into the vehicle, on-road testing of vehicle with different velocities and results of on-road vehicle testing and the ride comfort quantification by using ISO 2631 standard.

Chapter 7 provides the summary of the research work based on MR damper and its vehicular application, quarter car analysis with McPherson strut and the quarter car testing with single sensor system. The conclusion of the work and the scope for future work are also discussed in this chapter.

CHAPTER 2

LITERATURE REVIEW

2.1 INTRODUCTION

MR fluid has grabbed the attention of the research community since its invention due to its capability of useful transformation from liquid to semi-solid phase with lower electric power requirement. This ability of MR fluid makes it possible to use it in various engineering applications. This chapter discusses some of the salient works reported on the MR fluid and its applications in the literature. Also, some of the control logics used for the MR fluid devices and simulations works are reported in this chapter.

2.2 MR FLUID

The magneto rheological fluid was first introduced for clutch application by Rabinow (1948) and explained the merits of using 'magnetic fluid' in engineering applications.
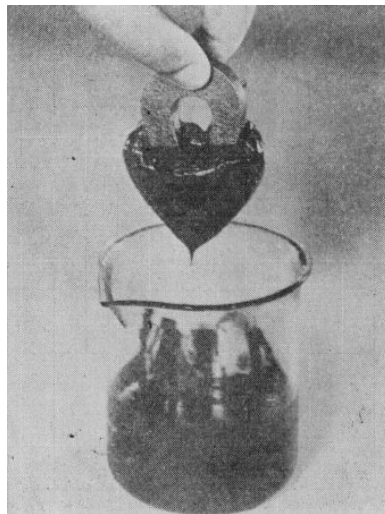
Figure 2.1 MR fluid as demonstrate by Rabinov (*Courtesy: Rabinow (1948)*)

A review on salient researches performed on magneto-rheological fluid and its fluid properties was summarized by Alghambi et al (2014). The study also summarized the

preparation of MR fluids and the compatibility among the constituents of MR fluids. A review on preparation of magneto rheological fluids, its stabilization and various ferrous particles used for the preparation was presented by Ashtiani et al (2015). Also, the benefit of different particles and other constituents was discussed.

Various MR fluid samples were prepared and characterized by Kumbhar et al. (2015) for MR brake application. Author discussed about its rheological properties, also effect of constituents of MR fluid. Wahid et al. (2016) presented a review on difficulties and defects which may occur during the preparation or after the function of magneto rheological fluid. The author also presented the demerits of such prepared MR fluid.
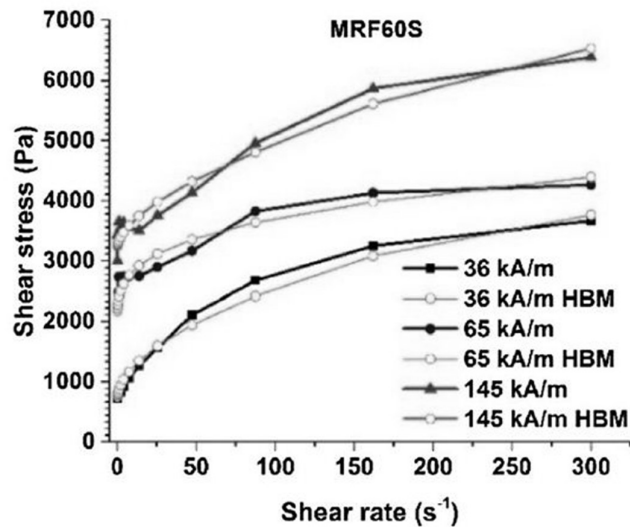
Figure 2.2 MR fluid flow behavior with variation in magnetic fields (*Courtesy: Acharya et al. (2019)*)

Gurubasavaraju et al. (2017) prepared various MR fluid samples and found out the optimal fluid composition by using particle swarm optimization method. The study conducted design of experiment mainly on ferrous particle volume fraction and fluid flow gap in the damper. Acharya et al. (2019) used carbonyl iron powder (CIP) in the preparation of magneto-rheological fluid where two sizes of particles were used for the purpose. Apart from this, the comparison between three different particle loadings was also reported when mixed with poly alpha olefin oil.

Preparation of magneto-rheological fluid and its rheological study analysis for specific engineering applications was discussed by Acharya et al (2020). The optimal fluid composition was found based on simulation studies performed over MR brake. Sedimentation studies of the prepared MR fluid samples were also discussed. An MR fluid sample was prepared for twin tube damper application by Desai et al. (2020) and the fluid characteristics were discussed for varying magnetic field. The fluid characteristics were modeled by using Hershel-Bulkley model.

2.3 MR DAMPER

Yang et al. (2002) discussed about large scale MR damper for seismic application with 20 ton capacity, its modeling and control through force-feedback.
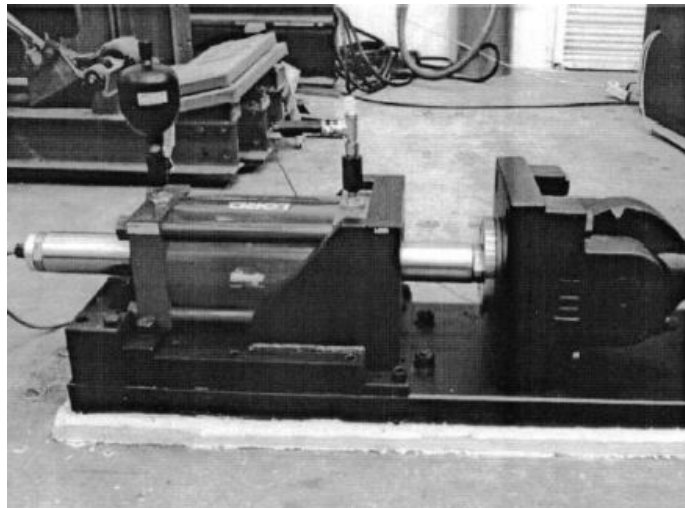
Figure 2.3 20 ton MR damper for seismic application (*Courtesy: Yang et al. (2002)*)

A flow mode MR damper was designed and developed by Yao et al. (2002) which was characterized using sinusoidal and triangular excitation. Dynamic range nearly equal to 8 was obtained and author explained the non-symmetry between compressive and rebound force. Sassi et al. (2005) proposed new approaches for MR damper piston development and corresponding magnetic flux distribution was discussed. The characterization of the newly developed MR damper was illustrated at different input DC current.

Hong et al. (2005) presented non dimensional design parameter scheme in the design and construction of MR damper by using Bingham plastic model. Single DOF vibration model with spring and MR damper was used to study the effectiveness of the proposed methodology.

Common hydraulic oil in a damper was replaced with MR fluid and characterized with triangular profile excitation by Ramirez et al. (2007). The damping force developed was analyzed against the displacement and a simple mathematical relationship was established. Shivaram and Gangadharan (2007) developed a low capacity shear mode MR damper and modeled the damper based on statistical modeling technique by using design of experiment. The DOE included volume fraction, magneto motive force and the operating frequency.

Figure 2.4 MR damper developed for quarter car testing and analysis (*Courtesy: Sung & Choi (2008)*)

Dimensions of the piston of an MR damper for middle sized commercial vehicle were optimised by Sung and Choi (2008) using finite element method. The developed damper was then characterized and then used in the quarter car assembly to measure the ride comfort without and with skyhook control. A simulation study based on finite element method was conducted by Nguyen (2009) to determine the optimal dimensions of the MR damper suitable for vehicle application.

Double ended types as well as a single ended type MR damper were differentiated by Guan et al. (2009). In the study, the author illustrated the design procedure for spring accumulator in the single ended MR damper. Xu et al. (2012) developed a large scale

MR damper suitable for earthquake mitigation using in house prepared MR fluid. The maximum damping force obtained was more than 190kN. Authors also used various parametric mathematical models to mathematically represent the MR damper behavior. An MR damper which could produce about 1.5 kN damping force was developed by Tu et al. (2012). The magnetic fiux generated was analyzed prior to the damper development through finite element method.

Zhu et al. (2012) reviewed and discussed about different design procedures adapted in development and analysis of MR damper for structural and vehicular applications by different research groups. A twin tube MR damper was developed and characterized by Zheng et al. (2012) at different input currents for the shear mode type. An unsymmetrical nature between compressed and rebound force was observed. An experimental analysis with quarter car set up was conducted along with on-off skyhook controller.

Figure 2.5 Damper testing setup (*Courtesy: Parlak and Engin (2012)*)

The nature of MR fluid in the fluid flow gap region was analyzed using CFD in the non-Newtonian region and the damper was developed for characterization by Parlak and Engin (2012). Authors presented the agreement between the experimental and

quasi static analysis using CFD. Simulation results of MR damper with 6-pole piston design was demonstrated by Shiao et al. (2013). Further, the quarter car simulation with this damper along with fuzzy controller at two kinds of road inputs was discussed.

Yazid et al. (2014) discussed about combination of shear and squeeze modes in the design of MR dampers and the results of simulation (using Finite Element Method Magnetics) of this mode was compared with MR damper designed with shear mode and squeeze mode alone. A comparative study was presented by Dezfouli (2014) among the characterization performance of different commercial dampers available for two wheeler vehicle. A prototype MR damper was also developed based on the design of commercial MR damper.

A large scale MR damper was developed by Sternberg et al. (2014) whose characterization was performed through multi-physics platform. The error between simulation and the experimental results was explained for different experimental conditions. An MR damper was experimentally characterized and the behavior was mathematically modeled for further analysis using quarter car model by Suresh (2015). Further, the effect of skyhook control was discussed with this MR damper model. Goldaz (2015) theoretically demonstrated the concept of magneto rheological damper with twin tube cylinder and simulated the damper at various conditions. The effect and variations due to dynamic input was also explained.

An MR damper with twin tube structure and commercially available MR fluid was presented by Hemanth et al (2016). The damper was modeled using non-parametric technique using the damper characterization and further used for quarter car model analysis. The presented work by Kima et al. (2017) used permanent magnet instead of electromagnetic coil to tune the damping force in the magneto rheological damper. Also, different shapes of cylinders were developed and characterized to understand the dynamic response.

A monotube MR damper developed by Rewabhai (2017) was used with in-house prepared MR fluid and characterized using dynamic testing machine. The MR damper could deliver the damping force above 1kN. Design of experiment was conducted to

determine the optimal dimensions of monotube MR damper through simulation study by Gurubasavaraju et al. (2017). Three different models were considered for the study and the comparative analysis was presented. A low capacity MR damper was considered in the work.

Rahman et al. (2018) reviewed about the versatile usage of magnetorheological dampers in different engineering applications ranging from low capacity to high capacity along with various designs involved. The work by Gurubasavaraju et al. (2018) presented a methodology to characterize the twintube shear mode MR damper through FE and CFD analysis. Also, the damping force development with varying shear gap has been illustrated. A low capacity MR damper was developed and the similar damper was characterized through simulation by using FE method and CFD by Tharehallimata et al (2018). The agreement between experimental and simulation result was presented and the simulation results were extended for quarter car analysis.

MR damper for All Terrain Vehicle (ATV) was modeled using COMSOL multi-physics for its application in SAE Baja by Unni and Tamilarasan (2018). The model was subjected to Design of Experiment (DOE) and optimized using Taguchi method. The simulation was conducted for two different MR fluids. A commercially available passive damper of a passenger van was characterized by Desai et al. (2019) and the response was used in the design of twin tube MR damper. The maximum damping force of MR damper recorded was about 1kN.

A monotube MR damper with intension of to be used in commercial vehicle was developed by Sherje and Deshmukh (2019). The characterization results showed the damping force development through this damper reaching above 1200 N for 2A DC input current. The performance comparison of an MR damper analytically was presented by Acharya (2019) based on the fluid properties of different MR fluids prepared in the laboratory. Optimized fluid properties was also found out for the damper designed based on design of experiment.

Figure 2.6 A shear mode monotube MR damper (*Courtesy: Meng & Zhou (2019)*)

A shear mode MR damper was developed and characterized by Meng and Zhou (2019) at definite dynamic condition as well as for different DC input current. A good dynamic range was observed and variations in the model parameters were observed with variation in current input.

2.4 MATHEMATICAL MODELING OF MR DAMPER

Chen et al. (2020) discussed about different mathematical models used to identify the hysteresis behavior of MR damper and their bounds. The author compared the results obtained with the results obtained from benchmark research. The effect of model parameters over the vibration suppression was also discussed. The importance of modeling the non-linearity of MR damper was described by Savaresi et al.(2004) and demonstrated two types of modeling approaches for MR dampers. The methodology included black-box method and semi-physical model approaches.

Kwok et al. (2006) proposed a novel parametric modeling technique to simulate the MR damper hysteresis behavior and compared it with well known Bouc-Wen model. The author described the advantages of the proposed model in terms of computational simplicity and error identification. Chooi and Oyadiji (2009) proposed a mathematical model to represent the MR fluid flow behavior in the annular gap and compared it

with the parallel plate approximation method. The common errors in parallel plate approximation were also discussed.

Ahn et al. (2009) used commercially available LORD RD-1005-3 MR damper in a research study and characterized it. The authors modeled the characterization results by using different modeling tools such as Bingham model, Bouc-Wen model, Kwok model and the proposed self-tuning fuzzy method. The study emphasized the superiority of proposed method over other methods.

A developed MR damper was characterized and the hysteresis behavior was modeled by using various modeling techniques by Sahin et al. (2010). The author also discussed about error and deviation occurred while modeling the damper among various mathematical models. A half car vehicle model was considered by Stutz and Rochinha (2011) to analyze the vehicle performance by using suspension with passive damper as well as MR damper. The non-linearity of MR damper was considered by using modified Bouc-Wen model. Performance analysis was done based on different road profiles.

Various hysteresis models available for MR dampers were demonstrated with their physical meaning by Eshkabilov (2016) and were analyzed with the help of quarter car model. The performance of quarter car with each model was compared. A piecewise linear approximation method was proposed by Kazakov et al. (2017) for modeling MR fluid properties. This model was then used to simulate the resistance force through MR damper.

Meng and Zhou (2019) characterized the in-house prepared shear mode MR damper and used hyperbolic tangent model to represent the hysteresis of the damper at different input currents. Hongzhan et al.(2020) reviewed on application of MR dampers in different fields, their modeling methodologies including parametric approaches and non-parametric approaches. Various control strategies adapted for controlling the dynamic behavior of MR dampers was also discussed. Devikiran et al. (2022) performed damper characterization which was designed for two wheeler application. The damper characteristic was then modeled using Kwok modeling technique and vehicle simulation was then performed by using MATLAB/ Simulink.

2.5 VEHICLE MODELS AND TESTING

An MR damper was characterized and modeled through Bouc-Wen model by Yao et al. (2002). The damper model was then implemented in quarter car simulation where semi-active nature of the suspension was achieved through sky-hook control.

Active control of the road noises reaching the vehicle frame was attempted by Roumy et al.(2004). A feedback controlled actuator was attached between the suspension point and the car frame for active vibration attenuation. LQR controller was designed and adapted for the active suspension. Vaes et al. (2005) used a half car test rig to understand the performance difference between two control criteria and compared the efficiency as well as discussed the beneficial factors. A fuzzy logic control was adapted by Rashid et al. (2006) to analyze the quarter car performance with magneto-rheological damper under random road input. Force-velocity characteristic of MR damper was used as the damper model for quarter car simulation.
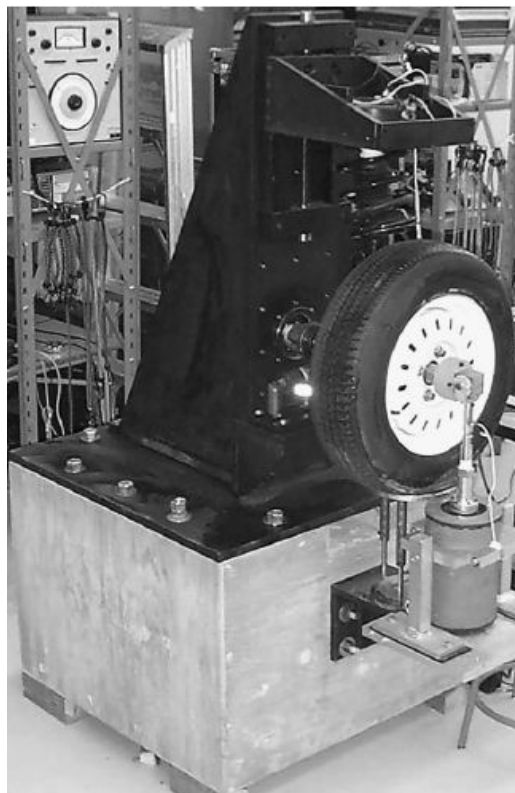
Figure 2.7 Quarter car test rig assembly (*Courtesy: Roumy et al. (2004)*)

A road hump as well as random road input profiles was used by El-Kafafy et al. (2012) for quarter car simulation using MR damper. Bouc-Wen model of MR damper was used to represent the damper in the suspension. Sprung mass acceleration and dynamic tire load were considered as the response terms from the quarter car. A comparison between passive and semi-active suspension with MR damper was reported by Prabhakar et al. (2013) based on quarter car simulation. Bingham and Bouc-Wen models were used to represent the MR damper. An LQR based controller was used with the MR damper for vibration suppression.

In a quarter car simulation using MR damper, modified algebraic model was used to represent the hysteresis behavior of the damper by Balamurugan et al.(2014). The comparison between passive, semi-active and active suspensions was made based on their performance over rough road condition. A better ride comfort was aimed through quarter car simulations by Mitra et al. (2014) where experiments were conducted based on Box-Behnken method of design of experiment. ANOVA and response surface method was adapted to find the optimal solution.

Balamurugan and Jeyaraj (2014) made an analytical characterization of MR damper by using algebraic models and implemented in quarter car model by using skyhook sliding mode controller. Later, the performance of semi-active system with MR damper was compared with active suspension system and found very close comparison between them in most of the aspects. A quarter car system with passive suspension in it was tested by Mitra et al. (2015) were number of experiments were chosen based on design of experiment with fractional factorial design. Analysis of variance was carried out to check the influence of individual parameters over ride comfort.

A quarter car model with passive suspension was analyzed by Reddy et al. (2016) targeting the ride comfort of a passenger. Response surface method was used to arrive at mathematical model for ride comfort based on design of experiment and then this model was used as objective function for genetic algorithm.

Design of experiment was conducted by Mitra et al. (2016) to understand the ride comfort and road holding of a quarter car system with passive suspension. Parameters

such as sprung mass, spring stiffness, damping coefficient and tire pressure were considered for designing the experiment. A quarter car system with seat-suspension-human model was simulated by Nagarkar et al. (2016). The study aimed at optimizing the parameter towards better ride comfort and to achieve good vibration dose value to achieve health criterion as per ISO-2631-1. Non-linearity in the suspension components was considered whereas the quarter car simulation was conducted over random road surface (Class C).

Quarter car simulation with road bump profile was reported by Reddy et al. (2016) to achieve better ride comfort. Response surface method and Taguchi method were used to arrive at optimal parameters. Chindamo et al. (2017) discussed a methodology where the required road profiles can be generated in the four poster rig or the full car set up and presented the validation. Two different piston schemes of magneto-rheological damper were compared by Park et al. (2017). Two dampers were characterized and the one without bypass hole produced more damping force. The dampers were then tested using quarter car test rig and the ride quality among the two were compared.

Two DOF quarter car model was solved using SIMULINK to investigate the vehicle performance in terms of ride comfort and road holding by Phalke and Mitra (2017). Analysis was performed using the bump height of 0.1 m.

Experimentation over a quarter car test rig with passive and active suspensions was reported by Omar et al. (2017). Both systems were analytically evaluated using Simulink's simscape library. For validation simplicity, the models were developed as single degree of freedom systems. Quarter car models with 2-DOF and 3-DOF schemes were compared by Zhao et al. (2017) under random road excitations. Driver RMS acceleration was measured without and with cushion effect for comparative analysis. A validation test conducted at different velocities showed the deviation against two models.

Response surface method along with genetic algorithm was adapted by Reddy et al. (2017) to minimize the RMS sprung mass acceleration of quarter car simulation

model. Sprung mass, spring stiffness and the damping coefficient were considered as variables in the design of experiment.

Quarter car simulation with magneto-rheological damper was reported by Abdelhafez and Omar (2017) where the active vibration suppression was evaluated. For this purpose authors simulated the suspension performance with proportional -derivative (PD) controller as well as positive position feedback (PPF) control. Yerrawara and Arakerimath (2017) conducted experiments on quarter car test rig based on design of experiments obtained from Taguchi method. An MR damper was used in the semi-active suspension of the quarter car test rig with McPherson arrangement. Parameters considered for designing the experiments were spring stiffness, sprung mass and the current input to understand their effect over ride comfort.

A quarter car model for a train car suspension was presented by Nguyen et al. (2018).The semi-active suspension of the train car consisted of magneto-rheological damper. The semi-active suspension was then tested in a quarter car test rig with different control schemes and their performance comparison was presented. Performance comparison of MR damper with skyhook controller, proposed quantitative feedback theory (QFT) controller against passive damper was illustrated by Jeyasenthil and Choi (2018). The quarter car simulation was demonstrated with two types of MR dampers: without fault and with fault.

An in-house prepared MR damper was characterized and used in quarter car simulation by Jamadar et al. (2020). An equivalent damping model was considered along with Bingham model and both were used in driver seat model in the quarter car simulation. Road bump as well as random road profiles was used in the simulation.

Multi-dynamics model of a quarter car was developed by Vivas-Lopez et al. (2021) using FEM tool to analyze the stress concentration in the suspension components. The stress concentration with passive as well as semi-active suspensions was reported. The commercial MR damper characterization was reported to use it in the modeling and controlling application.

2.6 CONTROLLER APPLICATIONS

Chn et al. (1999) used sky hook algorithm and implemented in the quarter car test rig. The control gains were tuned using road detective algorithm. The performance of this semi-active system showed improvement when compared to the passive one.

Sliding mode controller was adapted by Lam and Liao (2001) in a semi-active suspension using MR damper to improve the ride comfort in a quarter car simulation. Comparison was made against constant current, passive and with controlled inputs to the damper. The skyhook control algorithm was implemented in the quarter car simulation study using MR damper by Li et al. (2006). The sprung mass displacement was used to evaluate the performance of MR damper.

The work by Vassal et al. (2006) emphasized on the implementation of skyhook control for semi-active suspension using MR damper. The sprung mass response was analyzed using single accelerometer. Savaresi and Spelta (2009) demonstrated a technique to use a single sensor with skyhook control strategy to reduce the cost occurrence due to minimal requirement of two sensors in the closed loop control systems. The technique was demonstrated with an illustration of two wheeler vehicle.

Song (2009) made an attempt to develop a cost effective sky hook controller for suspension system using MR damper by reducing the number of sensors used for data measurement. Later simulation study was conducted using full car model. Sename et al. (2010) considered the non-linearity of MR damper and accounted the same in design of control strategy involving the skyhook scheme. A random road scheme was considered in the study.

Spelta et al. (2010) designed a layout for sensor placement in a vehicle to reduce the sensor requirement in the semi-active suspension in a four wheeler vehicle and adapted Mix-1-sensor to control the suspension activity. Commercially available MR damper was characterized by Metered et al. (2010) and the comparative analysis was carried out among different control strategies. The MR damper modeling was done using non-parametric model technique in terms of neural network.

de Jesus Lozoya-Santos et al. (2011) presented a controller synthesis for an MR damper in a quarter vehicle model. Two controllers were presented based on hysteresis and nonlinear behavior: LPV controller and Frequency Estimation Based control. Simulation results showcased their response for comfort and road holding.

Characterization of MR damper was done and the data were used to develop a fuzzy-PID based controller by Kasemi et al. (2012). The control algorithm was developed by Kasemi et al. (2012) based on the behavior of the MR damper through the characterization results. Fuzzy logic and PID control were adapted for the quarter car simulation model. The characterization was done using commercially available MR damper. Truong and Ahn (2012) described about the characterization of commercial MR damper and its modeling. Also, proposed the force-sensor less control system in combination with fuzzy logic.

Simulation and experimentation on quarter car was carried out with active suspension control by Hyniova (2016). For this purpose, h-infinity control was adapted. Nie et al. (2017) proposed and developed a modified SH-ADD control algorithm to improve the ride comfort and road holding of a vehicle. The developed algorithm was tested with MR damper in a quarter car test rig. The algorithm showed upto 18% improvement in the ride quality of the vehicle. A hardware controller was developed to the quarter car test rig to improve the ride quality using an active suspension system by Ehteshum (2018). The passive nonlinear model was used to develop the idealized controller.

The study by Babawuro et al. (2019) compared the performance of LQR and LMI controllers in quarter car suspensions using passive and active dampers. The performance of MR damper in the quarter car simulation was compared with different designed control strategies along with skyhook control scheme by Florean-Aquino et al. (2021).

The relative displacement between sprung and unsprung mass was considered as the control input by Desai et al. (2021) in the quarter car testing. The testing was carried out on suspension system of an SUV vehicle replacing passive damper by MR damper. Rakheja-Shankar control scheme was utilized in the quarter car analysis.

2.7 VEHICULAR TESTING

The on road real time testing of a two wheeler vehicle with MR damper retrofit into the suspension system was reported by Gravatt (2003). The study used skyhook control for the testing and the performance comparison against the OEM damper suggested significant reduction of body acceleration with skyhook control.

A case study was described by Naude and Snyman (2003) illustrates the optimized parameters for passive dampers of a 22 ton three axle vehicle. The study also validates the experimental results with those of analytical ones made through particular software. Akutain et al. (2007) developed a full car simulation model and used control algorithm to understand the performance comparison in the semi-active suspension system. Semi-active dampers such as continuously variable dampers (CVD) and Discrete Stage Variable Dampers (DSVD) were used. The difficulties and the practical problems associated with the control algorithms were also discussed.

The difficulties in achieving ride comfort and road handling simultaneously in off-road vehicles were addressed by Els et al (2007). The opposite nature of ride comfort and road holding was demonstrated by three case studies. Ride comfort and road holding was measured by Shirahatt et al. (2008) to compare the performance between passive and active suspension systems. Optimization techniques with different constraints were adapted in the due course. ISO 2631 was used to analyze the comfort parameters of the full vehicle model.

Ride comfort, kurtosis and VDV evaluation were carried out by Nahvi et al. (2009) for a passenger vehicle with curb weight 1336 kg. The vehicle was passed over variety of road profiles for comparative analysis. The ride comfort evaluation was carried out by using British Standard BS 6841. A benchmark passive damper was considered by Messer (2015) for designing the MR damper for off-road vehicles. The pressure drop characteristics were studied for the designed and developed MR valve. Modified Bingham model was used to model the damper characteristics.

Schiehlen and Iroz (2015) discussed about the five critical parameters in designing the suspension for the vehicle where two of them were spring and the damper. The author

also projected the uncertainties in these parameters and attempted to provide a way to make a decision based on pareto-optimal solution.

Patil and More (2016) used FFT analyzer to understand the vibration level of three different four wheeler vehicles to understand the ride comfort capability. The vehicle testing was conducted over three varieties of road surfaces and vibration levels were compared in terms of displacement, velocity and accelerations. Ryabov et al. (2016) discussed an analytical analysis of efficiency of shock absorbers in vehicles based on damping characteristics of the linear shock absorbers.

Steišūnas et al. (2017) evaluated smoothness of the ride and ride comfort considering vertical acceleration of passenger vehicle with one tire flat condition. Tire flat condition was defined using software package called Simpack. Yang et al. (2018) used ADAMS software tool to analyze the ride quality of an electric vehicle with McPherson front suspension. Weighted vertical acceleration and the pitch angle acceleration were the key responses used to optimize the stiffness and damping of the suspension.

A ride comfort analysis over an automated people mover was carried out by Budiwantoro et al. (2018) using ISO 2631 and Sperling ride index. It was observed that the acceleration levels were well above highly comfortable ride quality index and the comfort duration was also provided. A theory of variational feedback control (VFC) was utilized in development of control scheme for MR damper suspension by Pepe et al.(2019). The damper and the control was tested in a BMW series four wheeler vehicle. The experiments were carried over a bump on the road and the performance comparison between different controllers was carried out.

2.8 OTHER APPLICATIONS OF MR FLUID

Teresawa and Sano (2005) used an MR damper between ground floor and the first floor to mitigate the seismic shock effect. Commercially available MR damper RD-1097-1 was used as the semi-active damper. Park et al. (2006) proposed a design for MR brake system where braking torque was controlled by sliding mode controller.

MR brake design with two rotating disk was optimized using simulated annealing in combination with finite element method.

Hiemenz et al. (2007) attempted to mitigate the rotorcraft vibration reaching the crew in the helicopter system. The MR damper was used with skyhook controller in the experimental set up where SH-60 crew seat was installed. Use of magneto-rheological damper in washing machine to reduce the noise and vibration was demonstrated by Spelta et al. (2009). Commercially available MR controllable friction damper was utilized for the purpose by replacing the original dampers. Application of magneto-rheological dampers in landing gear of an aircraft was demonstrated by Shixinga et al. (2011). The drop test platform with landing gear assembly was utilized for the experimentation and parameters identification.
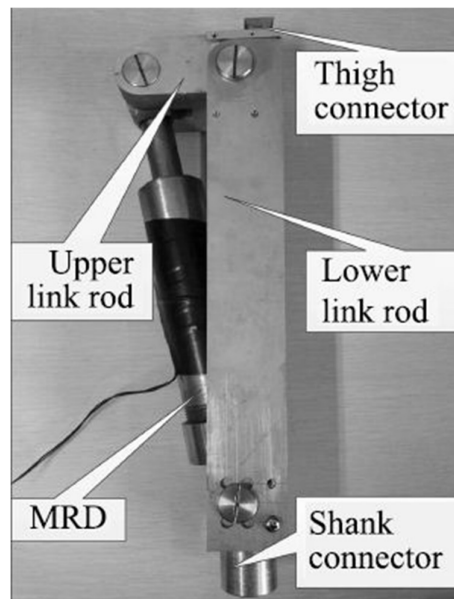
Figure 2.8 MR damper for lower limb prosthetic knee (*Courtesy: Fu et al. (2017)*)

Orecny et al. (2014) used MR damper in the suspension of a working machine to analyze the vibration mitigating capability. Two conditional studies were presented by the authors with MR damper.
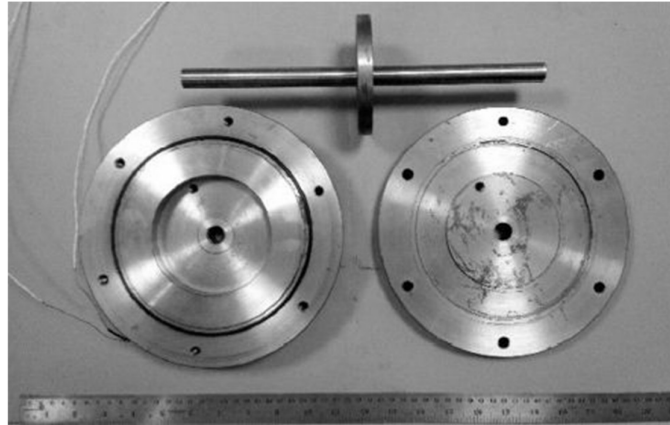
Figure 2.9 Components of MR brake (*Courtesy: Acharya et al. (2020)*)

The ride comfort and road holding of a monorail vehicle with semi-active suspension was analyzed by Yildiz and Sivirioglu (2016). The semi-active system comprised of MR damper and the study simulated the suspension performance under lateral as well as vertical loading.

Fu et al. (2017) developed an MR damper designed for prosthetic knee application and characterized it at different input DC current. The design was based on two bar linkage principle and the application was controlled by using sliding mode control.

2.9 STANDARDS ON RIDE COMFORT

Paddan and Griffin (2002) subjected about 100 vehicles under 14 different categories to evaluate the whole body vibration. The standards ISO 2631 (1997) and BS 6841 (1987) were taken into consideration for the evaluation. Authors differentiated the merits as well as demerits of each standard and compared the health criteria defined in two standards.

Fischer and Isermann (2004) differntiated passive, semi-active and active suspension systems and tabulated their energy requirements. The active and semi-active suspensions were then modeled and the model parameters were identified through experimentation in quarter car system. Validation of the models was also presented. Authors stressed the importance of time constants of semi-active systems and their influence over the performances. Marjanen (2010) found from previous literatures

about lack of studies on validation of ISO 2631 standard for whole body vibration. Method to validate the standard was demonstrated in the study keeping in mind about multi axes measuring environment for a vehicle.

Faris et al. (2012) reviewed about ride quality of passenger cars based on various literatures available in that research trend. Authors demonstrated numerous methods including theoretical as well as experimental techniques to quantify the ride comfort of a vehicle. Park and Subramaniyam (2013) studied the parameters such as frequency weighted root mean square, frequency weightings, maximum transient vibration values, vibration dose values and ride comfort which are associated with the whole body vibrations. The study involved whole body vibration evaluation standards such as ISO 2631 and British standard BS 6841.

Cieslak et al.(2019) made an attempt to estimate the ride comfort by combining acceleration measurements and anthropometric data. Also, the study explored the benefits of neural network in estimation of ride comfort. The ride comfort evaluation was performed based on ISO 2631:1997. A comparison between passive suspension and the semi-active suspension with MR damper was demonstrated by Negash et al. (2021). The suspension with MR damper was analyzed with two control algorithms: skyhook and skyhook-ADD. Improved performance of semi-active suspension was compared with passive one at different harmonics.

2.10 RESEARCH GAP

- Literature study indicated that the study of MR damper application in vehicles was performed majorly through analytical and computer simulation or through quarter car test rig. Only few studies reported its application in actual vehicle and analysis.

- Commercially available MR damper have been implemented in foreign countries in vehicle suspensions used for racing purpose and in high end expensive vehicles. No vehicles on Indian road are currently running with suspension system with MR damper, whereas India is one of the biggest markets for cost effective four wheelers.

- Performance and efficiency of MR damper in terms of road holding and vehicle stability have been reported through analytical or quarter car simulation using standard road spectrum input. Only few studies have been reported using real time road profile input.

- Majority of the works reported in the literature used commercially available MR fluid for the research purpose. Even though various studies reported application of different control strategies to the MR dampers through analytical studies, a very few works have reported practical implementation of control tactics to semi-active suspensions.

2.11 OBJECTIVES

- To design and develop the MR damper for four wheeler vehicular application.

- To mathematically model the MR damper based on the experimental characterization of the damper.

- To develop the control strategy for the semi-active suspension system by using MR damper to provide better ride comfort.

- To study the performance of developed MR damper with McPherson suspension system by using the quarter car test rig.

- To implement the MR damper into the front suspension system of the four wheeler vehicle.

2.12 SCOPE OF THE RESEARCH WORK

- Synthesis of in-house prepared MR fluid with different iron particles and the study of rheological properties of the prepared fluid.
- Development of the MR damper suitable for a particular test vehicle and with a spring accumulator.
- Characterization of the developed MR damper by using in-house prepared MR fluid at different current conditions.

- Modeling of the MR damper mathematically by using parametric modeling technique known as Kwok model.
- MR damper performance analysis in the McPherson suspension system in quarter car testing.
- Implementation of MR damper in the front suspension system of the test vehicle and on road testing of the damper at various current conditions including skyhook control.

2.13 METHODOLOGY
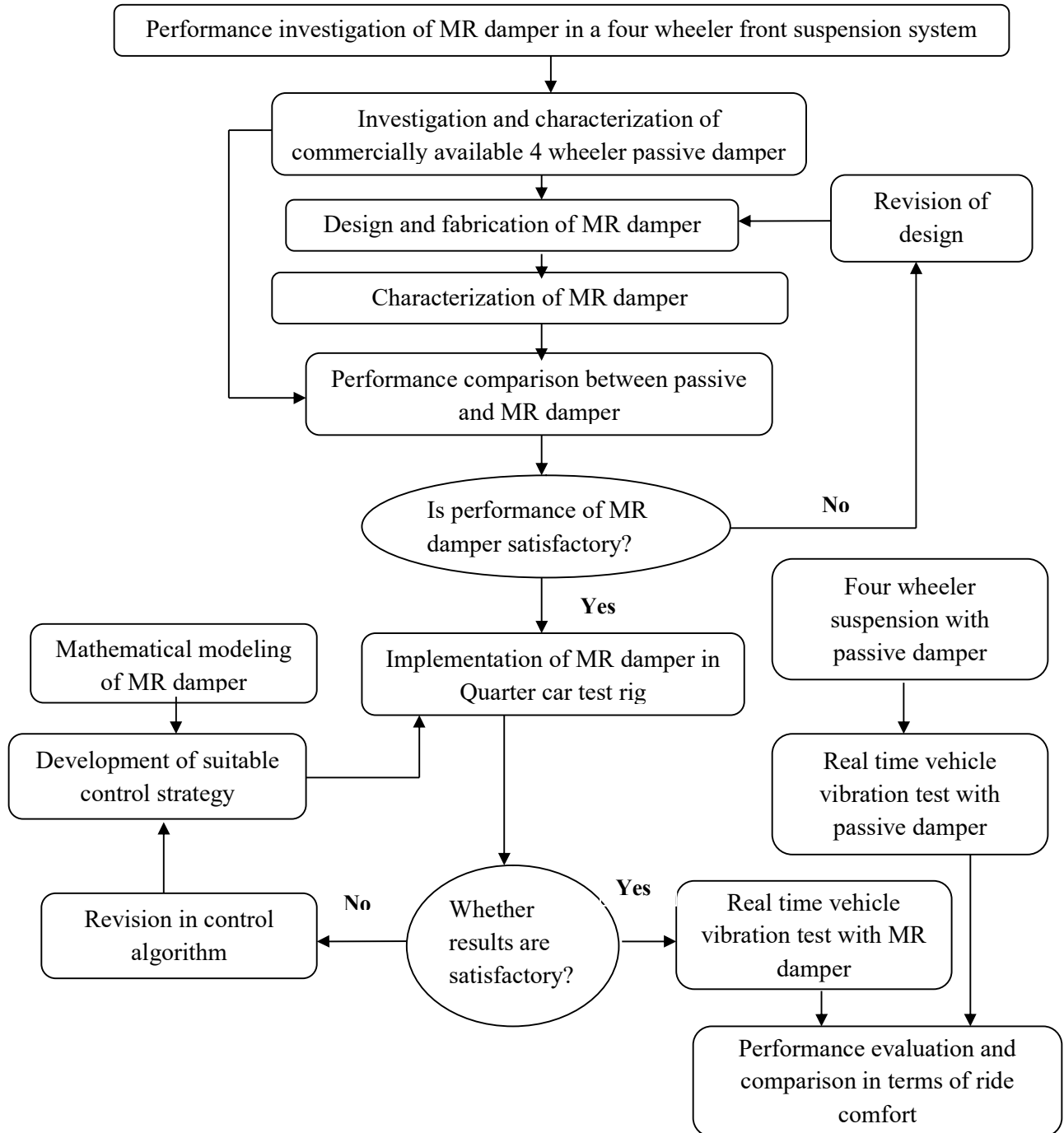
Figure 2.10 Flowchart of the methodology

The current work emphasizes on the design and development of magneto-rheological damper and its implementation in quarter car testing as well as real-time vehicular testing. The methodology followed is illustrated in figure 2.1.

2.13.1 Passive damper characterization

In this study, the passive damper in the suspension of the desired test vehicle has been extracted and characterized to understand the passive damper performance under controlled excitation. This is a crucial primary step in order to understand the damping force limit for the specific vehicle.

2.13.2 Synthesis of MR fluid and its rheological characterization

The magneto-rheological fluid is prepared in-house using definite constituents of iron particles, carrier fluid and the additive. Additive is needed in a very small amount to increase the stability of the fluid. The prepared fluid has undergone rheology testing using the rheometer to understand the fluid properties on varying the magnetic field intensity.

2.13.3 Design and development of MR damper

The magneto-rheological fluid damper is designed on the basis of theoretical expressions considering fluid properties and with reference to the data obtained from passive damper characterization. The piston dimensions are determined by optimization process with suitable constraints. The obtained piston dimensions are undergone magnetic analysis using FEMM software. Finally, the MR damper is developed on the basis of determined dimensions.

2.13.4 Characterization of the MR damper and mathematical modeling

The developed MR damper is characterized by using dynamic testing machine to understand the dynamic behavior of the MR damper under various dynamic excitation conditions and the current input. These hysteresis behaviors are then modeled with the help of parametric modeling technique. The parameters of the model are determined by comparing the experimental and theoretical values.

2.13.5 Quarter car simulation and experiments

The quarter car analysis is one of the simplest and the effect way to understand the suspension nature under the road excitation. The quarter car is modeled by using MATLAB/Simulink and the parametric model of the MR damper is substituted as the damping element in the quarter car model. The quarter car model is excited under different amplitude and frequency conditions. Also, the damper is excited with different constant currents and the skyhook controlled current and the results are compared. The simulation result is validated with quarter car experiment where similar excitation is provided.

2.13.6 Real time on-road testing with MR damper

As an important phase of this research, the passive damper in the suspension of the test vehicle is replaced with the developed MR damper. The on-road testing is carried over a road with bump and the testing is conducted at two different velocities. Also, the damper is excited with different current conditions including controlled current. The results are then compared and the comfort level is quantified based on ISO 2631 standard.

2.14 SUMMARY

This chapter presented various studies on MR fluid synthesis and applications, MR damper with different designs, quarter car simulation and experimental work, vehicle implementation of MR damper, mathematical modeling of the damper and different control logics to MR damper. Observation from the literature and the research gaps are presented based on the literature reviews. Finally, objectives are defined for the current research work and the methodology to complete the objectives is briefed.

CHAPTER 3

DEVELOPMENT OF MAGNETO-RHEOLOGICAL DAMPER (PROTOTYPE-1)

3.1 INTRODUCTION

Majority of vehicles running over the roads use passive dampers in the suspension element. These dampers use hydraulic oil as the damping medium and the grade of the oil depend on the type of vehicle used and some other crucial design points. These dampers perform in a similar manner against repetitive conditions since the oil property remain same and does not change with the condition. This chapter presents characterization of passive damper of a light motor vehicle. This preliminary study is needed to set a benchmark for the next stages. Also, this chapter discusses about the quarter car simulation with passive damper in it.

Before developing an actual scale prototype, an attempt has been made to develop a small stroke MR damper (prototype-1) for better understanding. This chapter also discusses about the design and development of the small stroke MR damper. The MR fluid required for this damper is developed in the laboratory. Later, the characterization results of this damper are also presented. A quarter car simulation work is presented in the next step to analyze the damping effect through MR damper.

3.2 PASSIVE DAMPER OF THE VEHICLE

Several vehicles over the Indian roads use passive dampers as the damping element. The passive damper in the vehicle can be assembled in the strut under different design schemes. They may be McPherson system, single wishbone or double wishbone system etc. The current research utilizes a passive damper of a four wheeler vehicle assembled in a McPherson strut. The passive damper in the McPherson strut is shown in figure 3.1.

The passive damper present in the McPherson strut is dissembled to analyze the damper performance. The passive damper consists of piston-cylinder arrangement

where the movement of piston rod inside the cylinder restricts the motion of the element. The damping of the motion or the vibration depends over the damping medium used inside the cylinder. Generally, hydraulic oils are used in the passive damper for the purpose and different dampers may consist of different grades of oil depending on the application.

Figure 3.1 Suspension scheme in McPherson strut (*Courtesy: Fallah et al. (2009)*)

The passive damper used in this research has the stroke length of 82 mm and has the cylinder diameter of 28 mm. The passive damper is attached with two eyes so as to conduct characterization experiments in the damper testing machine. The damper is connected at the upper and the lower eyes to the damper testing machine through fixtures. The damper testing machine with passive damper attached is shown in the figure 3.3.

Figure 3.2 Passive damper of the test vehicle

3.3 PASSIVE DAMPER CHARACTERIZATION
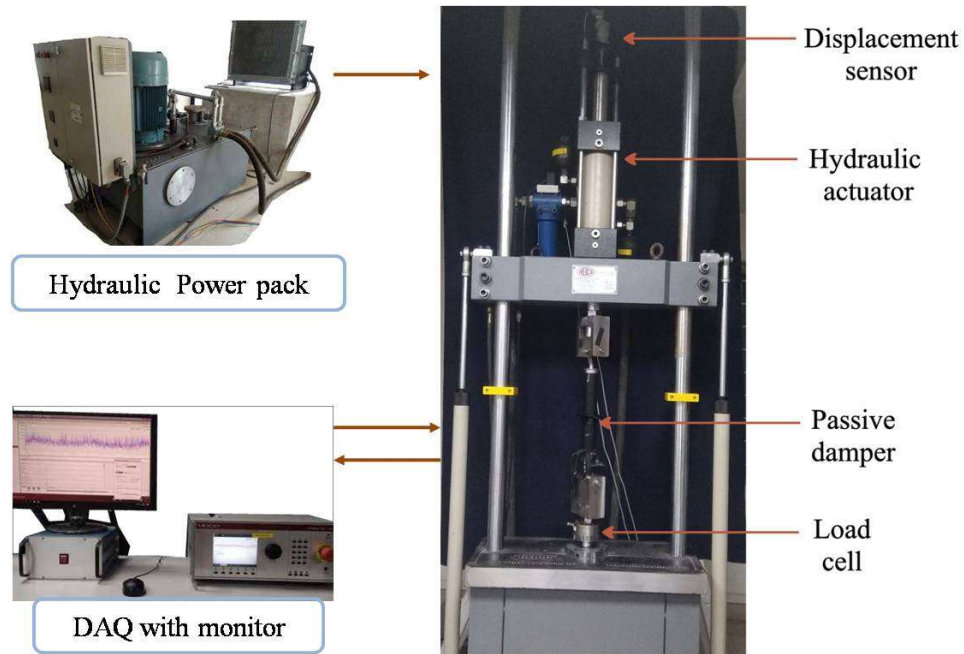
Figure 3.3 Passive damper characterization in damper testing machine

To conduct the characterization testing, the passive damper has been subjected to various dynamic inputs in terms of amplitude and frequency. The dynamic input is given to the machine with the help of controller (make: MOOG Ltd.). The damper testing machine (make: HEICO Ltd.) is aided with linear position transducer as well as load cell for displacement and load measurement, respectively. The controlling as well as data acquisition is done by the same controller. The eye attached to the piston rod is connected to the upper portion or the movable frame of the testing machine. The lower eye is connected to the fixed end of the damper testing machine. The motion to the piston rod is given from the upper end through the hydraulic actuation. The total developed force is measured by the load cell fixed at the lower portion of the damper testing machine.

The characterization tests were performed in the damper testing machine by choosing three distinct frequency and amplitude conditions. The experiments were conducted for frequencies of 0.5, 1 and 1.5 Hz and each with variation in displacement

amplitudes of 10, 15 and 20 mm, respectively. During the testing, the data were collected at the rate of 1000 samples per second.
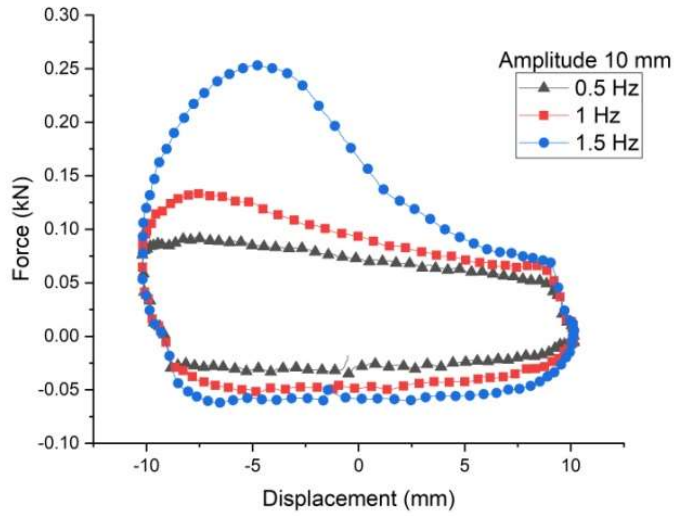
(a)
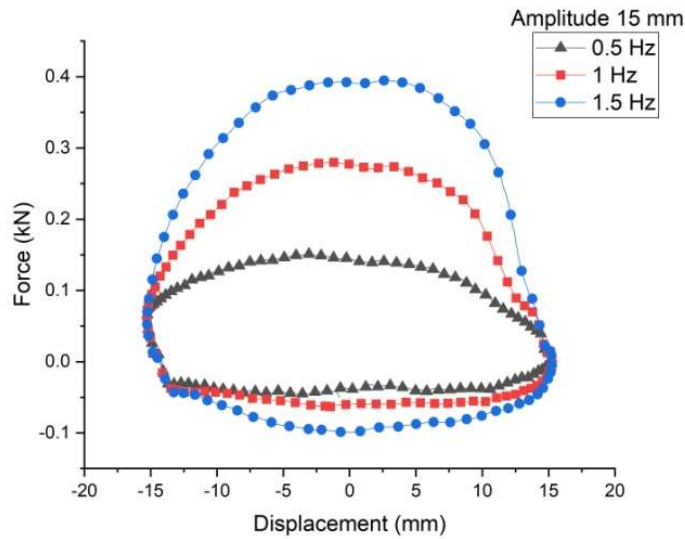
(b)
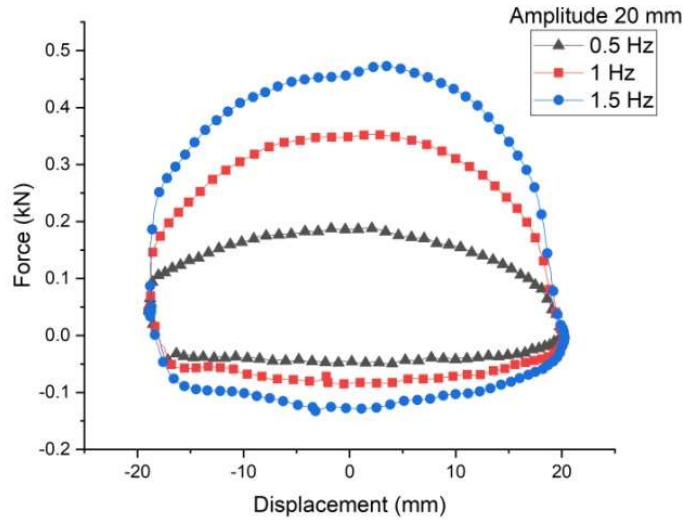
(c)

Figure 3.4 Passive damper characterization results for amplitudes (a) 10 mm (b) 15mm and (c) 20 mm

The characterization tests with combination of each frequency and amplitude provide force–displacement curve. This curve gives the useful information over energy dissipation in every cycle of operation. The area enclosed within the force-displacement curve of a cycle has a direct relation with the total energy dissipated by the damper.

$$E = \pi C \omega A^2 \qquad\qquad (3.1)$$

Where, E = Energy dissipated per cycle (Nm), ω = Frequency of the operation (rad/s), C = Damping coefficient of the damper (Ns/m), A = Amplitude of the cycle (m).

The equation not only helps to estimate the energy dissipation but also to evaluate damping coefficient of the damper in a cycle. The damping coefficient is assumed to be fixed for a cycle since the damping medium is passive in nature.

The damping coefficient corresponding to each operational cycle has been evaluated based on equation 3.1. The energy dissipated in each cycle is nothing but the area enclosed with the force-displacement curve. Table 3.1 provides the damping

coefficient evaluation corresponding to each combination o dynamic testing condition.

Table 3.1 Damping coefficients for different cycles.

Sl No.	Amplitude (mm)	Frequency (Hz)	Damping coefficient (Ns/m)
1	10	0.5	1943.9
2	10	1	1347.9
3	10	1.5	1406.2
4	15	0.5	2079.3
5	15	1	1800.9
6	15	1.5	1747.2
7	20	0.5	1850.3
8	20	1	1718.5
9	20	1.5	1588.8

Evaluation of the damping coefficient of the passive damper is helpful in further analysis stage, where the design of experiment is prepared for a quarter car simulation.

3.4 DESIGN OF EXPERIMENT (DOE)

Currently, design of experiments (DOE) is one of the salient techniques used by several researchers before conducting the actual experiments and this can provide number of experiments to be carried out based on the technique of DOE preferred. The time saving characteristic of the DOE made it popular where the number of input parameters involved is more. In this research, central composite design (CCD) has been used to design the experiments by using Minitab software. The controlling parameters considered are sprung mass (kg), vehicle velocity (m/s), damping coefficient (Ns/m) and the spring stiffness (N/m). To design the experiment, three levels of each parameter have been considered in this work which could able to provide 31 sets of experiments, as per CCD design. The damping coefficient

considered for designing the experiment is considered from Table 3.1, where the highest, lowest and the mean values were adapted for DOE.

The level of parameters considered to design the experiments are provided along with the magnitude of all parameters in Table 3.2.

Table 3.2 Variables for quarter car model and their levels.

	Level 1	Level 2	Level 3
Sprung mass (kg)	280	330	380
Vehicle velocity (m/s)	10	20	30
Damping coefficient (Ns/m)	1348	1718	2079
Spring stiffness (N/m)	24000	28000	32000

The factors and levels mentioned in table 3,2 were used to form design of experiment and central composite design (CCD) was used to design the experiment using MINITAB software which developed 31 sets of experiments. The 31 sets of experiments based of CCD are provided in Table 3.3.

Table 3.3 Design of experiment for quarter car simulation.

Sl No.	Sprung mass (kg)	Vehicle velocity (m/s)	Damping coefficient (Ns/m)	Spring stiffness (N/m)
1	330	20	1718	28000
2	380	30	1348	32000
3	330	20	1718	28000
4	380	20	1718	28000
5	280	20	1718	28000
6	330	20	2079	28000
7	330	20	1718	28000
8	280	30	1348	32000
9	380	10	2079	32000

10	330	20	1718	28000
11	330	20	1718	28000
12	380	10	1348	24000
13	330	10	1718	28000
14	280	30	1348	24000
15	280	30	2079	32000
16	380	30	1348	24000
17	380	30	2079	32000
18	330	20	1348	28000
19	330	20	1718	28000
20	330	20	1718	24000
21	330	20	1718	28000
22	380	10	1348	32000
23	330	20	1718	32000
24	380	30	2079	24000
25	280	10	1348	24000
26	280	10	2079	32000
27	380	10	2079	24000
28	330	30	1718	28000
29	280	10	1348	32000
30	280	30	2079	24000
31	280	10	2079	24000

Among 31 experiments, it can be seen that some testing sets are repetition of certain combination to ensure the repeatability of experimental results. These 31 sets are the input for the quarter car analysis using Matlab/Simulink which is discussed in the later sections.

3.5 QUARTER CAR ANALYSIS WITH PASSIVE SUSPENSION USING SIMULINK

Quarter car model is exclusively used to understand the effect of certain vehicle parameters on the four-wheeler by simply using $1/4^{th}$ of the of the vehicle model. A quarter car model involves sprung and unsprung mass, spring, damper and tire. Quarter car model can be mathematically represented with the help of Newton's second law of motion and are represented by equations 3.2 and 3.3.

$$m_2\ddot{y}_2 + c_2(\dot{y}_2 - \dot{y}_1) + k_2(y_2 - y_1) = 0 \qquad (3.2)$$

$$m_1\ddot{y}_1 - c_2(\dot{y}_2 - \dot{y}_1) - k_2(y_2 - y_1) + c_1(\dot{y}_1 - \dot{R}_d) + k_1(y_1 - R_d) = 0 \qquad (3.3)$$

where, m_1= unsprung mass, m_2= sprung mass, R_d= road displacement, k_1= tire stiffness, k_2= spring stiffness, c_1= tire damping coefficient, c_2= damping coefficient of damper, y_1= unsprung mass displacement, y_2= sprung mass displacement.
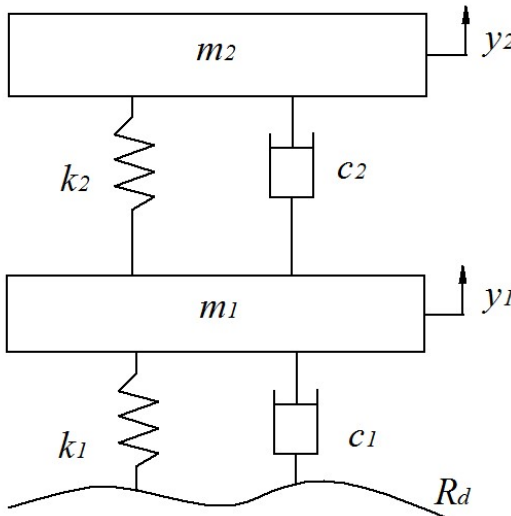
Figure 3.5 Quarter car model with passive damper

In this work, a sine profile has been considered as the road input to be given for quarter car model with amplitude of 6cm and 10m wavelength.

A relation between wavelength (υ), vehicle velocity (v) and angular frequency (ω) can be used to input the vehicle speed in quarter car model and is given in equation 3.4.

$$\omega= 2\pi v/\upsilon \qquad\qquad (3.4)$$

With the help of all the mentioned control parameters, a quarter car model has been constructed using Matlab/Simulink for the simulation and is depicted in figure 3.6.

The parameters such as sprung mass, vehicle velocity, damping coefficient and the spring stiffness are considered from the table of design of experiment for each set of experiment. Other parameters essential for quarter car models are unsprung mass, tire stiffness and tire damping coefficients. These parameters were maintained constant for all the test runs. The values maintained for these parameters were unsprung mass= 55 kg, tire stiffness = 254800 N/m and tire damping coefficient= 12050 Ns/m.
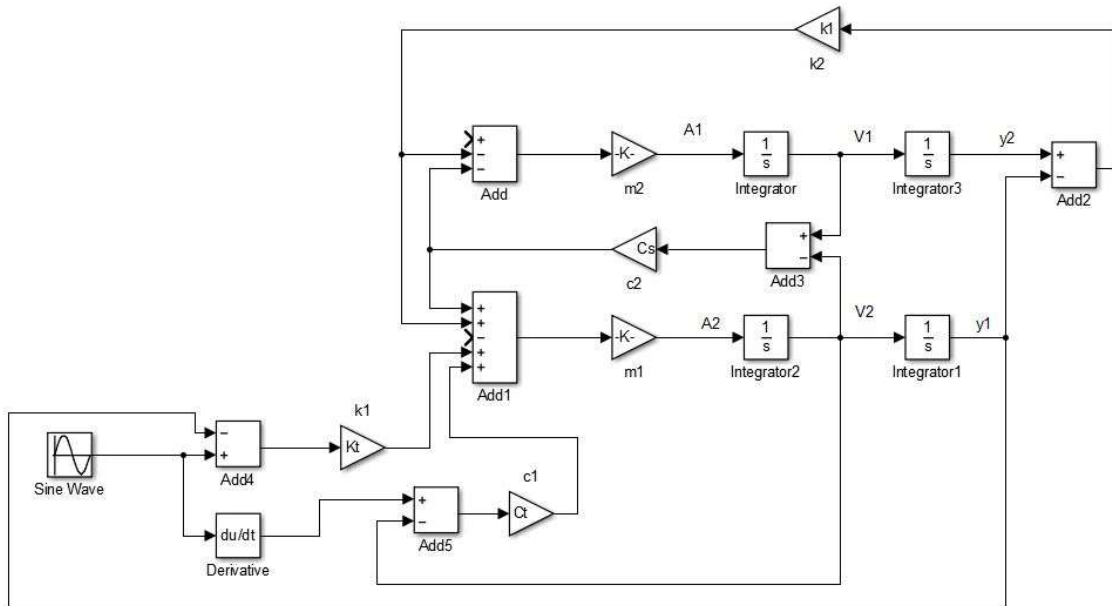
Figure 3.6 Matlab/Simulink model for quarter car simulation using passive suspension

31 experiments were totally carried out using the Quarter car Simulink model as per DOE to evaluate ride quality and road holding in every case. The ride quality can be simply quantified as RMS acceleration of sprung mass. Also, the relative displacement between the unsprung mass and road can be used to quantify road holding (Phalke and Mitra (2017)).

Hence, the ride quality and the road holding were the responses noted against the variables such as sprung mass, vehicle velocity, damping coefficient and the spring

stiffness. The 31 sets of experiments as per DOE table and their responses from quarter car simulations are presented in table 3.4.

Table 3.4 The simulation results based on DOE.

Sl No.	Sprung mass (kg)	Vehicle velocity (m/s)	Damping coefficient (Ns/m)	Spring stiffness (N/m)	Ride quality (m/s^2)	Road holding (m)
1	330	20	1718	28000	6.32	0.007
2	380	30	1348	32000	5.20	0.0047
3	330	20	1718	28000	6.32	0.007
4	380	20	1718	28000	5.29	0.0066
5	280	20	1718	28000	7.72	0.0075
6	330	20	2079	28000	6.37	0.0073
7	330	20	1718	28000	6.32	0.007
8	280	30	1348	32000	7.51	0.0054
9	380	10	2079	32000	3.07	0.0048
10	330	20	1718	28000	6.32	0.007
11	330	20	1718	28000	6.32	0.007
12	380	10	1348	24000	3.91	0.0059
13	330	10	1718	28000	3.07	0.0042
14	280	30	1348	24000	5.98	0.0045
15	280	30	2079	32000	8.45	0.0071
16	380	30	1348	24000	4.22	0.0041
17	380	30	2079	32000	5.98	0.0064
18	330	20	1348	28000	6.36	0.0068
19	330	20	1718	28000	6.32	0.007
20	330	20	1718	24000	5.39	0.006
21	330	20	1718	28000	6.32	0.007
22	380	10	1348	32000	3.37	0.0052
23	330	20	1718	32000	7.41	0.0083

24	380	30	2079	24000	5.21	0.0059
25	280	10	1348	24000	3.08	0.0037
26	280	10	2079	32000	2.61	0.0032
27	380	10	2079	24000	3.20	0.0049
28	330	30	1718	28000	6.00	0.0055
29	280	10	1348	32000	2.75	0.0034
30	280	30	2079	24000	7.24	0.0063
31	280	10	2079	24000	2.75	0.0033

The relationship between the responses (ride quality and road holding) and the input variables is established based on Analysis of variance (ANOVA) and the regression equations.

3.6 ANOVA AND RESPONSE SURFACE OPTIMIZATION

Response surface method (RSM) is an important statistical tool used to understand the relationship between the control variables and responses. Obtaining an optimal surface with the help of designed experiments is a basic idea behind RSM. Analysis of variance (ANOVA) is another useful statistical tool to check the significance of the result by separating the total variance. ANOVA helps in the estimation of interaction between parameters and in identifying the desirable parameter. This also explores the significance and influence of one parameter over the response. One of the important tests in ANOVA is '*p-test*' or probability test. For 95% confidence level, if *p-value* is lesser than or equal to 0.05, then the null hypothesis will be rejected for total population and the parameter is said to significant and if p>0.05, then the parameter is not significant.

Using the response (ride quality and road holding) and the control variables, a relationship between them can be established using regression equations. But before doing so, it's very important to check the significance level of parameters, interaction between them and the desirable parameters. This can be achieved by using analysis of

variance (ANOVA) for both the responses. Table 3.5 and table 3.6 show the results of ANOVA, for both ride quality and road holding respectively.

As mentioned in the earlier section, the individual parameter or interaction of parameters with p value<0.05 are said to be significant. The closeness of the model with the actual values can be identified with the R^2 values. In this work, full quadratic model has shown higher R^2 values when compared to linear or linear+ interaction or square+ interaction model.

Table 3.5 ANOVA for ride quality.

Source	df	Adj SS	Adj MS	f-value	p-value
Model	14	83.4916	5.9637	37.55	0.000
Linear	4	49.64	12.41	78.14	0.000
Vel	1	43.55	43.55	274.21	0.000
Mass	1	4.15	4.15	26.11	0.000
Stiff	1	1.59	1.59	10.06	0.006
Damp	1	0.35	0.34	2.18	0.159
Square	4	22.36	5.59	35.20	0.000
Vel×Vel	1	8.72	8.72	54.90	0.000
Mass×Mass	1	0.05	0.05	0.30	0.592
Stiff×Stiff	1	0.0019	0.0019	0.01	0.913
Damp×Damp	1	0.0001	0.0001	0.00	0.979
2-way interactions	6	11.43	1.90	11.99	0.000
Vel×Mass	1	7.45	7.45	46.91	0.000
Vel×Stiff	1	1.98	1.98	12.48	0.003
Vel×Damp	1	1.85	1.85	11.64	0.004
Mass×Stiff	1	0.09	0.08	0.56	0.465
Mass×Damp	1	0.06	0.05	0.37	0.550
Stiff×Damp	1	0.0007	0.0007	0.00	0.948

The R^2 value observed for full quadratic value was 97.05%. Adjusted R^2 (R^2 adj.) was observed as 94.46% and predicted R^2 (R^2 pred.) was observed to be 86.83%. Based on this a regression equation for ride quality was developed and is given in equation 3.5.

Table 3.6 ANOVA for road holding.

Source	df	Adj SS	Adj MS	f-value	p-value
Model	14	0.000056	0.000004	20.54	0.000
Linear	4	0.000011	0.000003	13.46	0.000
Vel	1	0.000007	0.000007	36.15	0.000
Mass	1	0.000001	0.000001	4.77	0.044
Stiff	1	0.000001	0.000001	4.31	0.054
Damp	1	0.000002	0.000002	8.59	0.010
Square	4	0.000034	0.000008	43.34	0.000
Vel×Vel	1	0.000013	0.000013	64.08	0.000
Mass×Mass	1	0.000000	0.000000	0.00	0.996
Stiff×Stiff	1	0.000000	0.000000	0.14	0.717
Damp×Damp	1	0.000000	0.000000	0.00	0.985
2-way interactions	6	0.000012	0.000002	9.97	0.000
Vel×Mass	1	0.000006	0.000006	28.21	0.000
Vel×Stiff	1	0.000001	0.000001	5.11	0.038
Vel×Damp	1	0.000005	0.000005	25.87	0.000
Mass×Stiff	1	0.000000	0.000000	0.32	0.580
Mass×Damp	1	0.000000	0.000000	0.21	0.651
Stiff×Damp	1	0.000000	0.000000	0.12	0.729

RQ= -2.6 + 0.933* Vel – 0.0018* Mass – 0.000082* Stiff – 0.00034*Damp – 0.01833*Vel*Vel + 0.000054*Mass*Mass – 0.001365*Vel*Mass + 0.000009*Vel*Stiff + 0.000093*Vel*Damp – 0.000003*Mass*Damp   (3.5)

Where, RQ= Ride quality, Vel= velocity, Mass= sprung mass, Stiff= spring stiffness and Damp= damping coefficient.

In the similar manner, ANOVA was performed over road holding also, the results of which are given in table 3.6 which provided the significance parameters and terms over road holding model.

When checked for effectiveness of the model, the R^2 for the road holding was found to be 94.73%. Similarly, adjusted R^2 was found to be 90.12% and prediction R^2 was 76.7%. Based on this, similar to ride quality model, a full quadratic regression model was developed for road holding also. This is given in equation 3.6, where RH is road holding.

RH= -0.0045 + 0.000891*Vel + 0.000041*Mass – 0.000002*Damp –
0.000022*Vel*Vel – 0.000001*Vel*Mass + 0.000000* Stiff*Damp (3.6)
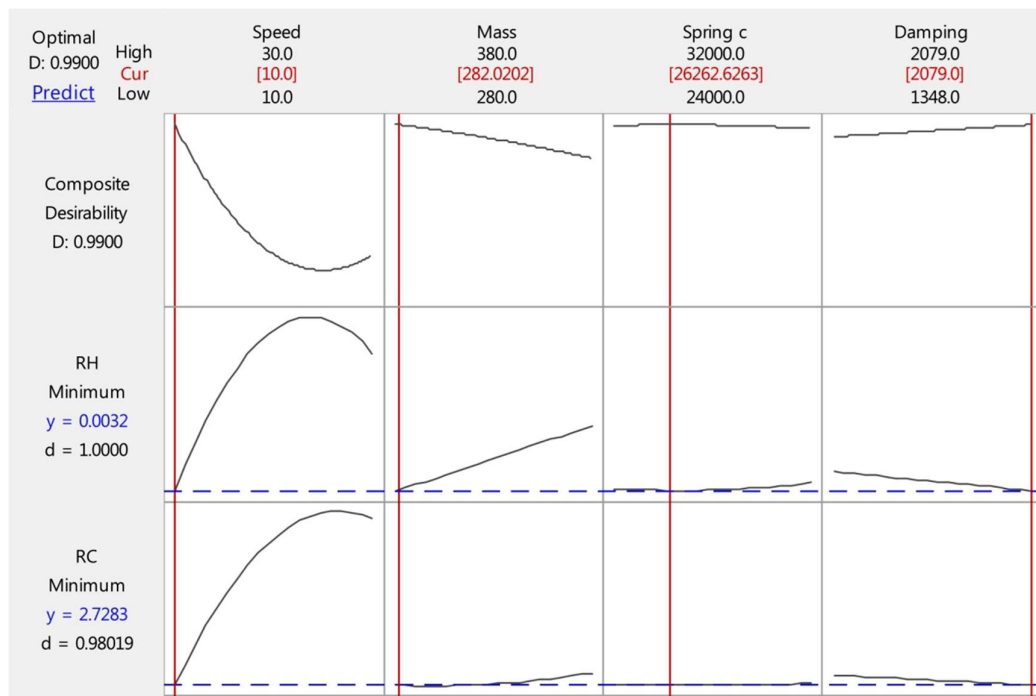
Figure 3.7 Result of RSM optimization

It is a general assumption that the model can be said to be valid if the adjusted R^2 value is closer to R^2 of the model and this is true in this case also both in terms of ride

quality and road holding. Hence, these models can be considered to establish relationship between the responses (ride quality and road holding) and the control variables in an effective way.

To optimize the response, it is necessary to set the boundaries with upper and lower limits of control variables. The goal for response can be set in terms of 'Response maximization' or 'target the response' or 'response minimization'. Based on the problem definition and requirements the goals can be set for single response or multiple responses. In this problem, it is desired to minimize the magnitudes of ride quality and road holding, by optimizing the control variables. A multiobjective optimization approach is required in this case to minimize the quantity of ride quality and road holding together.

As explained by Els et al. (2007), certain parameters seek opposite nature of settings when considered ride quality and road holding. Hence it is very difficult to design the suspension variables so that both ride quality and road holding meet the passenger satisfaction. Therefore, an attempt has been made in this work to optimize the quarter car suspension parameters, for better ride quality and road holding simultaneously. This is nothing but a multiobjective approach. This was achieved through response surface optimization. The intension of the optimization was to minimize the magnitude of ride quality and road holding. The response optimization plot is shown in figure 3.7.

Table 3.7 Results of optimization.

Optimum conditions				Response output	
Sprung mass	Velocity	Damping constant	Spring stiffness	Ride quality	Road holding
282.0202	10	2079	26262.62	2.73	0.0032

The response optimization plot provided the optimal condition for all the four control variables for 'compromised' minimum conditions of ride quality and road holding. It can be observed that the desirability value achieved was 1 for road holding and it was

close to unity in case of ride quality. The optimum conditions indicated, and the corresponding response values are tabulated in table 3.7.

The optimum conditions indicate that, combined minimization of ride quality and road holding preferably require minimum vehicle velocity and maximum damping coefficient value. The other parameters such as sprung mass and spring stiffness were intermediate values of provided input magnitude.

Table 3.8 Result of validation simulation.

	RSM optimization	Validation test	% error
Ride Quality	2.7283	2.7280	0.01
Road Holding	0.0032	0.0033	3.03

To check the validity of the result, the optimum values were substituted back in the quarter car Simulink model. The result of this simulation and the deviation of this result with the result of response optimization is given in table 3.8 in terms of percentage error.

The results in the table 3.8 indicate that the regression model for both ride quality and road holding obtained using response surface method efficiently served the purpose. The percentage error between the predicted and validation through simulation is well within the acceptable limit. Even though RSM is one of the oldest statistical methods and considering the fact that the study is involving multi objective optimization, the method was able to model the conditions well.

3.7 DEVELOPMENT OF MR DAMPER (PROTOTYPE-1)

The non-linear behavior of MR fluid in a damper with variation in current helps to attain a semi-active nature. Hence, the design of MR piston is a challenging task which requires a multi-dimensional thought process. Before developing an MR damper for vehicular application, a prototype of MR damper has been developed whose discussions are provided in following sections.

3.7.1 Geometric Design of MR damper (Prototype-1)

The design of MR damper is basically dependent of the dynamic range which can be stated as the ratio of 'controllable force' (C.F.) to 'uncontrollable force' (U.F.). The entire damping force of an MR damper is depending on three forces; force due to viscosity (F_η), force due to field induced shear (F_τ) and friction force (F_f). Hence, the dynamic range (DR) can be defined as (Xu et al. (2013)),

$$DR = \frac{C.F}{U.F} = \frac{F_\tau}{F_\eta + F_f} \tag{3.7}$$

In this present work, the design of MR damper has been made on the basis of dynamic range and maximum damping force expected (Xu et al. (2013)). According to Bingham model, the plastic viscous force (F_η) and field induced shear force (F_τ) can be written as,

$$F_\eta = \left(1 + \frac{whV}{2Q}\right)\frac{12\eta QLA_P}{wh^3} \tag{3.8}$$

$$F_\tau = \left(2.07 + \frac{12Q\eta}{12Q\eta + 0.4wh^2\tau_y}\right)\frac{\tau_y pA_p}{h} sgn(V) \tag{3.9}$$

where, Q is the volumetric flow rate, A_p is the effective cross section of piston ($A_p = \pi(d_p^2 - d^2)/4$), d is the diameter of piston rod, V is the relative velocity between cylinder and piston, p is the pole length, L is the total length of axial pole ($L = m+p$), w is the average circumference of annular flow path ($w = \pi(d_p+g)$), d_p is the diameter of piston head, η is the apparent viscosity of MR fluid without magnetic field, τ_y is the yield shear strength of fluid and g is gap of annular flow path.

The geometric nomenclature is as shown in figure 3.8.
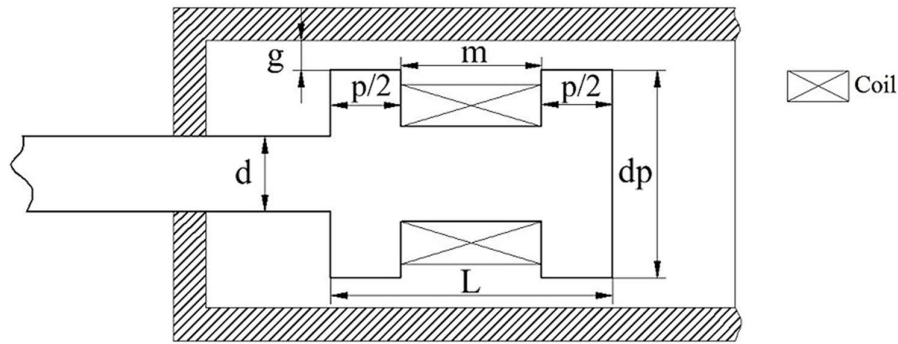
Figure 3.8 Geometric nomenclature of MR damper piston

For a damper to be designed, it is always necessary to keep both dynamic range and the damping force as high as possible or for an expected level. Hence, to find the essential dimensions of the piston, the problem boundary is considered as optimization problem

The optimization of the dimensions is subjected to achieving maximum damping force of 2 kN with a dynamic range of at least 3 and with an operating velocity of 0.2 ms^{-1}. The design variables considered were piston head diameter (d_p), piston rod diameter (d), pole length (p), total length of axial pole (L) and height of annular flow path (g). These design variables were to be optimized with above mentioned conditions. Along with this, for achieving better design, the fluid property of commercially available MR fluid 132 DG (from Lord Corporation), has been considering during design phase.

Table 3.9 Optimized dimensions of MR damper piston

Sl. No.	Design variable	Optimized dimension (mm)
1	Piston head diameter (d_p)	24.92 ≒ 25
2	Piston rod diameter (d)	10
3	Pole length (p)	4
4	Total length of axial pole (L)	29.91 ≒ 30
5	Height of annular flow path (g)	0.69 ≒ 0.7

Achievement of dynamic range was considered as objective function along with maximum damping force as constraint. The MATLAB fmincon function was used to reach the objective, with proper adjustment of design parameters (in this case, dimensions of piston). Optimized dimensions of the MR damper piston geometry is provided in table 3.9.
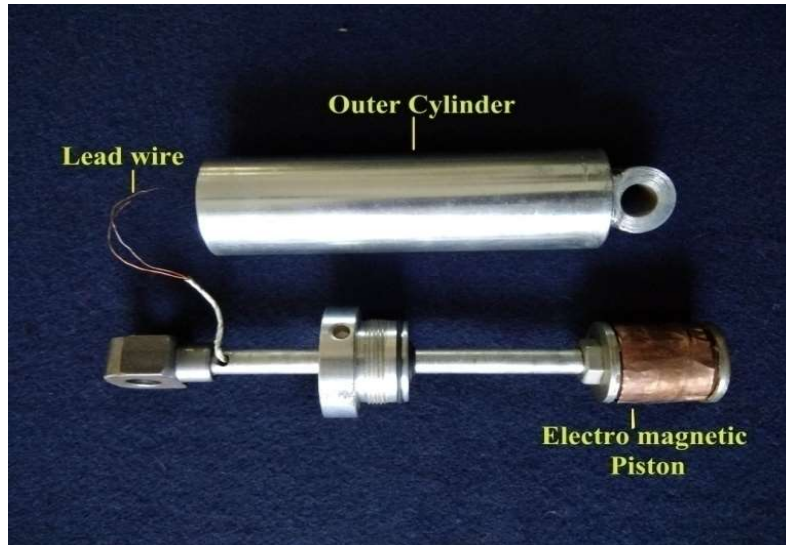
Figure 3.9 Fabricated MR damper (prototype-1)

The designed MR damper has been fabricated and is shown in figure 3.9. The outer cylinder of the MR damper and the piston were fabricated using AISI 1018 steel which is having good magnetic permeability.

3.8 EXPERIMENTAL SETUP
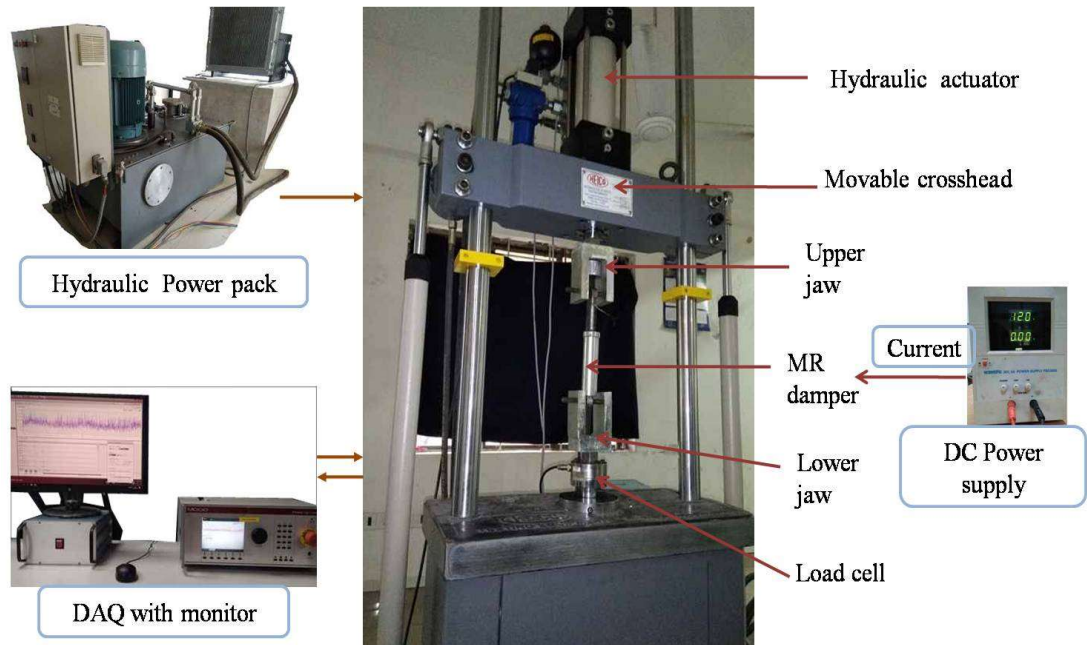
Figure 3.10 MR Damper (prototype-1) characterization

The damper characterization has been performed to understand the dynamic nature of MR damper in terms of force versus displacement data. The characterization tests were carried out in the dynamic testing machine (figure 3.10).

3.9 CHARACTERIZATION OF MR DAMPER (PROTOTYPE-1)

The dynamic performance of the designed MR damper is primarily understood with the force-displacement data obtained using characterization in damper testing machine. In this work, characterization of MR damper has been performed for different frequencies, amplitudes and currents supplied. The characterization has also been performed with no supply of current, as well. These conditions are listed in table 3.10. The MR fluid for this experimentation purpose was prepared in the laboratory, with 70% weight fraction of electrolytic iron powder and remaining weight fraction of paraffin oil as base fluid. To avoid quick sedimentation of iron particles, a little amount of oleic acid was added as additive.

Table 3.10 Conditions in damper characterization experiment

Sl. No.	Frequency of operation (Hz)	Amplitudes (mm)	Supplied Current (A)
1	1.5	5	0.25
2	2	10	0.75
3	2.5	15	1.25

3.10 RESULTS OF CHARACTERIZATION

This section describes the force-displacement behaviour of MR damper when subjected to different amplitudes, frequencies and currents as detailed in table 3.10. It is necessary to observe the differentiation of force behaviour with change in current supplied.
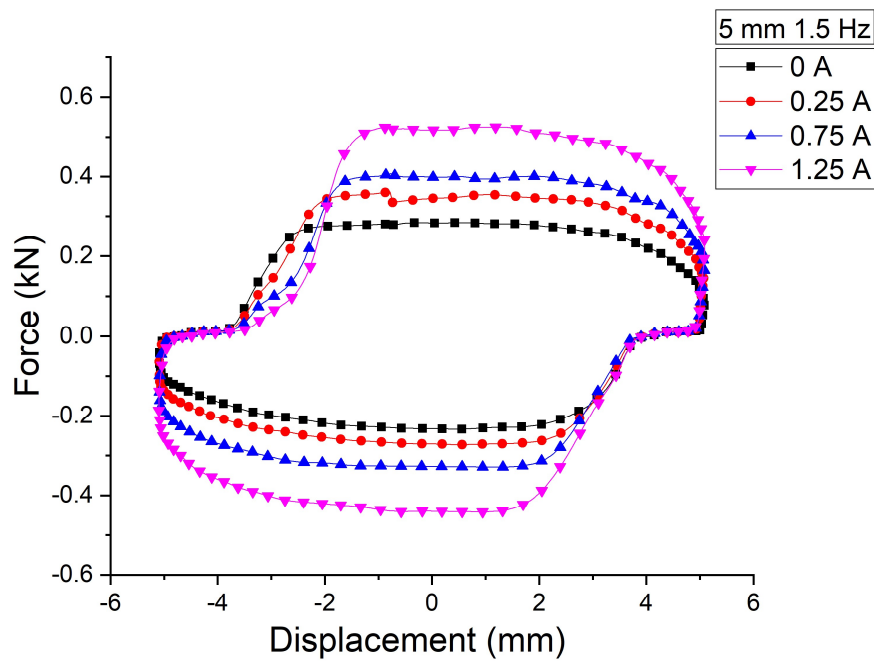
(a)
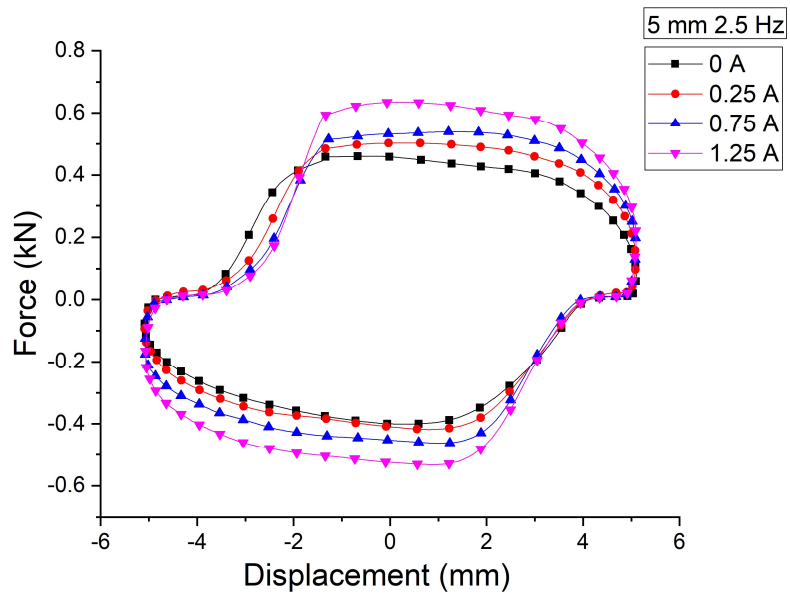
(b)
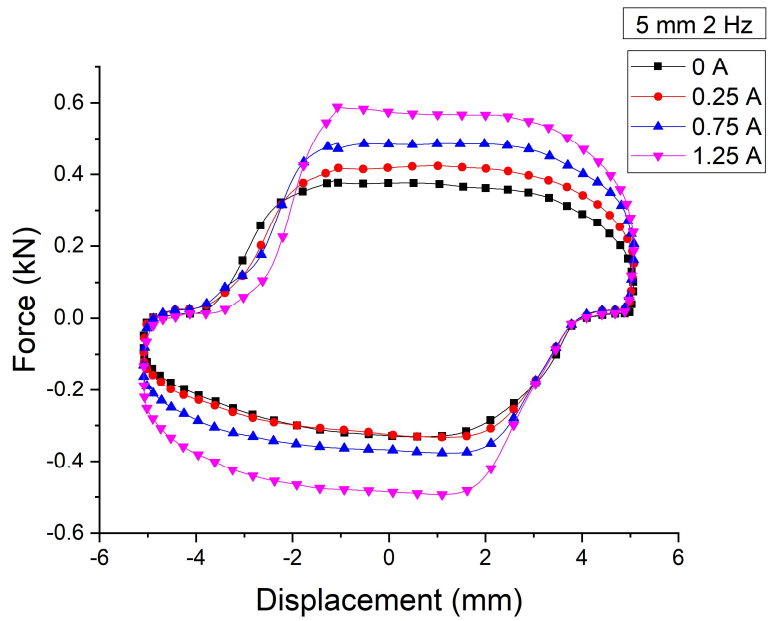
(c)

Figure 3.11 Force- displacement curves with variation in current, for 5mm and (a) 1.5 Hz, (b) 2 Hz and (c) 2.5 Hz

Figure 3.11 describes the distinction in damping force achieved with variation in current for 5 mm amplitude test condition. From the figure, a clear distinguished behavior in force enhancement has been observed when tested without and with supply of current. With variation of current supplied, a significant amount of increase in damping force has been noted for the designed MR damper. Similar, nature of damping force has been observed for 10 mm and 15 mm amplitude test conditions. The maximum force achieved in each test condition has been listed in table 3.11, where 'f' represents frequency of operation (Hz), 'A' represents displacement amplitude (mm), 'I' for current (A) and max force in kN.

A maximum damping force of 1.254 kN has been achieved form the designed damper at 15mm amplitude, 2.5 Hz and 1.25A current supplied. Hence, it is evident from the characteristic curves that there is a direct correlation between damping coefficients and the current supplied to MR damper.

Table 3.11 Maximum force for different displacement amplitudes, frequencies and currents

f	A	I	Max Force	f	A	I	Max Force	f	A	I	Max Force
1.5	5	0	0.28	1.5	10	0	0.51	1.5	15	0	0.87
1.5	5	0.25	0.36	1.5	10	0.25	0.53	1.5	15	0.25	0.90
1.5	5	0.75	0.41	1.5	10	0.75	0.61	1.5	15	0.75	0.95
1.5	5	1.25	0.52	1.5	10	1.25	0.66	1.5	15	1.25	0.96
2	5	0	0.39	2	10	0	0.63	2	15	0	1.04
2	5	0.25	0.42	2	10	0.25	0.63	2	15	0.25	1.09
2	5	0.75	0.49	2	10	0.75	0.75	2	15	0.75	1.11
2	5	1.25	0.59	2	10	1.25	0.81	2	15	1.25	1.13
2.5	5	0	0.46	2.5	10	0	0.74	2.5	15	0	1.17
2.5	5	0.25	0.5	2.5	10	0.25	0.74	2.5	15	0.25	1.23
2.5	5	0.75	0.54	2.5	10	0.75	0.86	2.5	15	0.75	1.24
2.5	5	1.25	0.64	2.5	10	1.25	0.91	2.5	15	1.25	1.25

But for each set of amplitude and frequency, the characteristic equation may be different. Hence, for each case of frequency and amplitude, damping coefficient has been found out based on relation between damping force and velocity.

The relation between damping coefficient and current supplied to MR damper has been plotted in figure 3.12 for each case of amplitude. After knowing the damping coefficient value for each case, it is easy to find the correlation between damping coefficient and current supplied. This is done by using curve fitting method for each characteristic curve.

The table 3.12 provides the curve fitting equations for each set of combination of frequency and amplitude, which relates damping coefficients (C) with current supplied (I).
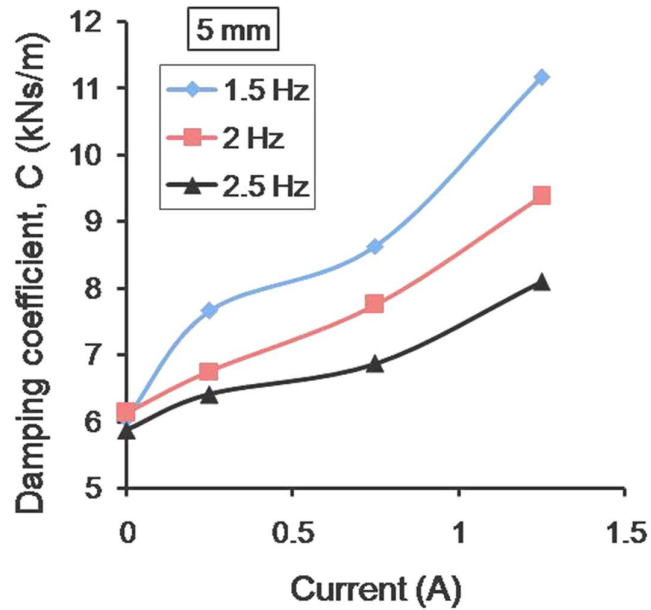
(a)
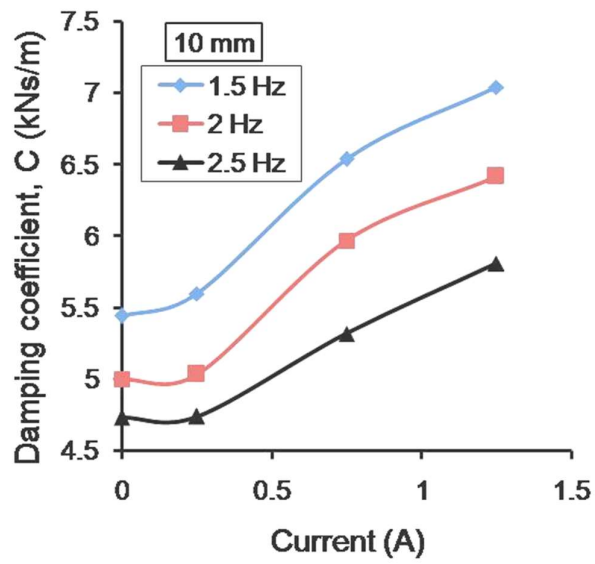
(b)
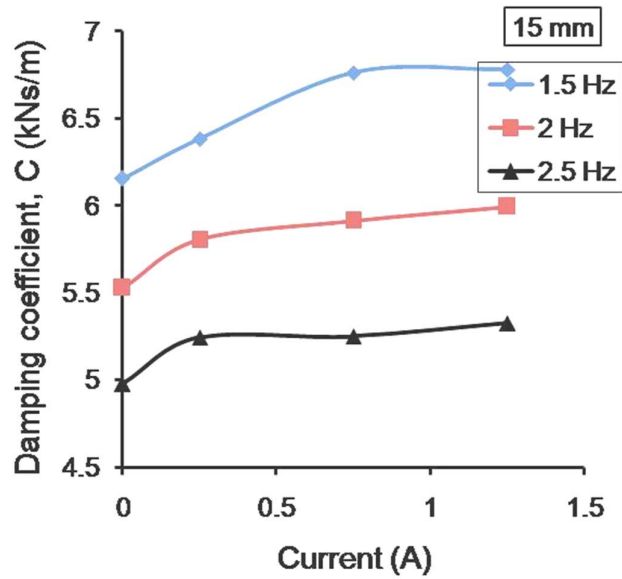
(c)

Figure 3.12 Variation of damping coefficient with variation in current, for (a) 5mm,
(b) 10mm and (c) 15mm

82

These correlations have been found out with an intension to find the MR damper performance when applied in quarter car simulation.

Table 3.12 Equations relating damping coefficients and currents

Frequency (Hz)	Amplitudes (mm)	Correlation equation in terms of current
1.5	5	$C = 7.396I^3 - 13.51I^2 + 9.434I + 6.033$
2	5	$C = 1.512I^3 - 2.159I^2 + 2.933I + 6.129$
2.5	5	$C = 2.519I^3 - 4.150I^2 + 3.030I + 5.866$
1.5	10	$C = -2.044I^3 + 3.717I^2 - 0.174I + 5.440$
2	10	$C = -2.613I^3 + 4.916I^2 - 0.931I + 5.001$
2.5	10	$C = -1.354I^3 + 2.871I^2 - 0.614I + 4.734$
1.5	15	$C = -0.429I^3 + 0.242I^2 + 0.866I + 6.156$
2	15	$C = 0.888I^3 - 2.056I^2 + 1.554I + 5.528$
2.5	15	$C = 1.236I^3 - 2.643I^2 + 1.651I + 4.976$

3.11 QUARTER CAR SIMULATION
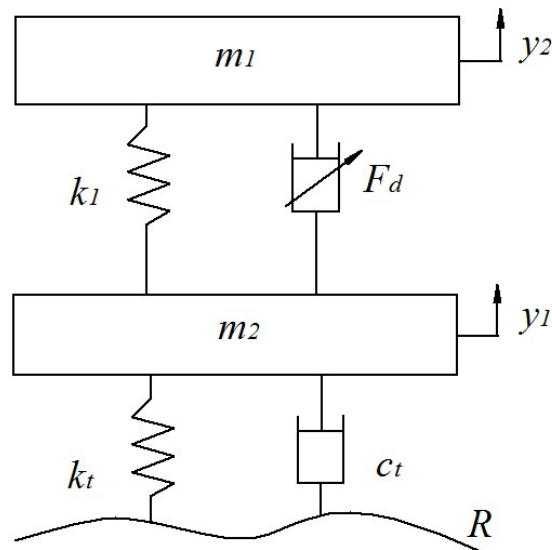
Figure 3.13 Quarter car with MR damper

The equation of motion for the quarter car by considering tire stiffness and tire damping too, can be written in accordance with Newton's second law of motion and can be mathematically represented as,

$$m_1 \ddot{x}_1 + k_1(x_1 - x_2) + F_d = 0 \tag{3.10}$$

$$m_2 \ddot{x}_2 + c_t(\dot{x}_2 - \dot{R}) + k_t(x_2 - R) - k_1(x_1 - x_2) - F_d = 0 \tag{3.11}$$

The parameters chosen for quarter car simulation have been listed in table 3.13.

Table 3.13 Quarter car parameters (Gurubasavaraju (2017))

Parameters	Values of parameters
Sprung mass, m_1 (kg)	450
Unsprung mass, m_2 (kg)	50
Spring stiffness of suspension, k_1 (N/m)	49000
Tire stiffness, k_t (N/m)	250000
Tire damping coefficient, c_t (Ns/m)	1500

Using the correlation equations as listed in table 3.12, the damping in the suspension has been varied in the MATLAB/Simulink model for each case of dynamic condition. For the simulation purpose, the quarter car has been run over a sinusoidal wave profile (as road) which has 10 cm amplitude and 12 m wavelength. The quarter car has been moved with the velocity of 20 m/s. The variation in root-mean-square (RMS) acceleration of the sprung mass (in m/s^2) with variation in current for each dynamic condition has been plotted in figure 3.14. The correlation between the damping coefficient and the current has been used in the analytical study to represent the variable damping of the MR damper, which is provided in table 3.12.

(a)

(b)

85
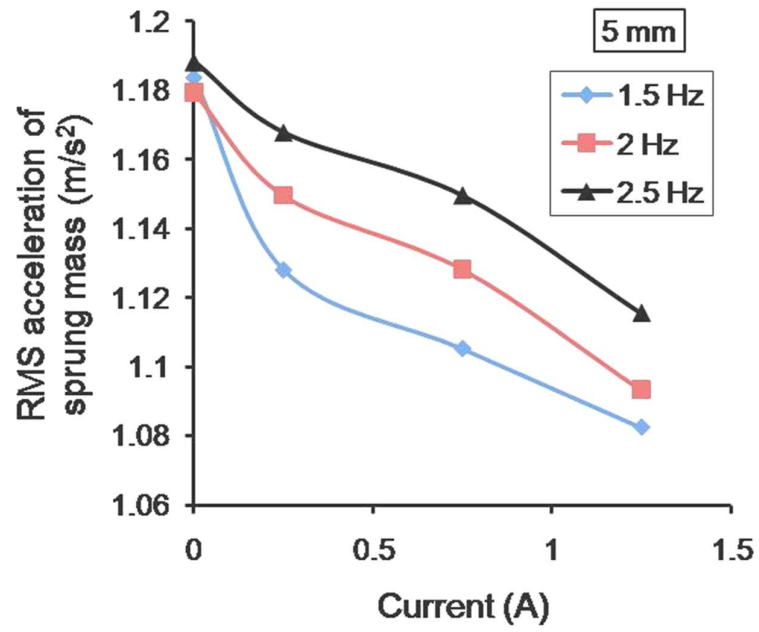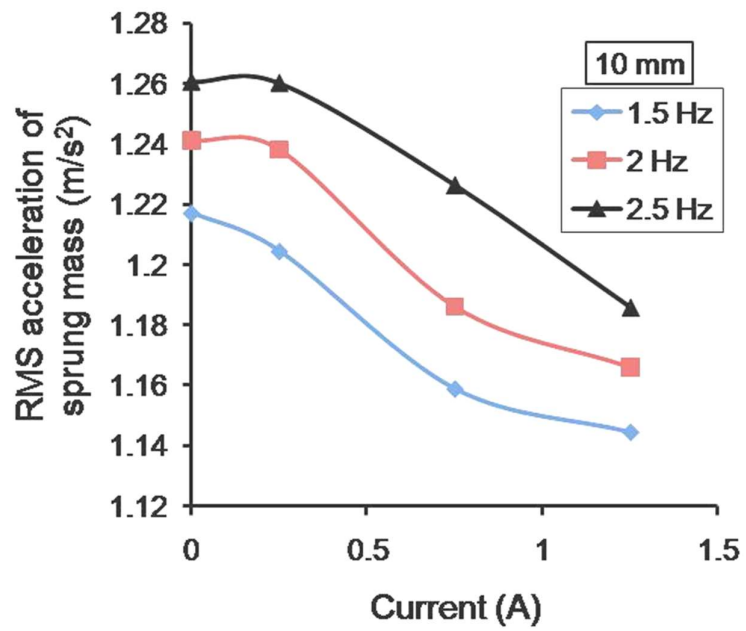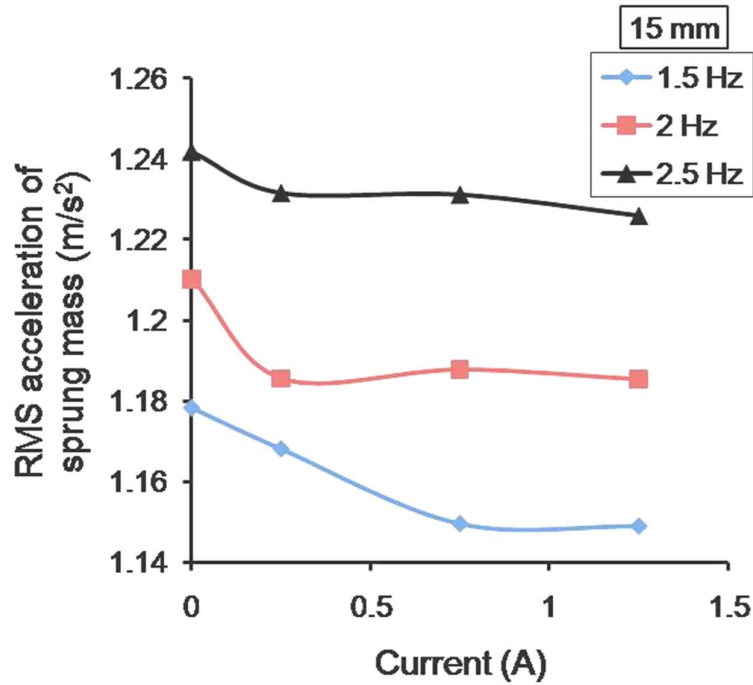
(c)

Figure 3.14 RMS acceleration variation with variation in current, for (a) 5mm, (b) 10mm and (c) 15mm.

It is evident from the plots shown in figure 3.14 that, there is a decrement nature in RMS acceleration of sprung mass with hike in the current provision to the MR damper. Reduction in amplitude of RMS acceleration of sprung mass always provides a comfort feeling to the passenger. Therefore, the semi-active MR damper is always helpful to provide better suspension feeling when compared to the normal passive damper.

3.12 SUMMARY

As a prior work to the development of the MR damper, a passive damper of the suspension of the test vehicle was extracted to know its dynamic behavior. The characterization experiments were conducted at definite frequencies of 0.5, 1 and 1.5 Hz and for amplitude conditions of 10, 15 and 20 mm. The force versus displacement nature of the passive damper showed that maximum damping force of 470 N

(rebound) was seen for 20 mm amplitude and 1.5 Hz condition. Also, it is observed that the compression and the rebound forces are not symmetrical. The energy dissipated under each condition was used to calculate the damping coefficient under every excitation. Maximum damping coefficient of 2079.29 Ns/m was observed during the testing.

A design of experiment (DOE) was formed by considering sprung mass, vehicle velocity, damping coefficient and the spring stiffness as variables under three different levels. The damping coefficient was used from the passive damper characterization result. The central composite design (CCD) produced total 31 experiments with these variables and levels. The design of experiment was aiming to analyze the ride quality and the road holding at different conditions. Lower the magnitude better is the ride quality. Based on the DOE variables and the responses, analysis of variance (ANOVA) was conducted with the help of full quadratic model. The full quadratic model has shown better R^2 values when compared to linear, linear+interaction and square+interaction models. Also, regression models were obtained for ride quality and the road holding using the full quadratic model. The regression equations were then used in response surface optimization to find the optimal condition for ride quality and the road holding. Least magnitudes of 2.72 m/s^2 and 0.0032 m were obtained for ride quality and road holding respectively. The optimal parameters were then back substituted in the quarter car model to check the validation of the results. The errors were found to be 0.01% for ride quality and 3.03% for road holding.

An MR damper (Prototype-1) was aimed to develop before heading to the full scale MR damper. The MR damper (Prototype-1) was designed based on viscous force and shear force according to the Bingham model. The designed MR damper was then developed by using AISI 1018 steel owing to its good permeable nature. The MR damper was then characterized in the damper testing machine using in-house prepared MR fluid. The MR fluid was synthesized by using electrolytic iron powder (EIP) and paraffin oil. The MR fluid contained 70% weight fraction of EIP and remaining contribution was from paraffin oil and oleic acid as additive. Characterization of the MR damper was performed under 1.5, 2 and 2.5 Hz operational frequencies and at

amplitude levels of 5, 10 and 15 mm. The current inputs to the MR damper were namely 0.25, 0.75 and 1.25 A. The characterization was results showed a maximum damping force of 1.2 kN force at 15mm amplitude, 2.5 Hz and 1.25A condition. At higher velocity conditions, the difference between elevated currents was observed less. Also, shift in the force versus displacement plots revealed the lack of accumulator in the damper.

Similar to the passive damper, the damping coefficient for each condition was determined based on energy dissipation relationship. The damping coefficient for each amplitude condition was expressed in terms of current input to establish a correlation between them. A quarter car model was built in MATLAB/Simulink and the damping coefficient in terms of current was used in place of damping element in the quarter car model. The RMS acceleration plots revealed a drastic reduction in the magnitude with increase in the current input when compared to off-state condition.

CHAPTER 4

DESIGN AND DEVELOPMENT OF MR DAMPER FOR VEHICLE

4.1 INTRODUCTION

This chapter aims to develop a methodology to design a semi-active damper for a commercial four wheeler vehicle. The cost-effectiveness of the proposed semi-active suspension system is observed in developing an in-house MR fluid, modifying an already existing passive damper into a semi-active one. The methodology used in this paper is discussed next. A shear mode mono-tube damper suitable with magneto-rheological fluid is designed and developed with dimensions necessary to fit in the vehicle. The MR damper is provided with a spring accumulator. This MR damper is characterized in damper testing machine subjected to different frequencies, amplitudes and current supply.

Non-linearity of magneto-rheological fluid damper is one of the challenging task to represent analytically. Several parametric as well as non-parametric models have been discussed in the literature to illustrate the hysteresis of MR damper. This chapter discusses about one such non-linear mathematical theory known as Kwok modeling technique. The characterization results have been utilized for the modeling purpose. This chapter illustrates the implementation of Kwok theory to the characterized damper, parameter identification and its closeness to the experimental results.

4.2 SYNTHESIS OF MAGNETO-RHEOLOGICAL (MR) FLUID (MRF-1)

A class of smart materials, magneto-rheological fluid is the calculative mixture of ferrous particles, carrier fluid or base oil and additive. Different kinds of ferrous particles had been investigated by various researchers in the preparation of MR fluid to study their properties (Acharya et al. (2017)). In this work, electrolytic iron powder (EIP) is used as ferrous content of the fluid. The EIP used is having particle size less

than 10 μm. The scanning electron microscopy (SEM) in figure 4.1(a) shows the particle shape and size of EIP.

Electrolytic iron powder has flake shaped particles. The size distribution of particles is determined by means of Cilas 1064 Particle Size Analyser which revealed that mean particle size of the EIP was about 7.02 microns (figure 4.1(b)).

The electrolytic iron powder is mixed in paraffin oil (from Merck) which is the base fluid used in this study (kinematic viscosity 30 cS at 37ºC). Apart from ferrous particles and base fluid, additives are added to avoid sedimentation, coagulation and for better re-dispersion. In the current work, oleic acid is used for sedimentation stability and as antifriction additive.

Initially, base fluid and the additives are stirred constantly for about 6 hours ensuring the uniformity of mixture. Ferrous particle (EIP) are then added to this mixture and stirred for about 12 hours to synthesize the MR fluid. The prepared MR fluid has 65% volume fraction of EIP in 33% volume fraction of paraffin oil with 2% additive.
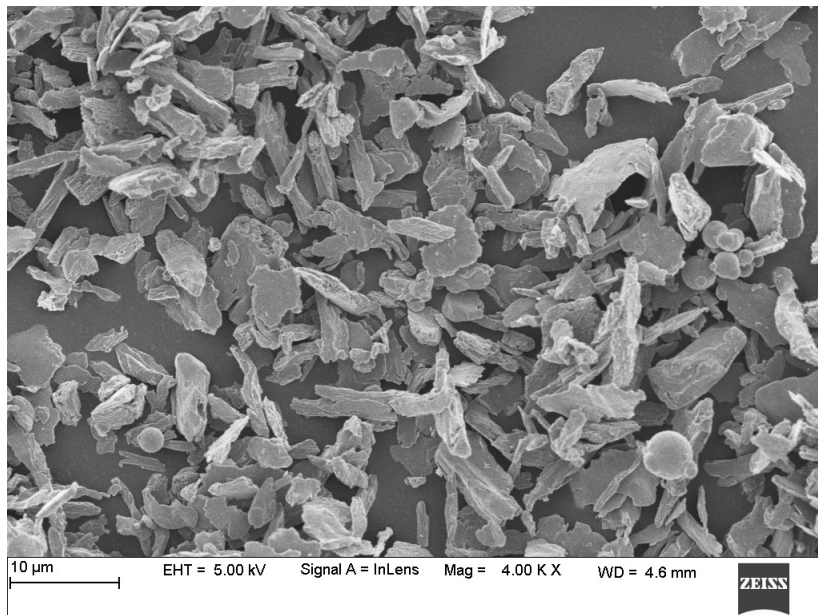
(a)
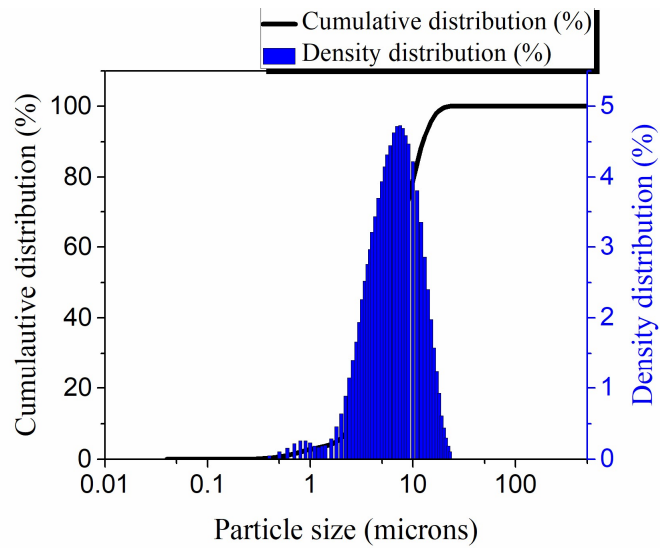
(b)

Figure 4.1 (a) SEM image and (b) Particle size analysis of EIP

The MR fluid thus synthesized is tested using a rheometer (make: Anton Paar), to understand the dynamic behavior of the fluid without and with the influence of magnetic field. The rheometer setup is shown in figure 4.2.
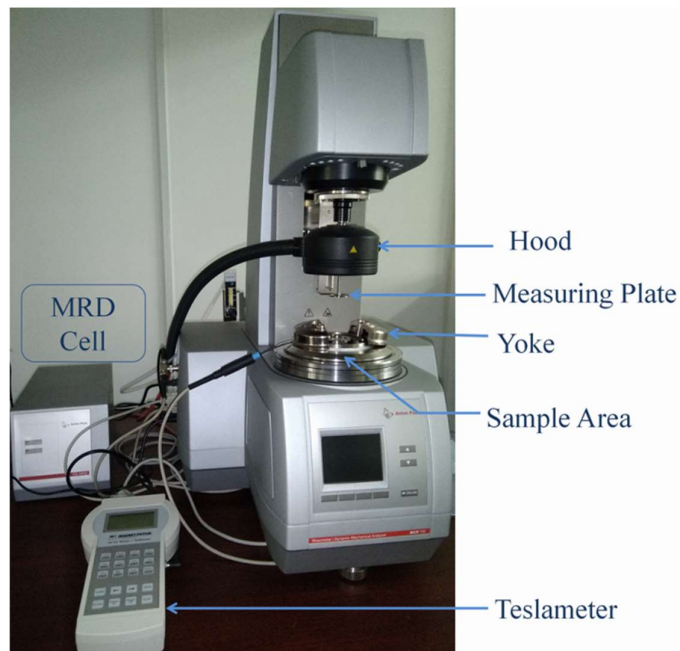
Figure 4.2 Rheometer for MR fluid rheology testing

Shear stress developed in a fluid can be known using the rheology testing under varying shear rate condition. The shear rate was varied from 0 to 800 s^{-1} and shear stress developed under different current conditions is shown in figure 4.3. For comparison purpose, the in-house prepared MR fluid (denoted by 'I') was tested along with commercial MR fluid (denoted by 'C') 132DG from Lord Corporation.

The yield stress of 8278 Pa was observed at 7.7 s^{-1} shear rate for in-house prepared fluid whereas yield shear stress of 7623 Pa at 4.3 s^{-1} for commercial fluid was noted at 2A current input and under same testing conditions. Yielding behavior was found different among two fluids at 1A current input. A notable change is observed in shear stress of the prepared MR fluid for different current inputs. Maximum shear stress for off-state condition is observed to be 117 Pa where as it reached 12635 Pa when 2 A current is supplied. Similarly, an off state viscosity of 147 mPa.s is observed at 800 s^{-1}. The commercial fluid could achieve 14778 Pa shear stress at 2A current. Also, a non-linear behavior is found in MR fluid rheology when there is a magnetic excitation when compared to the linearity in off-state condition.
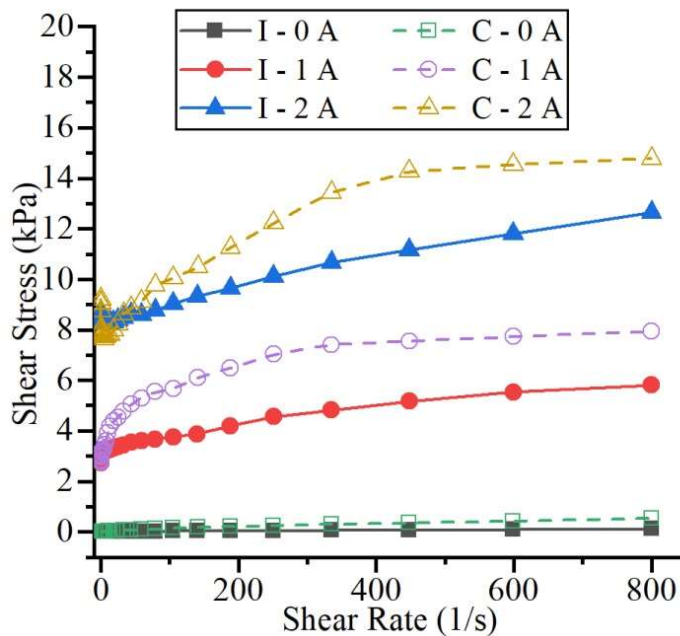
(a)
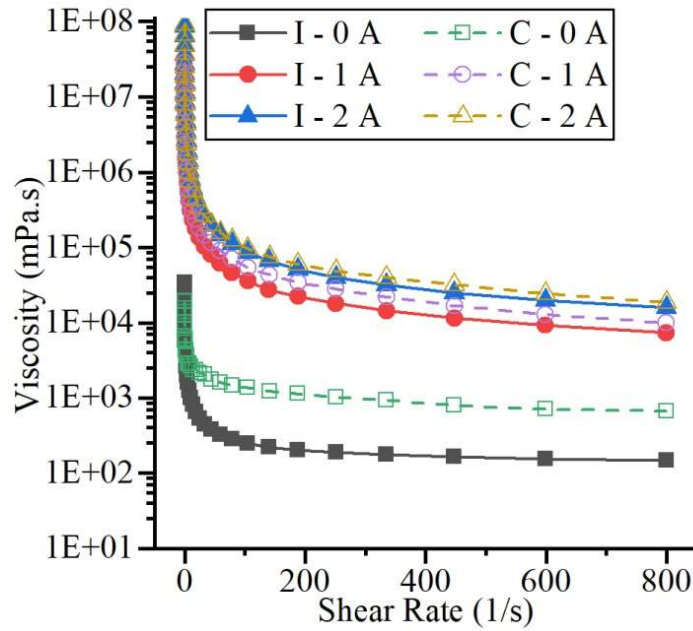
(b)

Figure 4.3 Shear rate v/s (a) Shear stress and (b) Off-state viscosity of in-house MR fluid

Reduction of viscosity is observed at higher shear rates. At maximum current condition, the in-house prepared fluid attained the viscosity of 15793 mPa.s where as commercial fluid was 18610 mPa.s viscous at highest shear rate of 800 s⁻¹. It can also be noted that, the viscosity variation between 1A and 2A was not same when compared to the same between 0A and 1A. This behavior was also observed in case of commercial MR fluid.

4.3 DESIGN AND DEVELOPMENT OF MR DAMPER

Design of MR damper discussed in this chapter follows the design procedure as discussed in previous chapter (Chapter 3). Again, the forces considered to design the MR piston are force due to shearing action, force due to viscosity of the MR fluid and the friction force. Overall frictional force is considered as 25N during the designing phase (Faisal and Muafag (2005)).

In this study, piston dimensions are optimized to achieve a maximum damping force of 2kN with a dynamic range of at least 3 at a 0.2 m/s working velocity. The dimensions {D,d,b,A,h} are considered as design variables. Further, maximum damping force and outer cylinder dimensions are applied as constraints. The dimensions of the outer cylinder are also recognized as constraints, since the damper should fit in the vehicle. Properties of the in-house prepared MR fluid such as off-state viscosity (η=0.77 Pa.s measured at shear rates between 300 to 800s-1), induced shear stress ($\tau_{y=}$7968 Pa at 2A current) are used from rheology data obtained for the fluid. Genetic algorithm was used in MATLAB^{TM} optimization tool box for the above mentioned optimization problem.

The design variables obtained are listed in table 4.1.

Table 4.1 Dimensions of MR damper piston

Design variable	Dimensions (mm)
Piston head diameter (D)	35.72≈ 36
Piston rod diameter (d)	20
Pole length (b)	9.65≈10
Total length of piston head (A)	49.78≈50
Height of annular flow gap (h)	0.92≈1

Finite Element Method Magnetics (FEMM) software is used to understand the flux distribution in the piston with the optimized dimensions. 320 numbers of turns of copper wire was used in the electromagnetic circuit. AISI 1018 steel was used as the piston material. The current of 0.75A was supplied across the coil cross section with 320 turns of coil. The analysis results showed that about 0.46T magnetic flux density is observed in the fluid flow gap region as shown in figure 4.4(b). Also, the flux density generated over the length of the piston is showed in figure 4.4(c).
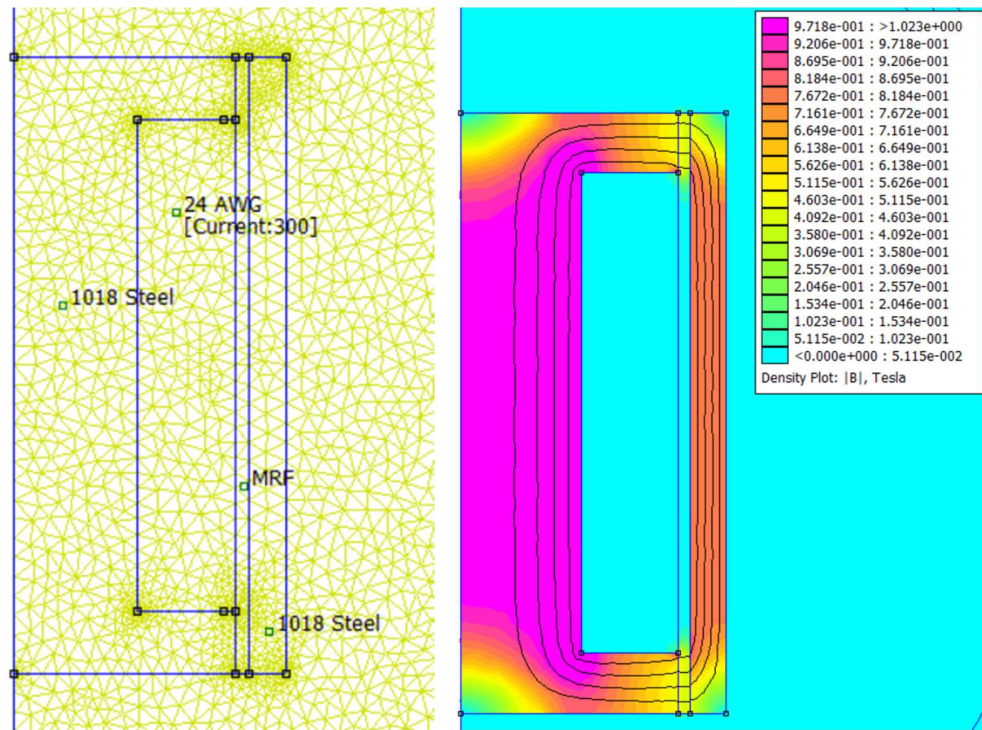
(a)   (b)
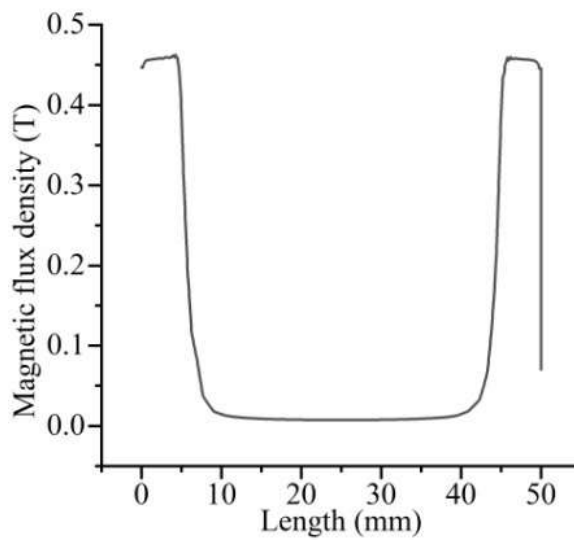
(c)

Figure 4.4 Magnetic flux density analysis using FEMM (a) boundary conditions, (b)
Analysis result, (c) flux density distribution in the fluid flow gap

The designed MR damper is fabricated using AISI 1018 steel which possesses good magnetic permeability. The piston of MR damper is wound using AWG 25 copper wire with about 320 turns.
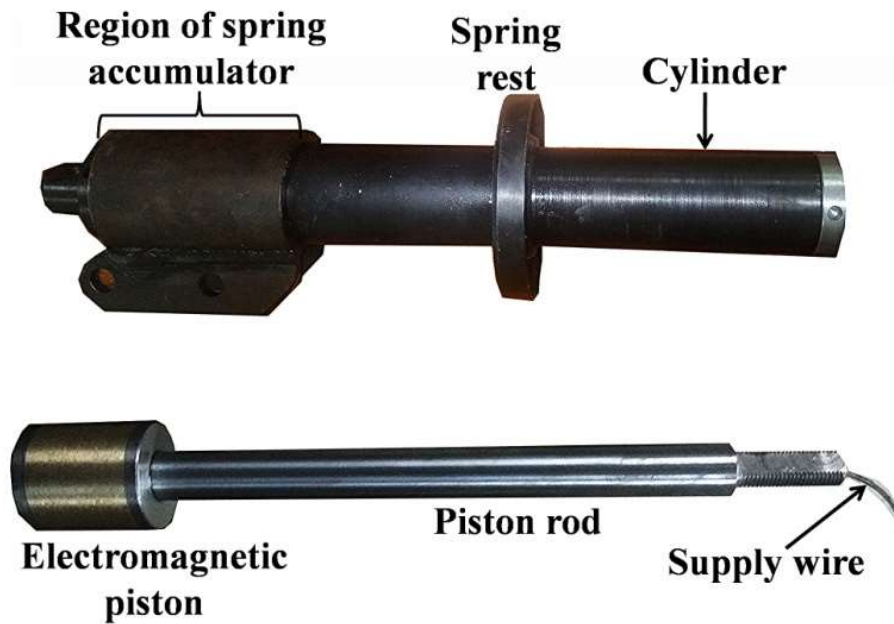
(a)

(b)

Figure 4.5 Manufactured MR damper

This work uses a spring accumulator in the mono-tube shear mode MR damper. The spring was designed using simple theoretical concepts and the spring accumulator chamber was separated by fluid chamber using a floating piston. The spring design considered properties of steel grade 5160 which is generally known as spring steel. The shear stress of spring wire (τ_s) can be given by (Guan et al. (2009)),

$$\tau_s = K \frac{2FR}{\pi r^3} \tag{4.1}$$

Where, F= load of operation, R= radius of the spring, r= radius of spring wire, K is a curvature coefficient (K is considered unity for $R>>r$). The ratio R/r is varied between 4 and 10 in general practices. In this study, the ratio of 4 is considered due to outer cylinder dimension constraint. With consideration of 275 MPa stress at yield point for the material chosen and maximum force of 1500 N for design consideration of spring, r= 3.72 mm and R= 14.9 mm are obtained. The total number of turns (n) of the spring can be obtained by,

$$\gamma = \frac{yr}{2\pi R^2 n} \tag{4.2}$$

Where, γ= strain of material, y=compression of spring. Considering strain of 0.02 from stress-strain curve of the spring material and for estimated 20 mm compression, a minimum number of turns obtained were 2.66. A total number of 6 turns were chosen for the spring with space availability in the long stroke MR damper. Leakage of MR fluid from the fluid chamber to spring accumulator is avoided with the use of dynamic seal in floating piton.
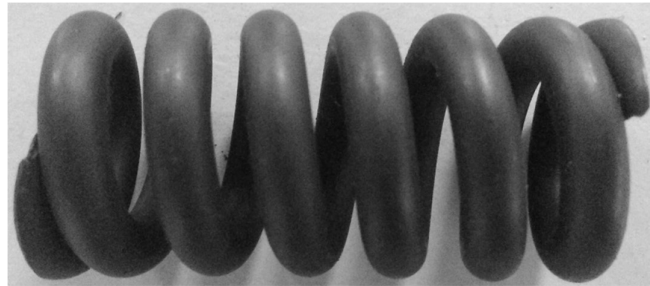
Figure 4.6 Spring for the accumulator

4.4 CHARACTERIZATION OF MR DAMPER

The characterization of MR damper specially designed to be fit into a vehicle can provide us a useful information regarding the development of total damping force when subjected to different dynamic input conditions. For this purpose, the damper is

characterized in the damper testing machine (DTM) under various dynamic inputs to collect the corresponding responses.
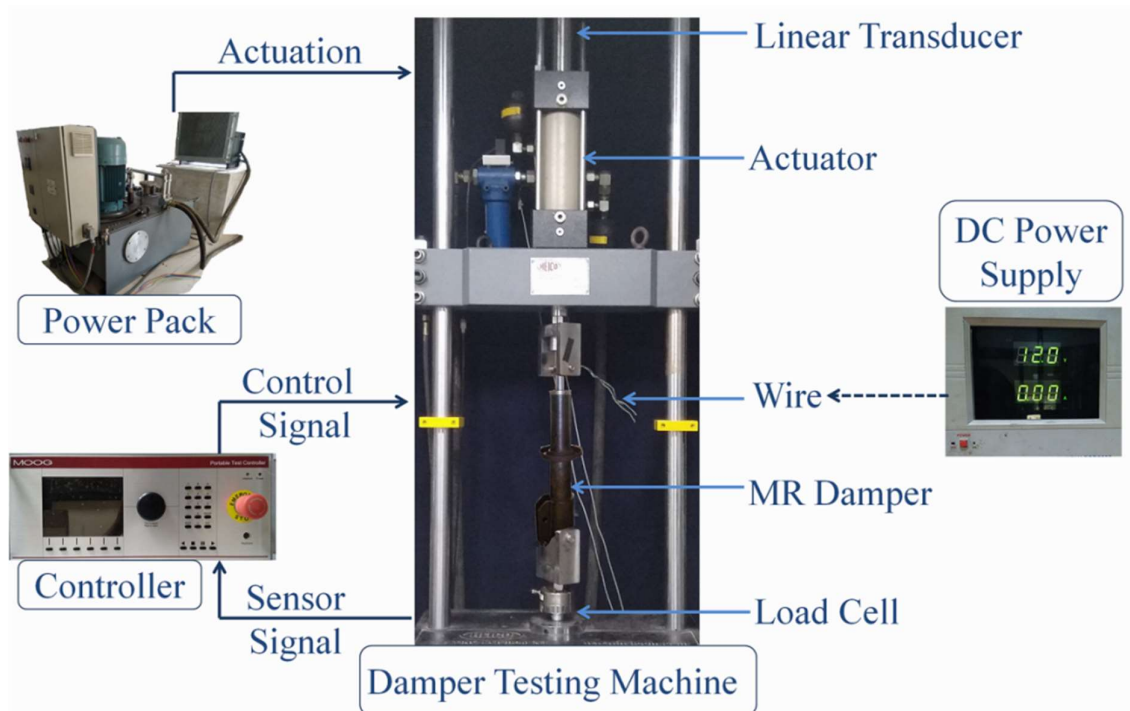
Figure 4.7 Damper testing machine for damper characterization

Testing of MR damper was performed for three amplitude conditions: 5 mm, 10 mm and 15 mm. The damper was excited with 1 Hz and 2 Hz frequency for all the amplitude conditions. To evaluate the performance variation of MR damper under different current conditions, the damper was supplied with 0.25A and 0.75A. The damper was tested in off-state condition too (i.e. without current supply). The force versus displacement behavior shown by the MR damper under above mentioned conditions is shown in figure 4.8 to figure 4.11.
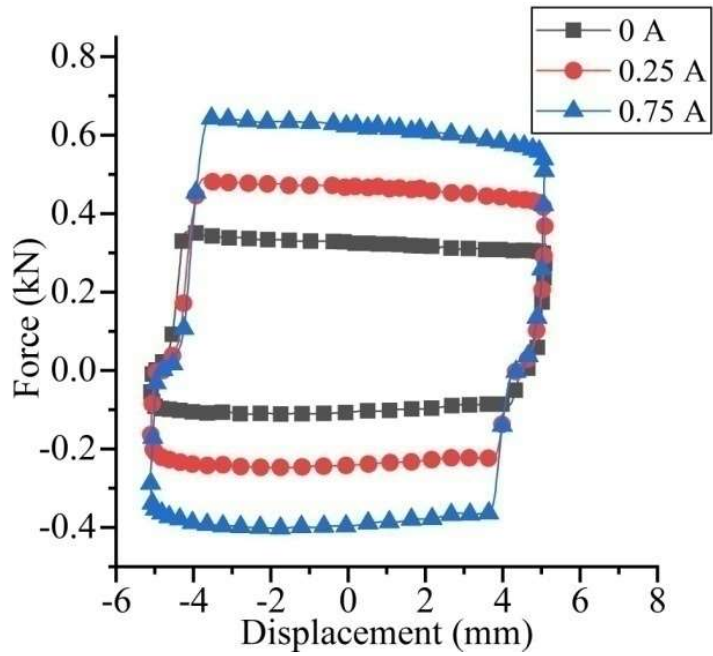
(a)
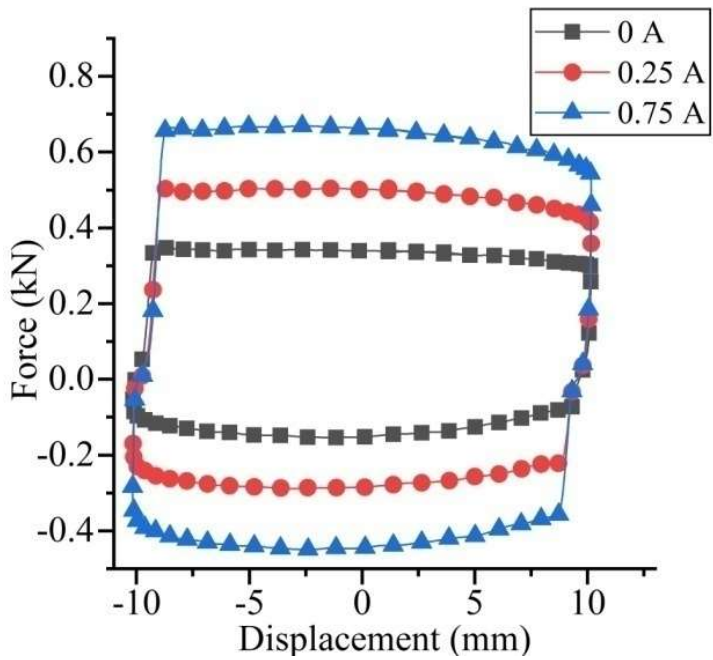
(b)

Figure 4.8 Force versus displacement at 1 Hz for (a) 5 mm amplitude and (b) 10 mm
amplitude condition
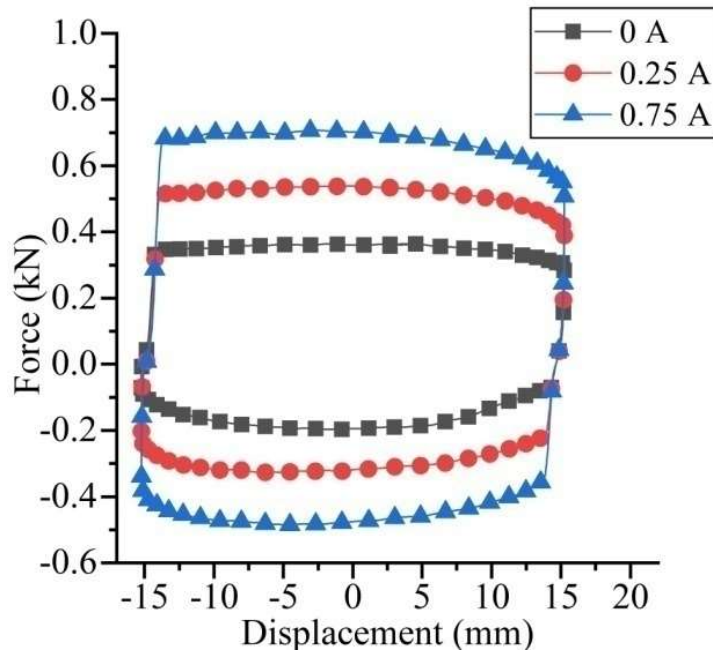
Figure 4.9 Force versus displacement at 1 Hz for 15 mm amplitude condition
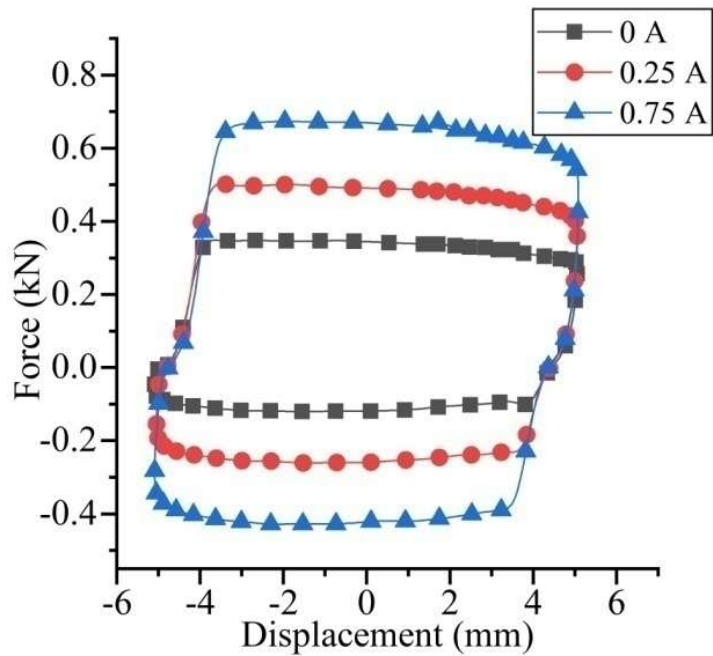
Figure 4.10 Force versus displacement at 2 Hz for 5 mm amplitude condition
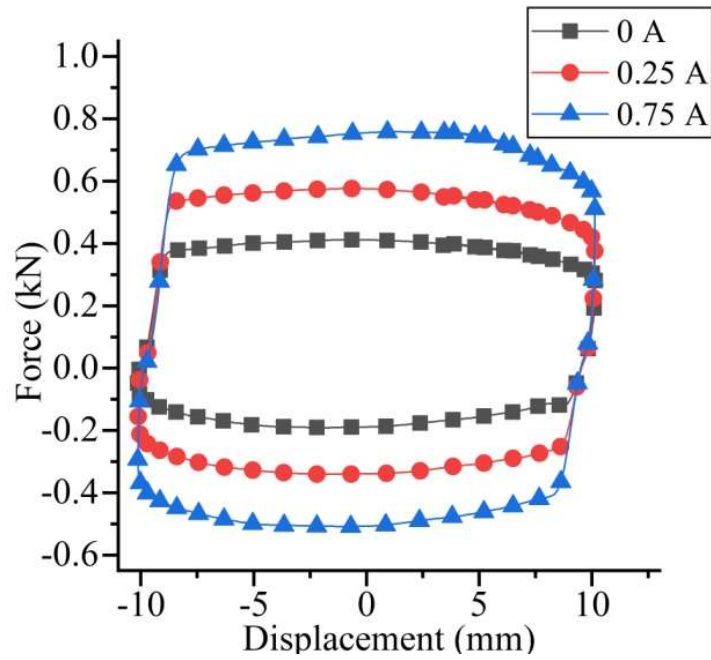
(a)
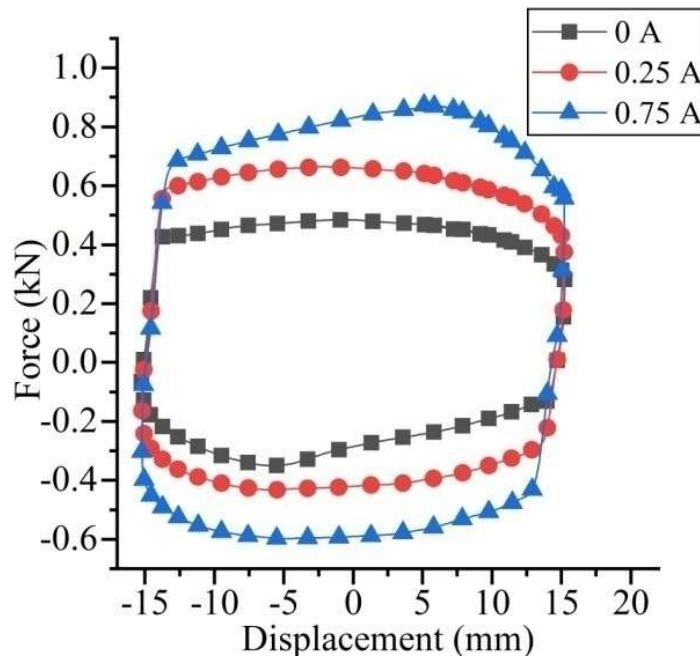
(b)

Figure 4.11 Force versus displacement at 2 Hz for (a) 10 mm amplitude and (b) 15 mm amplitude conditions

The MR damper characteristics as shown in figure 4.8 to figure 4.11 reveal a significant difference in the dynamic nature of the damper with and without supply of current. It can be seen in every amplitude conditions that the total force has doubled with 0.75A supply current when compared to the force without current supply. It is clear from the plots that maximum damping force of 873 N is achieved at 0.75 A DC current supply for 15 mm amplitude and 2 Hz operational frequency. Also, nature of the plots suggests that the spring accumulator used in the damper could able to work properly in the operated conditions.

4.5 MATHEMATICAL MODELING USING KWOK THEORY

Due to non-linearity behavior of MR fluid inside the damper, several mathematical models were proposed to represent damper characterization (Sahin et al. (2010)). Much more basic and simpler model such as Bingham model represents the hysteresis behavior, but the efficiency is generally compromised. Bouc-Wen model has more number of shape deciding parameters than Bingham model and obviously, it represents the hysteresis behavior in a more effective way (Wang and Liao (2011)).
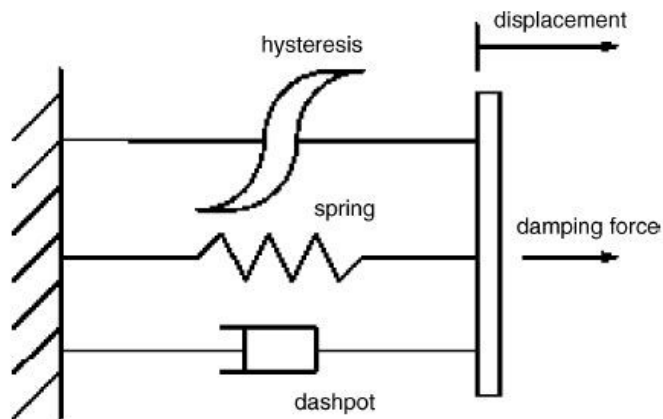
Figure 4.12 Kwok hysteresis model (*Courtesy: Kwok et al. (2006)*)

Kwok et al. (2006) proposed a model to represent the hysteresis behavior of MR damper which consisted of less number of parameters than the Bouc-Wen model. The research highlighted the benefits of the proposed model against to the Bouc-Wen model in terms of parameter identification error as well as identification efficiency. Also, it is obvious that the computational time needed in case of Kwok model is lesser

due to less number of parameters. Thus, this study uses Kwok theory to fit the hysteresis nature observed in the force-velocity characteristics. The Kwok model can be represented as (Kwok et al. (2006)),

$$F(t) = c_0\dot{x} + k_0 x + \propto z + f_0 \qquad (4.3)$$

Where, z is the hysteretic variable given by,

$$z = \tanh[\beta\dot{x} + \delta sgn(x)] \qquad (4.4)$$

Where δ determines the width of hysteresis and β decides the hysteretic slope. Parameters k_0 and c_0 represent conventional damper without hysteresis. α is the deciding factor for height of the hysteresis and f_0 is the offset shift of the hysteresis.
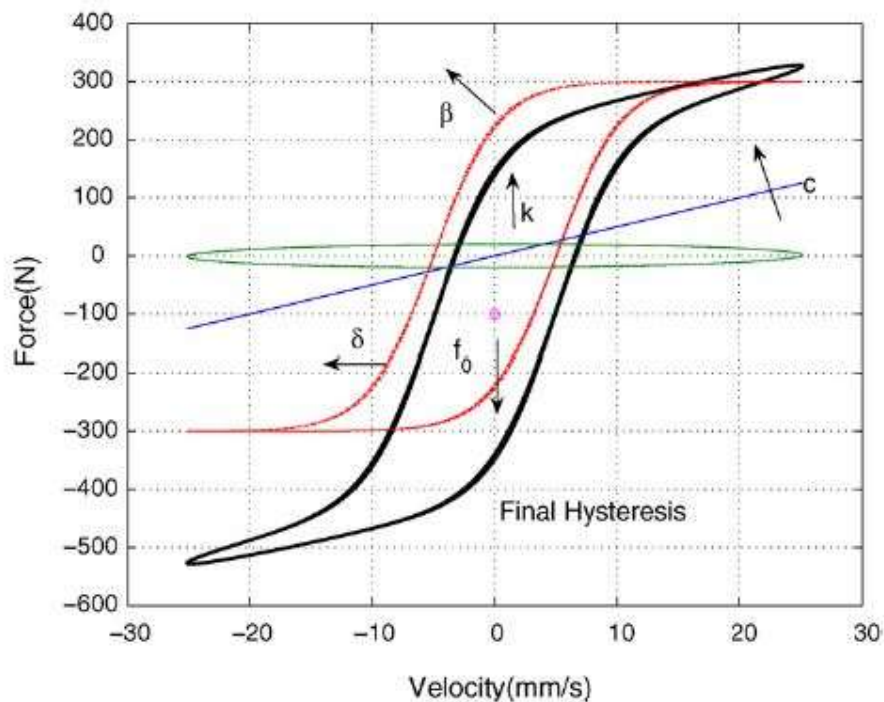
Figure 4.13 Kwok model parameters (*Courtesy: Kwok et al. (2006)*)

Hence, the Kwok model comprises of six parameters which decide the shape of the hysteresis of the damper characteristics. To obtain these parameters, the force-velocity nature of the damper for the tested conditions at different currents was obtained. The root mean square error between theoretical and experimental force was set as the

objective function. This root mean square error was minimized using genetic algorithm (GA) using the Matlab software. Population size of 100 was chosen which was run for 50 generations. Mutation function was chosen as 'Adaptive feasible', crossover function as 'Single point' and crossover fraction as 0.8. Other parameters of GA were kept default to obtain the optimized Kwok model parameters for different conditions. Thus obtained parameters were then used to understand their current dependency.

Each parameter was then represented using the polynomial model as,

$$c = c_0 I^2 + c_1 I + c_2 \qquad\qquad (4.5)$$

$$k = k_0 I^2 + k_1 I + k_2 \qquad\qquad (4.6)$$

$$f_0 = f_0 I^2 + f_1 I + f_2 \qquad\qquad (4.7)$$

$$\beta = \beta_0 I^2 + \beta_1 I + \beta_2 \qquad\qquad (4.8)$$

$$\alpha = \alpha_0 I^2 + \alpha_1 I + \alpha_2 \qquad\qquad (4.9)$$

$$\delta = \delta_0 I^2 + \delta_1 I + \delta_2 \qquad\qquad (4.10)$$

where, I is the DC current (A). The polynomial models were obtained for different dynamic conditions in terms of current. The sample of Kwok model parameters in terms of current for a particular dynamic condition (5 mm amplitude, 1 Hz frequency) is provided below.

$$c = 7738 I^2 + 2395 I + 5099 \qquad\qquad (4.11)$$

$$k = 11130 I^2 + 5503 I + 10041 \qquad\qquad (4.12)$$

$$f_0 = 33.34 I^2 - 5.778 I + 103.1 \qquad\qquad (4.13)$$

$$\beta = 726 I^2 - 288 I + 299.6 \qquad\qquad (4.14)$$

$$\alpha = -544.3 I^2 + 538.2 I + 73.6 \qquad\qquad (4.15)$$

$$\delta = 7.45 I^2 + 0.781 I + 3.563 \qquad\qquad (4.16)$$
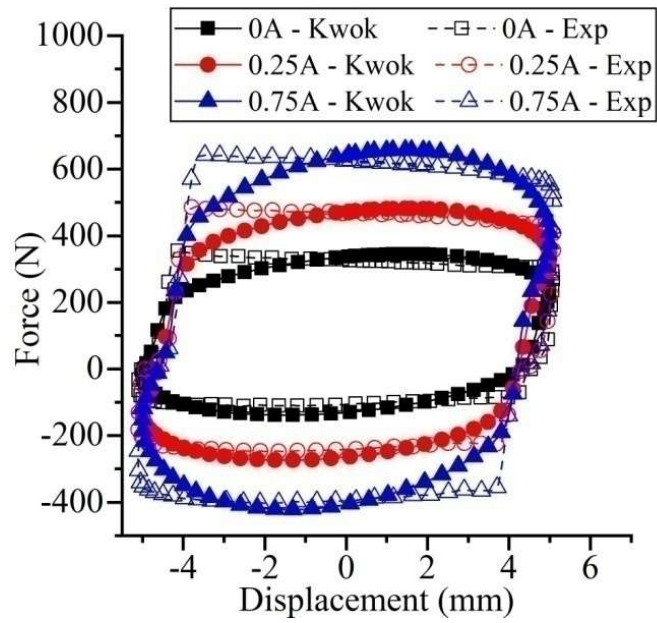
(a)
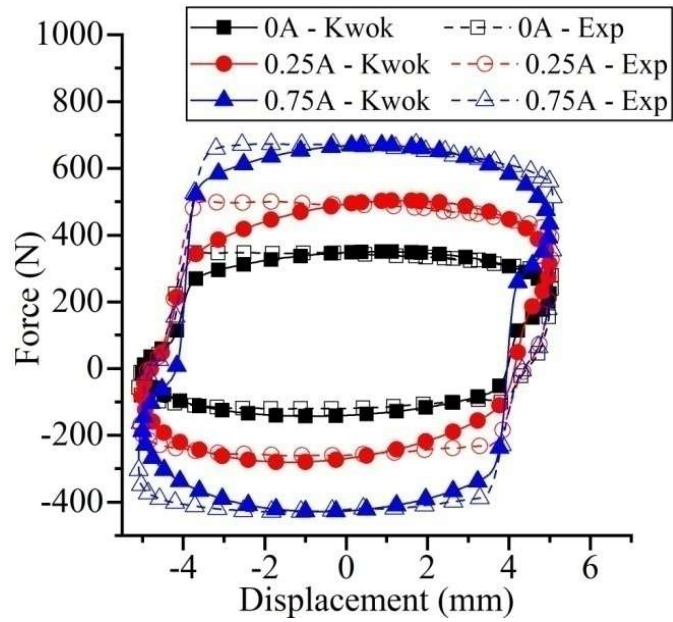
(b)

Figure 4.14 Comparison of data obtained through Kwok model and experimental data,

(a) 5 mm amplitude 1 Hz and (b) 5 mm amplitude 2 Hz conditions.
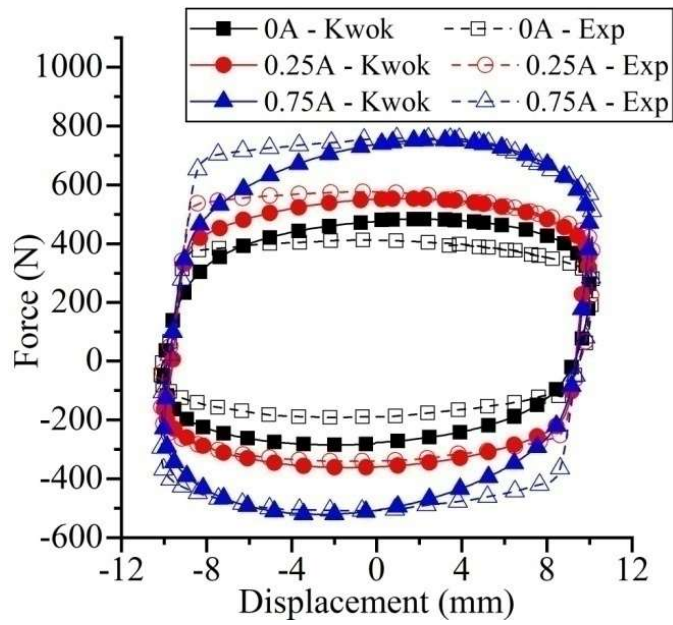
(a)
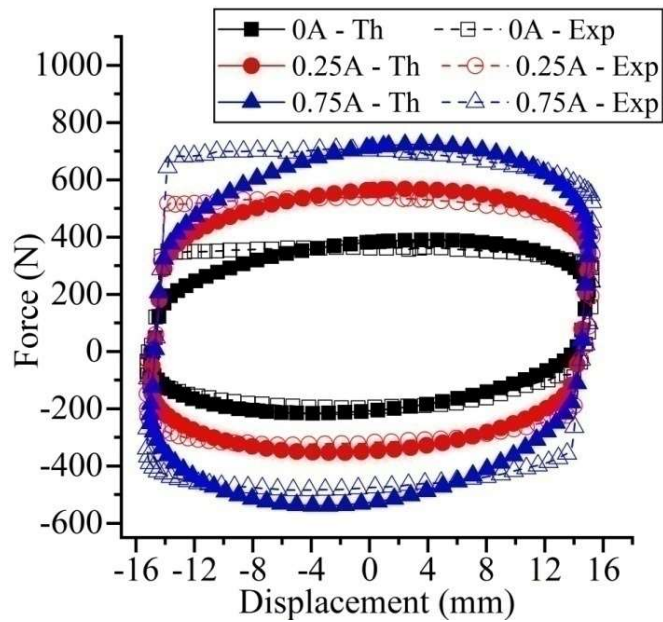
(b)

Figure 4.15 Comparison of data obtained through Kwok model and experimental data,
(a) 10 mm amplitude 2 Hz and (b) 15 mm amplitude 1 Hz conditions.
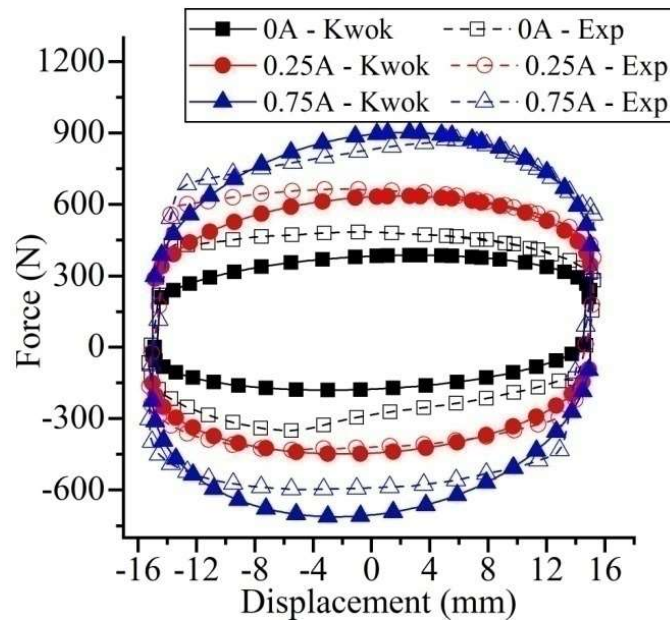
Figure 4.16 Comparison of data obtained through Kwok model and experimental data, 15 mm amplitude 2Hz condition.

Similar set of equations are obtained for other dynamic conditions too (for combinations of 5 mm, 10 mm, 15 mm amplitudes and 1Hz, 2Hz frequencies) using the data obtained through damper testing. The verification of these models has been validated and the comparison is shown in figures 4.14 to figure 4.16.

It is evident from these plots that the Kwok model parameters obtained using above methodology served the purpose by simulating the force-displacement behavior with minimum error between experimental and model force output. The comparison results show a positive remark that these models can further be used in quarter car simulation with the semi-active damper.

4.6 SUMMARY

This chapter discusses the in-house preparation of MR fluid and its implementation in the MR damper. The MR fluid was synthesized by using the electrolytic iron powder and paraffin oil with small amount of additive (oleic acid). The particle size analysis revealed the mean particle size of the EIP as 7.02 microns. Synthesized MR fluid was then tested using rheometer to reveal the rheological characteristics of the fluid under

the influence of different current inputs. The shear stress of the MR fluid was found to be increasing with increase in magnetic field and the difference was found to be significant. The yield stress of the fluid was used in designing the MR damper. The full scale MR damper was designed based on the Bingham model for viscous and shear force and also by considering MR fluid properties. A spring accumulator was also designed to accumulate the volume changes due to piston rod movement. The magnetic flux density in the fluid flow gap was analyzed using the FEMM software and the maximum flux density was recognized for the designed piston was 0.45 T.

The designed MR damper was developed using AISI 1018 steel and the electromagnetic piston was wound with AWG 25 copper wire. The developed MR damper was filled with synthesized MR fluid and characterized by using damper testing machine under various excitation conditions. The characterization results showed that maximum damping force developed was 873N and a minimum dynamic range of 2 was achieved. Also, the nature of the graph suggests that the shift in the plot was minimized due to usage of accumulator.

The representation of non-linear nature of MR the damper is an important criterion for further modelling or analysis. This chapter has presented a mathematical modelling of the MR damper hysteresis using a parametric modelling technique known as Kwok model. The characterized data of the MR damper was used for modelling purpose. The parameters of the Kwok model were determined for every test condition by using optimization method. Further, the parameters were converted into current dependent variables towards the ease of application in the later stages. The experimental and theoretical results showed a considerable match.

CHAPTER 5

QUARTER CAR TESTING AND ANALYSIS

5.1 INTRODUCTION

Literature studies illustrated the importance of quarter car analytical models along apart from experimentations. This chapter deals with quarter car simulations where the suspension with MR damper is utilized. The Kwok model of the MR damper is used to bring the semi-active nature for the suspension. The quarter car simulation is illustrated with sinusoidal road profile and with off-state, constant current as well as skyhook controlled current. The wheel and the spring data has been used in the quarter car simulation after characterizing them. Finally, validation of this study is presented after experimenting by using quarter car setup and the error plot is obtained.

5.2 CHARACTERIZATION OF TIRE AND SPRING

The tire characterization is subjected to the dynamic condition of 20 mm amplitude and 1Hz frequency.
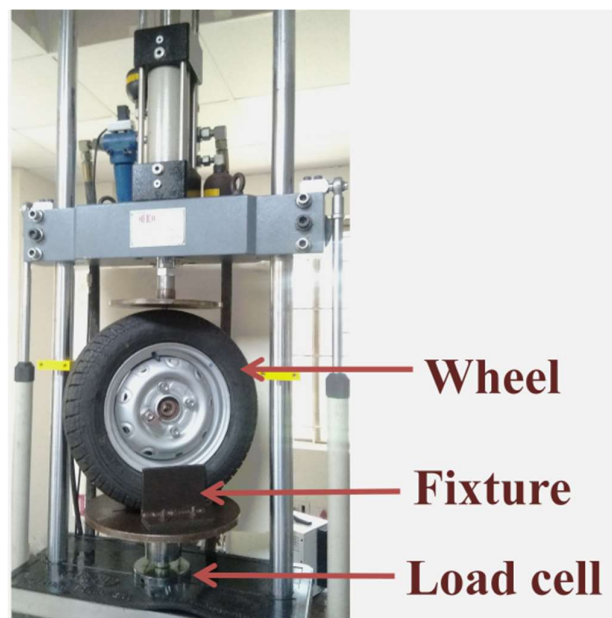
Figure 5.1 Tire characterization setup

The characterization testing is performed using the same dynamic testing machine which is used for damper characterization. The tire characterization setup and nature are as shown in figure 5.1 and figure 5.2 respectively.

Two important quarter car parameters to be obtained using the tire are the tire stiffness and the tire damping coefficient. Tire damping coefficient is obtained on the basis of area inside the curve, since area inside hysteresis is equivalent to the energy dissipation.
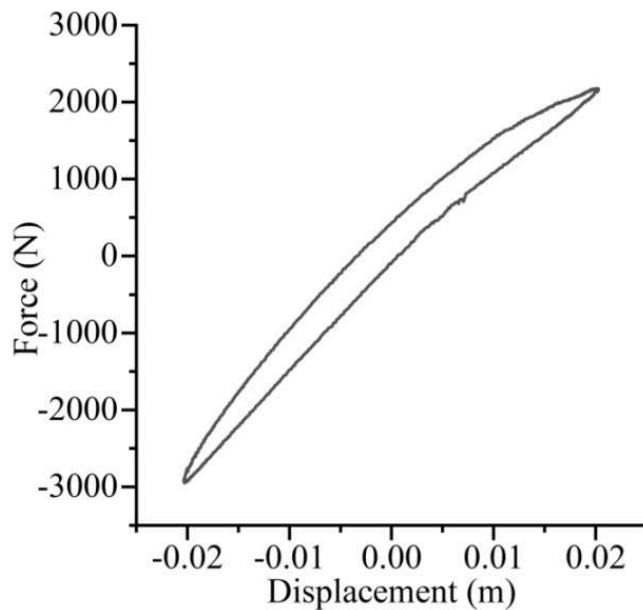
Figure 5.2 Tire characterization result

The tire damping coefficient is found to be 3100 Ns/m. The slope of the curve in the straight line region provides the stiffness of the tire which is found to be 129022 N/m.

Similar characterization testing is performed over the spring element of the strut to obtain the stiffness of the spring. The setup and plot of spring characterization is as shown in figure 5.3 and figure 5.4 respectively.
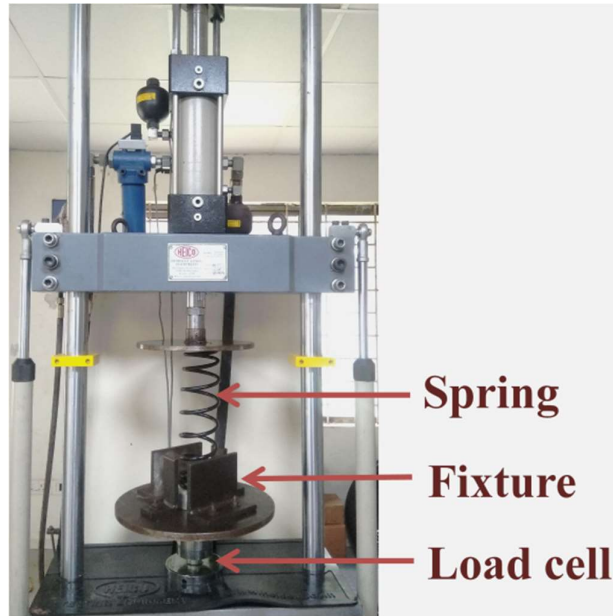
Figure 5.3 Spring characterization setup

Spring characterization is performed at 40 mm amplitude condition with 1Hz frequency using the dynamic testing machine. Slope of the line provides the stiffness of the spring and is found to be 14900 N/m.
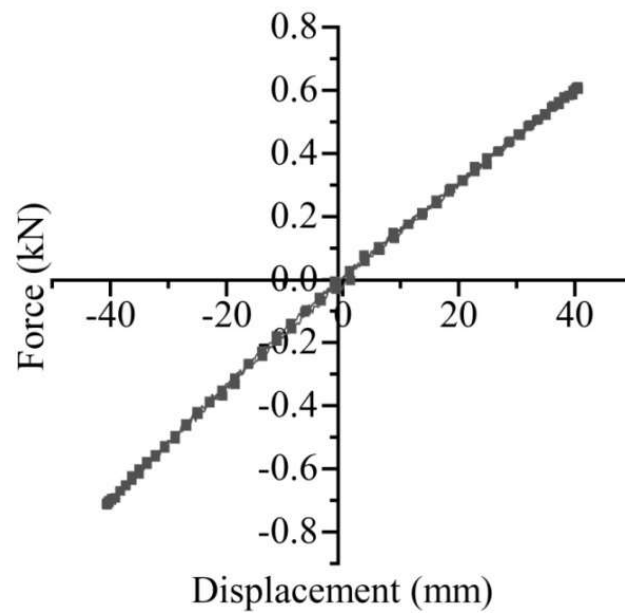
Figure 5.4 Spring characterization result

These characterization results of spring and tire as obtained using the mentioned procedure are further used in quarter car simulation using Matlab/Simulink.

5.3 MATHEMATICAL MODELING AND ANALYSIS USING QUARTER CAR MODEL

In this work, the quarter car simulation used Kwok model to represent the MR damper behavior in different dynamic conditions the sample of which was provided in equation 4.11 - 4.16. The Kwok parameters are changed according to the simulation condition. For example, Kwok parameters are different for 5 mm amplitude, 1Hz condition and 10 mm amplitude, 2Hz condition. Based on the dynamic input, the Kwok parameters which are in terms of current are altered. The quarter car simulations are performed for three current input conditions; 0A (off-state), constant current supply of 1A and current supply through skyhook control. Essentially, the parameters of the quarter car to be selected other than the spring and tire properties are sprung and unsprung masses. The sprung mass and unsprung masses are selected as 252 kg and 23 kg respectively. These parameters are selected based on the actual quarter car set up. The equation of motion for the quarter car can be written using Newton's second law of motion as,

$$m_s \ddot{x}_s + k_s(x_s - x_u) + f_d = 0 \qquad (5.1)$$

$$m_u \ddot{x}_u + c_u(\dot{x}_u - \dot{x}_r) + k_u(x_u - x_r) - k_s(x_s - x_u) - f_d = 0 \qquad (5.2)$$

Where, m_s= sprung mass (kg), m_u= unsprung mass (kg), c_u= tire damping coefficient (Ns/m), k_u= tire stiffness (N/m), k_s= spring stiffness (N/m), x_s= sprung mass displacement (m), x_u= unsprung mass displacement (m), x_r= road displacement (m). The parameter 'f_d' represents variable damping provided by the MR damper with change in current supply to the MR damper.

This work makes an attempt to simulate the quarter car using Matlab Simulink with the help of parameters of the actual elements. Hence, characterization testing is performed over the spring as well as the tire of the quarter car system. This data is further used in the quarter car simulation. The characterization results were discussed in previous section.

5.4 CONTROL LOGIC TO THE MR DAMPER

Skyhook control logic is one of the basic as well as a benchmark control logic which proved its efficiency in semi-active suspension control. Although the skyhook logic seems simpler, its effectiveness under different working environments was reported in various studies (Qazi et al. (2013), Sahin et al. (2010)). Based on these reasons, an attempt is made in this study to implement skyhook control logic during quarter car testing (figure 5.5).
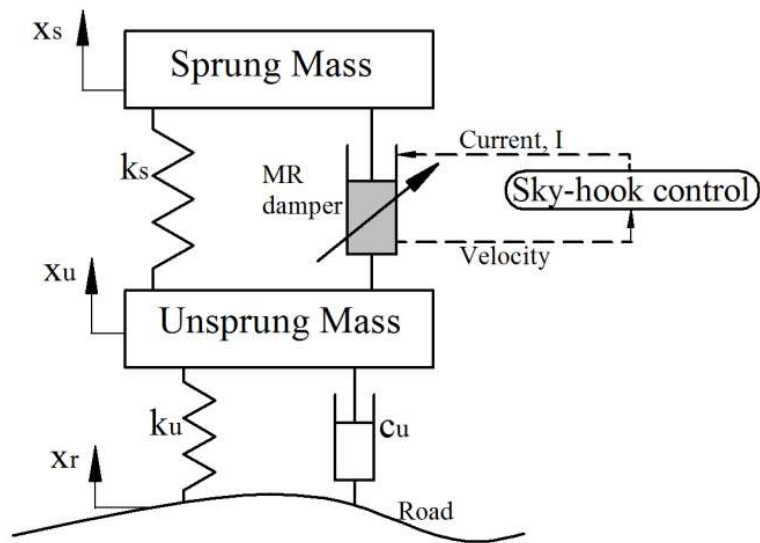
Figure 5.5 Quarter car scheme with Skyhook logic

The skyhook system controls the response of the sprung as well as unsprung masses by ON and OFF mechanism in the semi-active device. The control system turns ON and the maximum current flows into the system when the relative velocity between both masses and the sprung mass are in the same direction. When the directions are reversed, the system supplies minimum current to the damper. The control logic is simpler and hence a quick control action can be expected. The skyhook logic is as expressed in equation 5.3 and 5.4.

$$I = I_{max} \ when \ (\dot{x}_s - \dot{x}_u)\dot{x}_s \ is \ positive \qquad (5.3)$$

$$I = I_{min} \ when \ (\dot{x}_s - \dot{x}_u)\dot{x}_s \ is \ negative \qquad (5.4)$$

This control logic is used in the quarter car simulation to decide the maximum or minimum supply of current to the MR damper. Hence, a feedback system is developed to control the current supply to the MR damper based on the relative velocity between sprung and unsprung masses. In this work, minimum and maximum current supplies are assigned as 0A and 1A respectively.

The road input provided in the quarter car simulation is the sinusoidal profile of 5mm and 10mm amplitude. The simulation is carried out for 1Hz, 2Hz and 3Hz frequencies. These excitation frequencies are chosen based on vehicle body frequency which falls near 1-2.5 Hz (Fischer and Isermann (2004)). The sprung mass acceleration is considered as the deciding factor for performance comparison between three current input conditions. The power spectral density (PSD) plots for different conditions are as shown in figure 5.6 to figure 5.8.

The peaks in the respective frequencies are analyzed from PSD plots to differentiate MR fluid effect with variation of current supply. A clear difference in the peak value can be observed with different current supply condition. One can observe from these plots that when the current is supplied to the MR damper, the peak value reduces to an extent. It can also be noted that current supply through skyhook controller resulted in significant reduction in peak value which could result in better ride comfort.

Quantitatively, peak values for 5 mm excitations were recorded as 0.2441(at 1Hz), 1.2114(at 2 Hz) and 1.3695 $(m/s^2)^2$/Hz (at 3Hz) at off-state condition, while the peak values using sky-hook controllers were noted as 0.2181 (at 1Hz), 0.8271 (at 2Hz) and 1.1454 $(m/s^2)^2$/Hz (at 3Hz). Hence, the MR damper when used with skyhook controller brought down the peak values by 10.6 to 31.7% when compared to off-state condition.
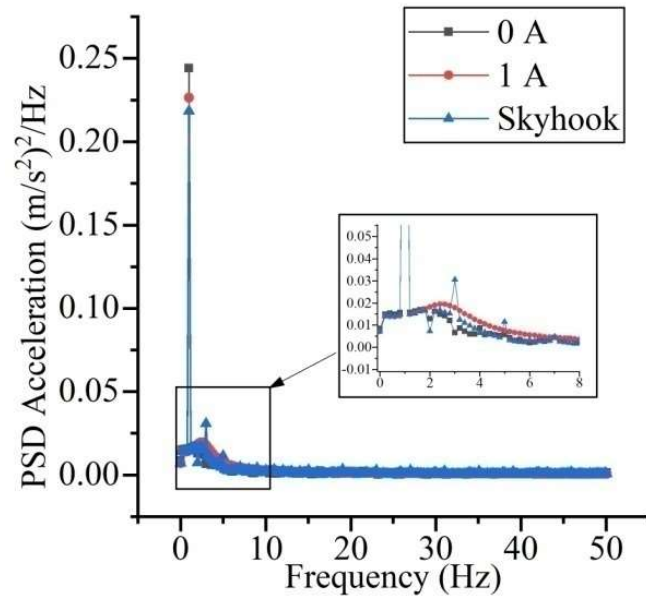
(a)
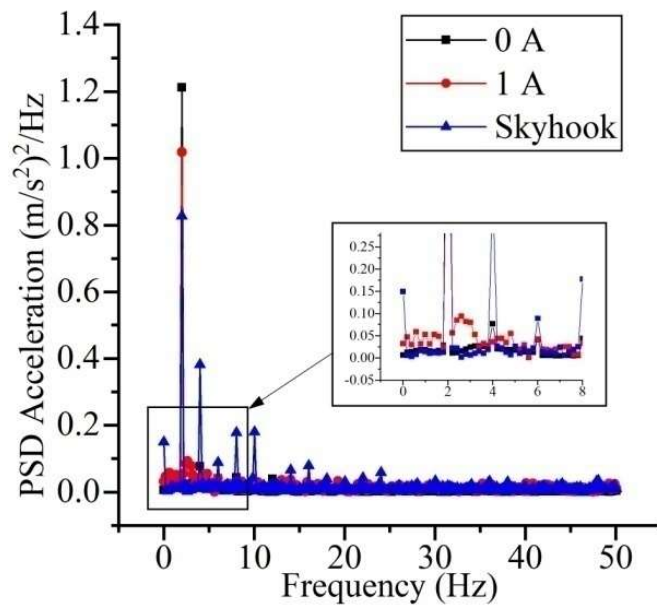
(b)

Figure 5.6 PSD acceleration plots of sprung mass for 5 mm amplitude at (a) 1 Hz and
(b) 2 Hz conditions from quarter car analysis using Kwok model.
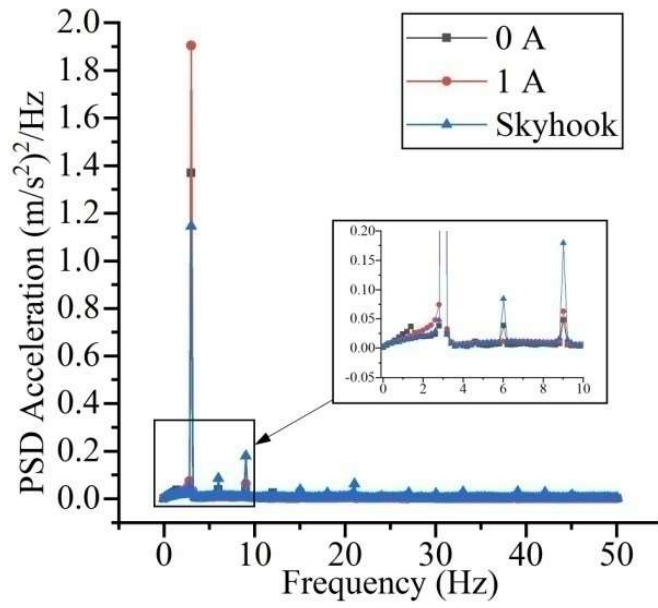
(a)
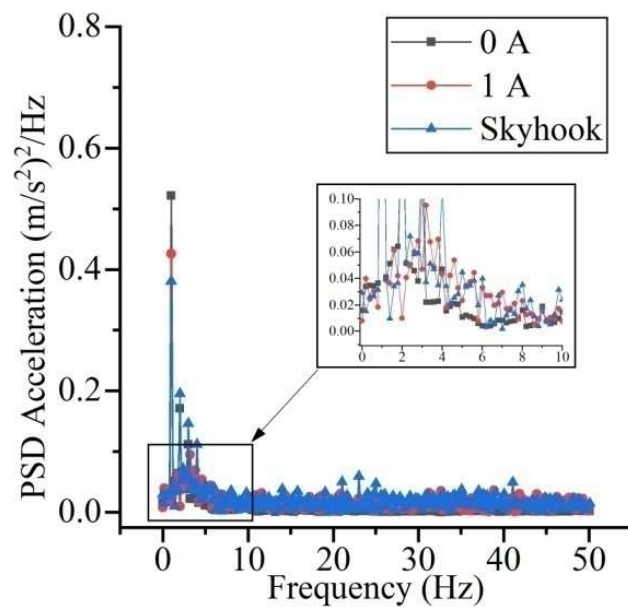
(b)

Figure 5.7 PSD acceleration plots of sprung mass for (a) 5 mm amplitude 3 Hz and (b) 10 mm amplitude 1 Hz conditions from quarter car analysis using Kwok model.
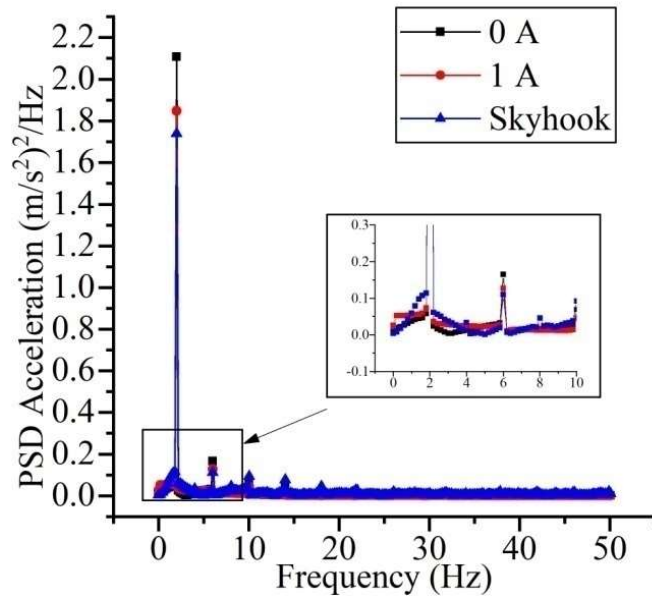
(a)
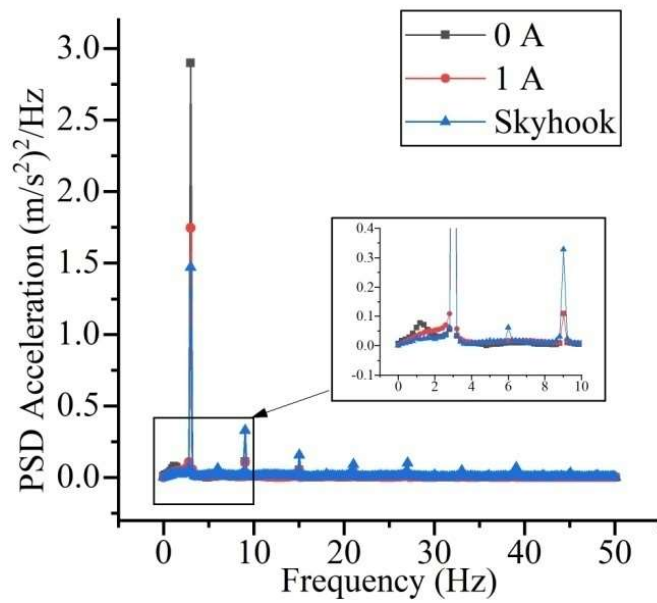
(b)

Figure 5.8 PSD acceleration plots of sprung mass for 10 mm amplitudes at (a) 2 Hz and (b) 3 Hz frequencies from quarter car analysis using Kwok model.

Similarly, a minimum improvement of 17% was analyzed for 10 mm amplitude conditions by using skyhook controller over the off-state condition.

(a)

(b)

(c)
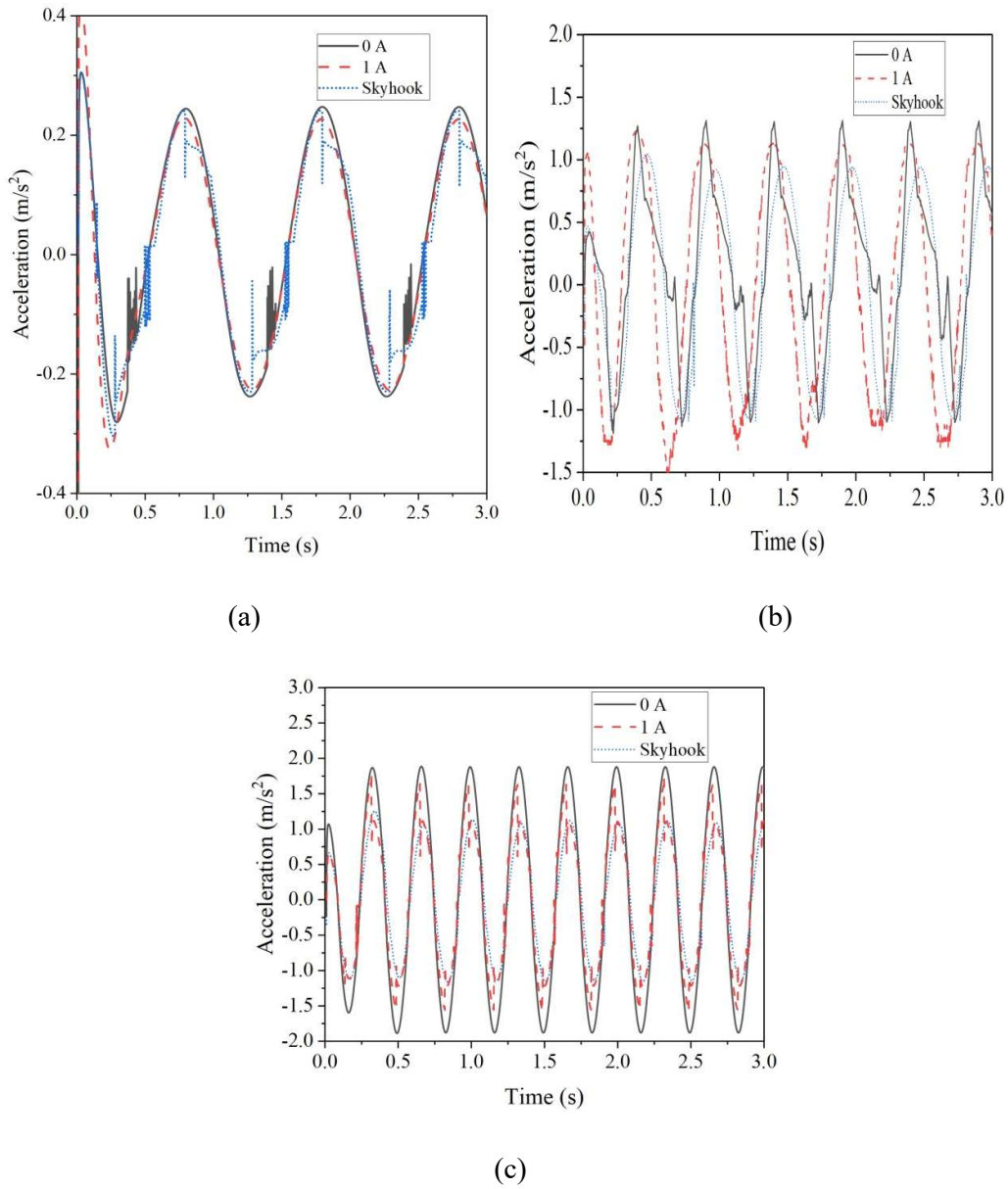
Figure 5.9 Performance comparison among three current inputs for 5 mm displacement with (a)1 Hz, (b) 2 Hz and (c) 3 Hz from quarter car model analysis
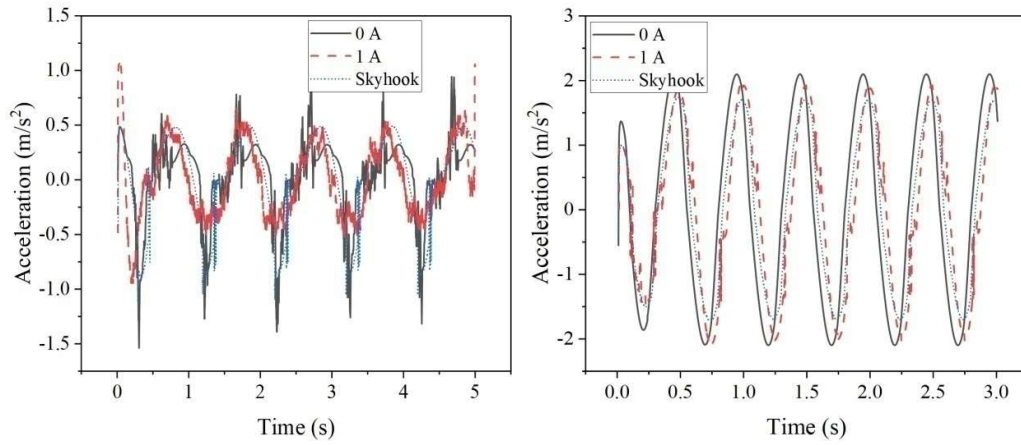
(a)   (b)
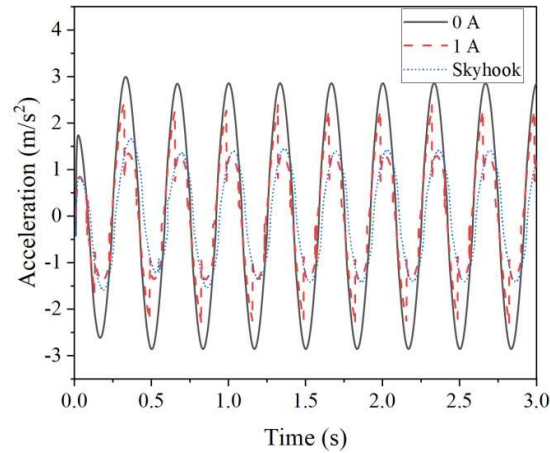
(c)

Figure 5.10 Performance comparison among three current inputs for 10 mm
displacement with (a)1 Hz, (b) 2 Hz and (c) 3 Hz from quarter car model analysis

A sample of time domain comparison for two conditions among three current
conditions is shown in figure 5.9 and figure 5.10.

5.5 IMPLEMENTING MR DAMPER INTO QUARTER CAR SYSTEM WITH
MRF-1

The developed MR damper is used in the McPherson suspension of a four wheeler
vehicle and fitted into the quarter car system as shown in the figure 5.11. The
experimentation using quarter car test rig has also intended to validate the simulation

results obtained in the previous step. The quarter car set up is hydraulic powered and is controlled using the same controller used for damper testing. A dead-weight is attached above the quarter car system to replicate the quarter sprung mass of the desired vehicle. The assembly of spring, damper, wheel components and sprung mass are attached to the quarter car system as shown in figure 5.11.
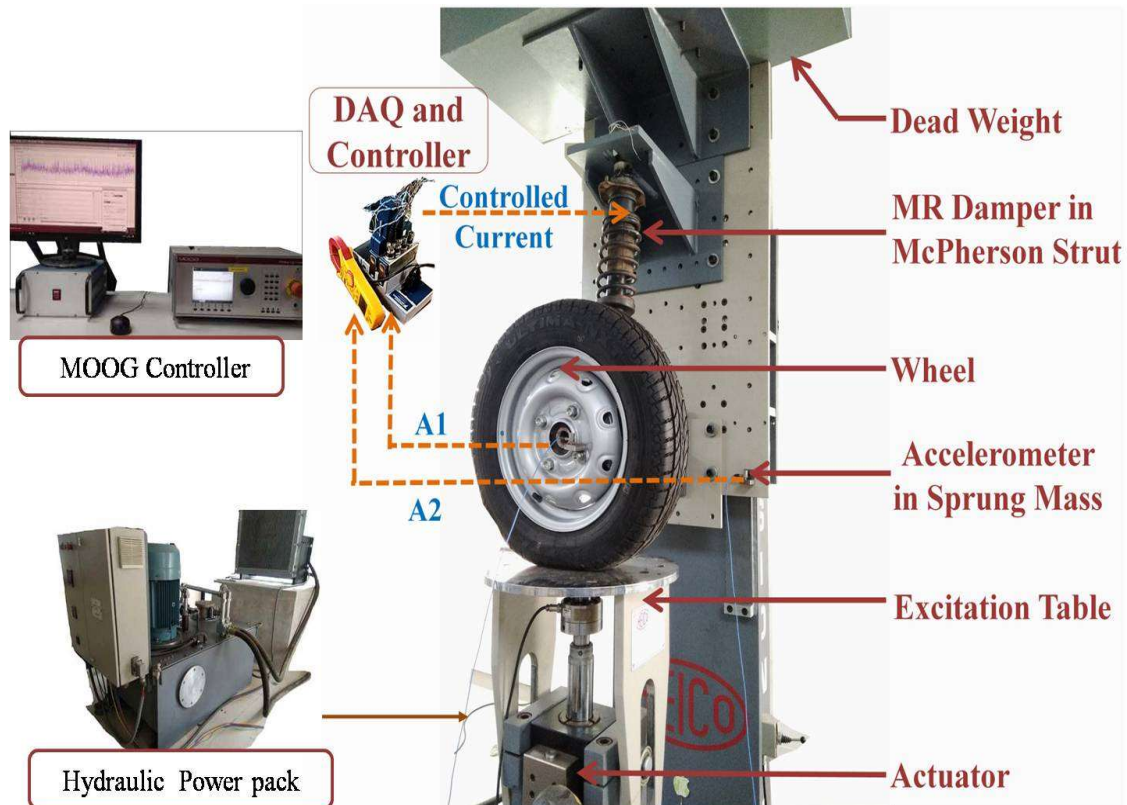
Figure 5.11 Quarter car test rig with MR damper in the McPherson strut

An accelerometer is attached to the sprung mass to record the disturbances during the excitation. Road disturbances with desired profile and magnitudes are provided through the hydraulic actuation.

The nature and the magnitude of excitation are provided in the table 5.1. Sinusoidal and trapezoid mode of road excitations are chosen with excitation conditions as mentioned in table 5.1.

Table 5.1 Operational conditions for quarter car system

Road amplitude (mm)	Excitation frequency (Hz)	Current supply (A)
5	1	0
10	2	1
-	3	Through skyhook

The performance of MR damper in each excitation condition is evaluated without supply of current (off-state condition), with supply of 1A current and current supply through skyhook controller. In figure 5.11, A1 represents acceleration signal from unsprung mass and A2 relates to the acceleration from sprung mass.
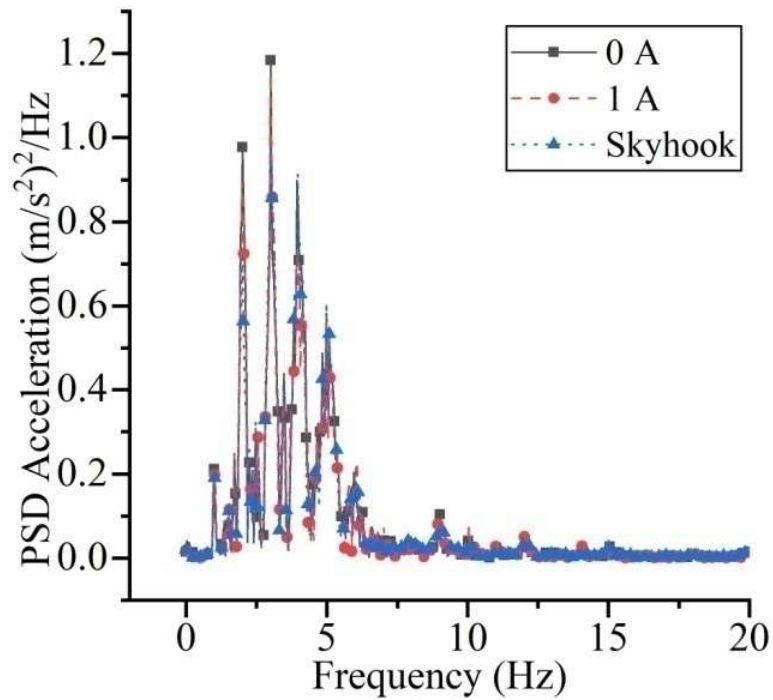
(a)
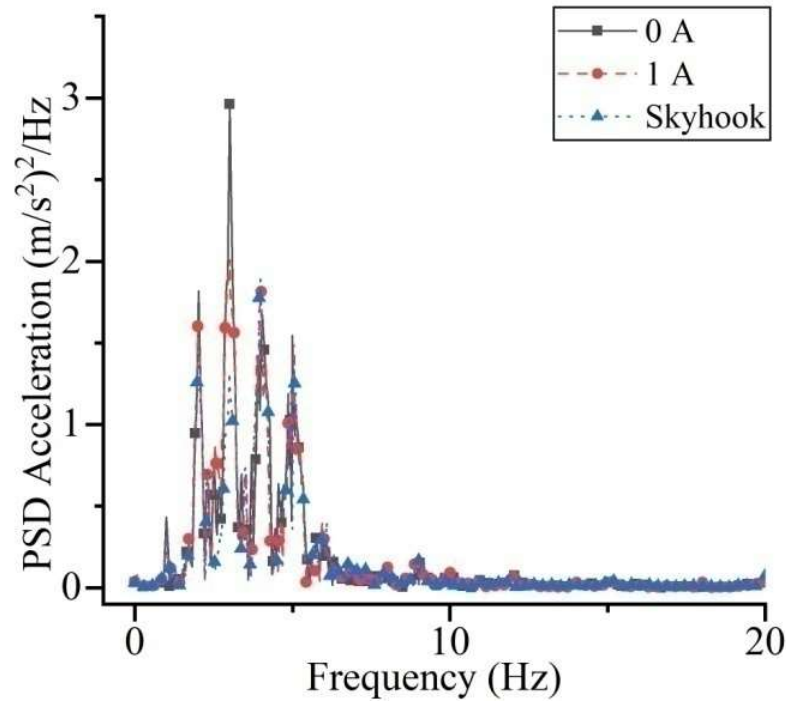
(b)

Figure 5.12 PSD acceleration plots for sinusoidal profile (a) 5 mm, (b) 10 mm
displacement amplitude

The response of the sprung mass for the above mentioned conditions are recorded in terms of the acceleration. The data from the quarter car test rig regarding acceleration has been taken from the accelerometers. The data from these accelerometers is acquired using NI 9234 DAQ (Data Acquisition). The data from these accelerometers is filtered and integrated using the sound and vibration toolkit in LabView software. The integrated signal is put into equation (5.3 and 5.4) and a control signal is transmitted to the current controller by means of digital input/output DAQ NI 9403 and through the current controller the MR damper is fed with the desired current. The sprung mass responses as PSD plots for 5 mm and 10 mm amplitude conditions are shown in figure 5.12 when the excitation are sinusoidal profile in nature.

The acceleration response in the frequency domain indicates a clear difference in the amplitude of acceleration with different current input conditions. The response magnitude is found to be reduced with constant current supply of 1A when compared

to that of off-state condition. The acceleration amplitude is observed the least when the current is supplied through sky-hook controller. The peak acceleration is observed for 3Hz excitation. Even though, testing excitations are limited to 1 Hz, 2 Hz and 3 Hz conditions, harmonics are observed at 4Hz and 5Hz which are not considered in this study since they showed diminishing nature after 3Hz.

Considering 5 mm amplitude condition, improvement of 10.08%, 26.6% and 17.28% is observed when the current is supplied through sky-hook controller against the off-state condition. It is evident from plots that higher magnitude responses are observed for 10 mm amplitude conditions. Stating in terms of percentage improvement, minimum 20% betterment is observed by using skyhook controller against the off-state condition. Collectively, a good improvement is observed when used with skyhook controller against off-state or passive condition considering both the amplitudes of sinusoidal road profile.

The peak values of the PSD acceleration obtained are compared among simulation and experimental results with sinusoidal profile road excitation. The percentage error observed between experimental and simulation results are shown in error plots for both 5 mm and 10 mm excitations (figure 5.13).
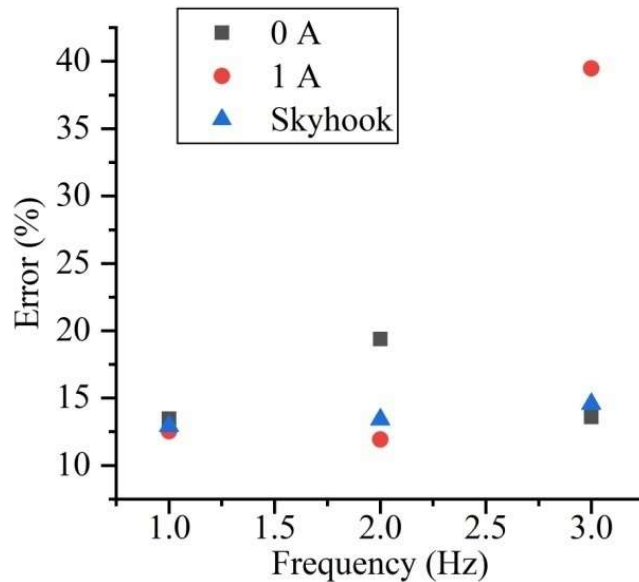
(a)
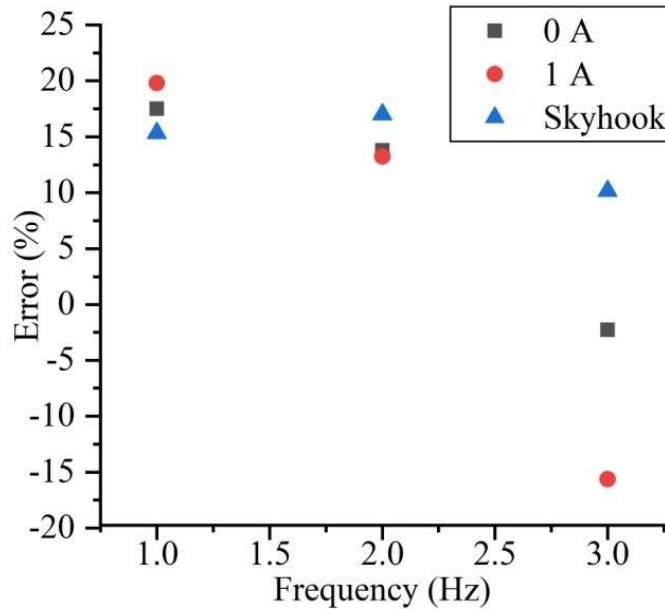
(b)

Figure 5.13 Error plots for (a) 5 mm and (b) 10 mm sinusoidal excitations

It can be observed that the percentage error for most of the trials lie within 20% except for one case.

The reason behind this error may be due to the deviation in the force output from the Kwok model from the experimental force (figure 4.14 to figure 4.16). Hence, a scope exists to eliminate to bring down this deviation to minimize further the percentage error. But, considering the non-linearity of the problem, the error is obvious.

The skyhook controller played a good role in improving the damper performance at relatively higher amplitude conditions also (10 mm displacement amplitude).

5.6 SINGLE SENSOR METHOD FOR QUARTER CAR

For the effective working of MR fluid when subjected to variety of non-uniform inputs, a suitable control strategy is must with feedback system. To receive suitable feedback in required form, several sensors are necessary which again depend on applied control tactics. As the number of sensors increase, the cost of the control scheme as well as the system also rises. This chapter extends the discussion with the

implementation of control scheme to the quarter car system which uses the single sensor in the entire loop. For the comparison purpose, a simulation of the quarter car model with proposed control scheme, skyhook control and constant currents are discussed. Finally, the response of quarter car experiments with proposed control scheme is narrated.

5.7 RHEOLOGY OF IN-HOUSE MR FLUID (MRF-2)

An MR fluid (MRF-2) with carbonyl iron as ferrous particles, poly alpha olefin as the carrier fluid, aluminium distearate and bentonite clay as additives is prepared in the laboratory. Aluminium distearate makes the redispersibility character of ferrous particles better in MR fluid whereas bentonite clay improves the stability of MR fluid in terms of settling of ferrous particles (Acharya et al. (2017)). In synthesizing the MR fluid, initially the additives are added in steps to the carrier fluid. The mixture is stirred for about 4 hours to ensure uniform distribution of additives into the base oil. The carbonyl iron particles are then added to this mixture and stirred for about 12 hours. The synthesized MR fluid contained 78% carbonyl iron particle and 20% base oil in terms of volume fraction. Both additives are added in equal amount constituting a total of 5% of base oil.

The synthesized MR fluid is then characterized to understand its rheology in terms of shear stress and viscosity for a given shear rate as well as for various current inputs. The characterization is conducted on Rheometer (make: Anton Paar Pvt. Ltd.), which enables rheology study of MR fluid with varying magnetic fields.

The rheology tests are performed with two conditions: varying shear rate with constant currents and constant shear rate with varying current. The change in current produces the changes in the magnetic field intensity during testing. A shear gap of 0.5mm is maintained between two parallel plates of rheometer for fluid characterization. Figure 5.14(a) depicts the shear stress variation with varying shear rate and different currents. The shear rate was varied from 1 to 600 s^{-1}. The rheological characterization is performed at four different current inputs: off-state (at 0 A), 1A, 2A and 3A. The shear stress of MR fluid recorded at different currents showed significant increase in the magnitude with increase in current input. The

linearity of MR fluid shear stress at off-state shows its behavior like Newtonian fluid. With application of magnetic field, non-Newtonian nature was clearly observed. The maximum shear stress at off-state condition has been observed as 163 Pa whereas it increased upto 29,505 Pa at 3A current input at 600 s^{-1} shear rate. A reduction in viscosity of MR fluid can be observed with increase in shear rate as seen in figure 5.14 (b). At a shear rate of 600 s^{-1}, viscosity of MR fluid at off-state condition is 271.29 mPa.s and the value increased to 49,175 mPa.s at magnetic field corresponding to 3A current.
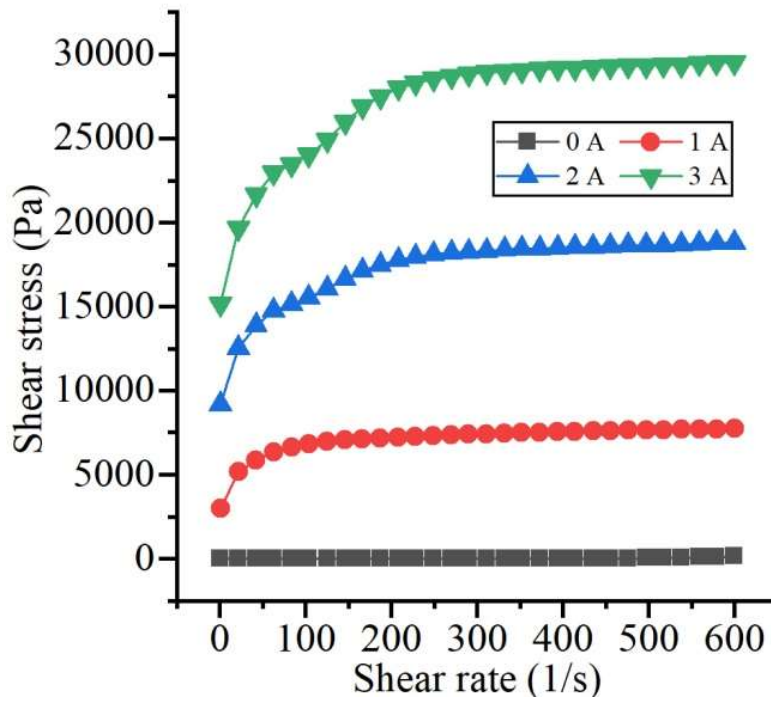
(a)
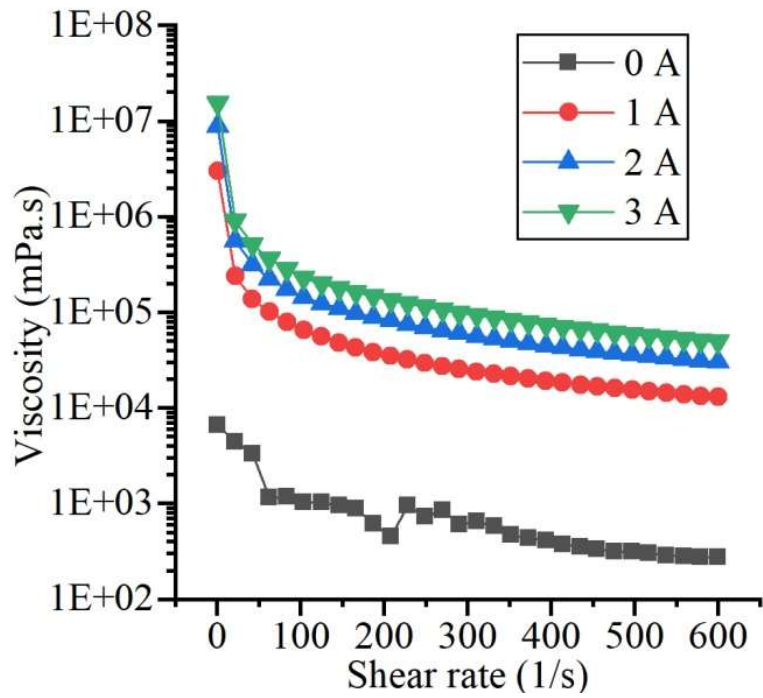
(b)

Figure 5.14 (a) Shear stress and (b)viscosity variation with varying shear rate

A set of experiments are also conducted to understand the shear stress and the viscosity variation with current sweep at constant shear rate.
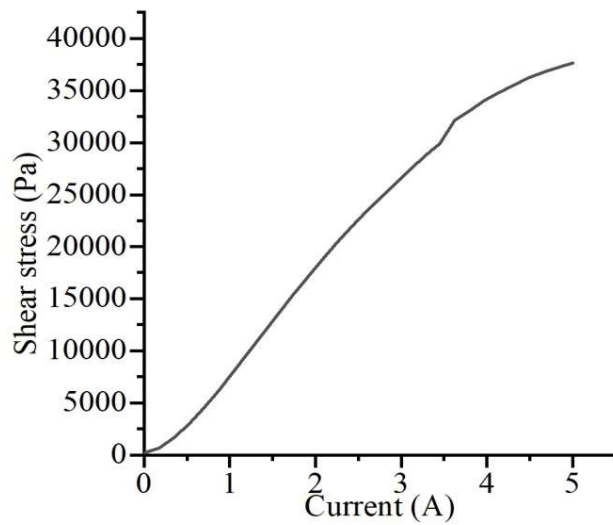
(a)
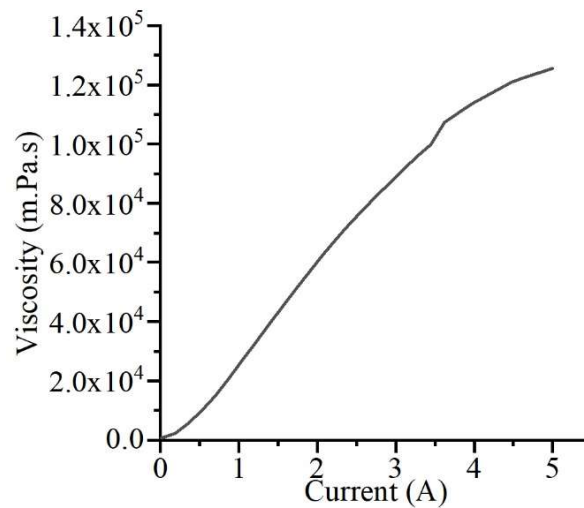
(b)

Figure 5.15 (a) Shear stress and (b) viscosity variation against current sweep

The current input is varied linearly from 0.01A to 5A and the response can be observed in figure 5.15.

With the current sweep, the shear stress rose from 245 Pa to 37,613 Pa and the viscosity increased from 819 mPa.s to 125,450 mPa.s. It is evident from the rheological characterization that the MR fluid responded well to the external magnetic field. It can also be observed from figure 5.15 that even though the current sweep was linear, the shear stress and the viscosity variation have deviated from linearity after a certain point. This can be attributed to the saturation limit of ferrous particles against the magnetic field application (Acharya et al. (2017)).

5.8 CHARACTERIZATION OF MR DAMPER WITH MRF-2

To understand the dynamic behavior of the MR damper, characterization of the assembled damper is performed for various harmonic inputs on a dynamic testing machine.

The MR damper is subjected to harmonic excitations with varying amplitudes and frequencies. Along with these, the performance of MR damper is observed for different current excitations varying from 0 A (off-state) to 1 A in steps of 0.25 A.

The current input to the damper is provided by DC power supply. For the sake of brevity, characterization results related to 10 mm amplitude and 2 Hz frequency for varying current inputs are provided. The characterization testing is performed for the sinusoidal input. The characterization results can be observed in figure 5.16.
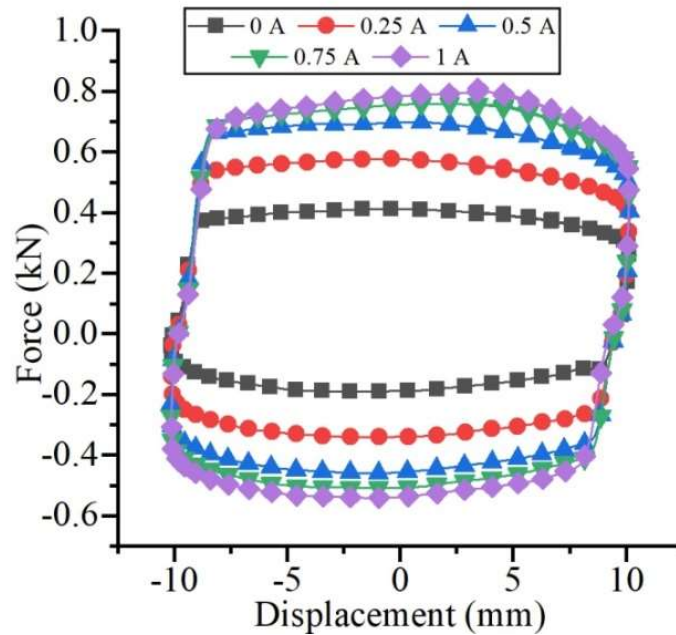
Figure 5.16 Damper characterization at different currents

From the MR damper characterization results, it can be observed that the total damping force developed is around 411 N (rebound) and -191 N (compressive) in the off-state condition. In the same way, 808 N (rebound) and -540 N (compressive) damping forces were recorded at 1A current input to the MR damper piston. A significant difference was observed when the MR damper was tested at other current conditions too (figure 5.16). A dynamic range (ratio of on-state to off-state force) of 2.3 was obtained for this design, which is on par with other dampers designed for vehicular applications (Yu et al. (2006), Devikran et al. (2021)).

5.9 CONTROLLER

The controllers used for controlling the current inputs to the MR damper are discussed below.

5.9.1 Skyhook control

This is a simple on/off strategy which switches between high and low damping coefficients in order to achieve the required levels of comfort or road holding (Akutain (2007)). The control law is given by the equation,

$$c_{in} = \begin{cases} c_{min} & if \ \dot{z}\dot{z}_{def} \leq 0 \\ c_{max} & if \ \dot{z}\dot{z}_{def} > 0 \end{cases} \qquad (5.5)$$

Here, c_{min} is the minimum damping constant equivalent to zero current, c_{max} is the maximum damping constant equivalent to high current, $\dot{z}$ is the sprung mass velocity and $\dot{z}_{def}$ is the deflection velocity. From an implementation point of view, it requires two measurements and thus two sensors for each wheel.

5.9.2 Acceleration driven velocity (ADV) control

Recent studies showed that road profile and surface condition can be estimated using the longitudinal acceleration of the car body. It was demonstrated that there is a correlation between the mean amplitude value of the body acceleration to that of road surface roughness (Prażnowski et al. (2020)). Using this result, the current supplied to the damper, subsequently the damping constant was controlled based on the RMS values of sprung mass accelerations. As only one sensor is required to measure the body acceleration, this will consequently reduce the overall cost of the controller.

In this control strategy, the damping constant is set to low when the RMS value of sprung mass acceleration increases above a threshold value, otherwise it is regulated to a maximum as given by the following equation 5.6.

$$c_{in} = \begin{cases} c_{min} & if \ \ddot{z}_{RMS} \geq a_{threshold} \\ c_{max} & otherwise \end{cases} \qquad (5.6)$$

Here, $a_{threshold}$ is the acceleration threshold which can be user controlled.

5.10 QUARTER CAR MODEL AND ANALYSIS

One of the simplest ways of analyzing the suspension performance is through the quarter car model.

Table 5.2 Quarter car simulation parameters (Tharehallimata et al.(2018))

Parameter	Value (units)
m_1	600 (kg)
m_2	75 (kg)
k_1	30000 (N/m)
k_2	300000 (N/m)
c_1	1516 (Ns/m)
c_2	0 (Ns/m)
c_{max}	4000 (Ns/m)
c_{min}	700 (Ns/m)

The mathematical model of quarter car model is:

$$m_1\ddot{z}(t) + k_1(z - z_t) + c_1(\dot{z} - \dot{z}_t) = 0$$

$$m_2\ddot{z}_t(t) - k_1(z - z_t) - c_1(\dot{z} - \dot{z}_t) + k_2(z_t - z_r) + c_2(\dot{z}_t - \dot{z}_r) = 0 \qquad (5.7)$$

Here, m_1 is the mass of sprung mass, m_2 is the mass of unsprung mass, k_1 is suspension spring constant, c_1 is the suspension damping constant which is being modulated by the controller, k_2 is the tire stiffness, c_2 is the tire damping, z is the sprung mass deflection, z_t is the unsprung mass deflection and z_r is the vertical deflection of road. The parameters used in the study are given in Table 5.2.

5.11 COMPARISON METRICS

To compare responses generated by various control algorithms, a method detailed in Savaresi et al. (2010) is used. The method is described below.

1. A sinusoidal road input given by equation (7.4) is fed to the quarter car model over a period of 10 cycles.

$$z_r = A\sin\left(2\pi ft\right)$$

<div align="right">(5.8)</div>

Here, A is the amplitude of the road profile, f is the frequency and t is time in seconds in the range $[0, 10/f]$.

2. The corresponding output displacement plots of sprung mass (z) and relative displacement of tire ($z_{rel} = z_t - z_r$) are recorded.

3. Power spectral densities of road input (Z_r), sprung mass displacement (Z) and relative tire displacement (Z_{rel}) are evaluated.

4. The corresponding frequency plots for ride comfort and road holding are generated as ratios $\dfrac{Z f)}{Z_r(f)}$ and $\dfrac{Z_{rel}(f)}{Z_r(f)}$ for all road input frequencies, $Z_r\left(f\right)$.

This methodology allows to derive Bode like diagrams for nonlinear systems and thus can be used in comparative studies of control algorithms.

5.12 EXPERIMENTAL TESTING ON QUARTER CAR

The developed MR damper has its compatibility in terms of dimension with the suspension system of a definite light motor vehicle. This work used the McPherson suspension system for the damper installment. This suspension is then fit along with other components required in a quarter car set up. The quarter car set up with the MR damper in the McPherson suspension is picturized in figure 5.17.
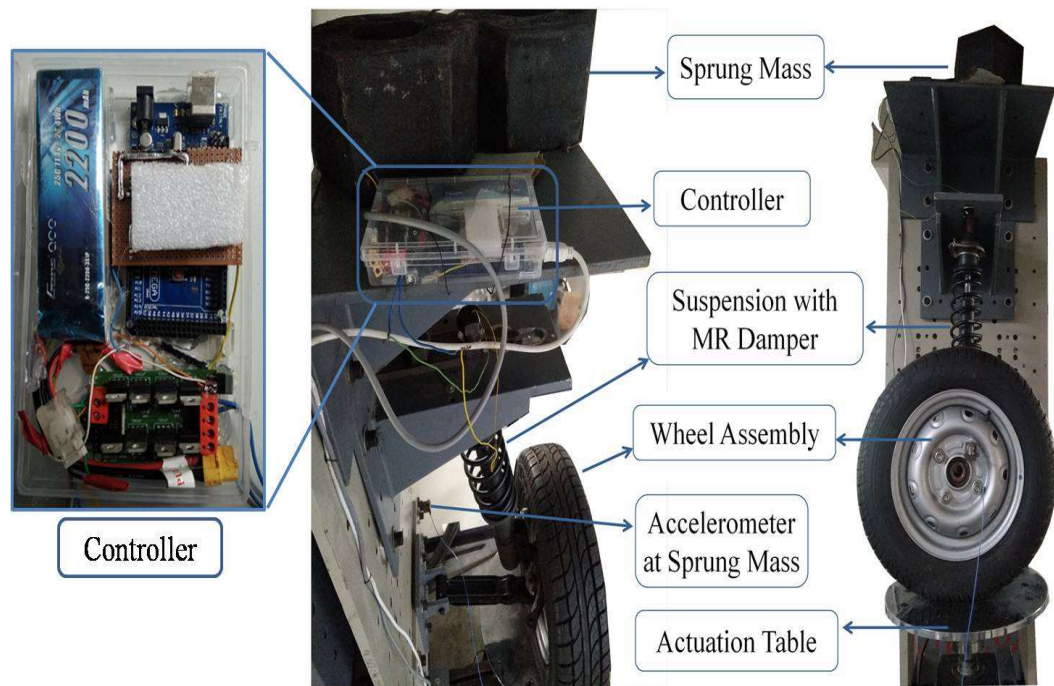
Figure 5.17 Quarter car set up

The sprung mass is placed over the suspension system and the sprung mass was set to be 210 kgs which represents the quarter mass of a commercial light motor vehicle. The spring element was the commercially available one which came along with the McPherson system of the vehicle.

The vibration measurement in terms of acceleration was carried out by placing an accelerometer on the sprung mass as shown in the figure 5.17. The actuation table of the quarter car set up imitates the road profile and the actuation is provided through hydraulic power. A data acquisition independent of the controller records the acceleration and displacement profiles of sprung, unsprung and road (actuation table) to be later used for analysis. While the accelerations are acquired through NI 9234 DAQ, displacements are recorded using LVDT and are monitored through LabVIEW software.

Due to experimental limitations and to avoid excessive vibrations, experiments have only been carried out in the range of 1 to 7 Hz in the interval of 0.1Hz and for an

amplitude of 10 mm in a sinusoidal profile. A compact controller has been developed to supply input current to the controller as shown in the figure 5.18.
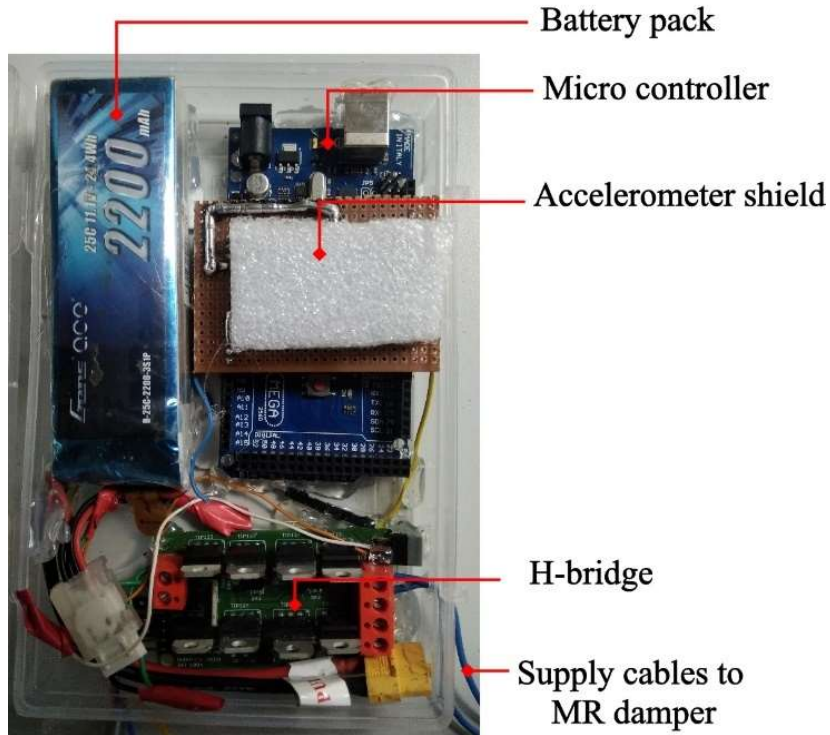
Figure 5.18 Compact controller developed

The controller consists of an arduino microprocessor, GY61 accelerometer sensor, a 12V DC power supply, and an H-bridge module. Based on the acceleration values of the sprung mass, the input current to the MR damper is regulated on-off corresponding to (C_{max}, C_{min}) damping constant. For a sampling frequency of 1000 Hz and RMS calculations for a moving window of 500 time steps was considered. Since the moving window is kept constant and to avoid redundant calculations, sum of square (SS) values of accelerations in the moving window are used instead of RMS values. The following steps which make use of previous time step calculations are used.

1. Initialize the parameters, *BufferSize* = 500, *counter* = 0, array *AR*[*BufferSize*] = 0.

2. Record the acceleration sensor reading in the variable *z*.

3. Calculate the sum of square values,

   *SS= RMS + z*z – AR [counter] * AR [counter]*.

4. Initialize *AR[counter] = z*.

5. Increment *counter* value.

6. Reinitialize the value of *counter* to 0, if *counter<BufferSize* – 1.

7. Regulate damper current based on *SS* values and repeat the process.

5.13 RESULTS AND DISCUSSION

Numerical studies have been performed for a displacement of 10 mm and nonlinear frequency plots for ride comfort and road holding are generated.
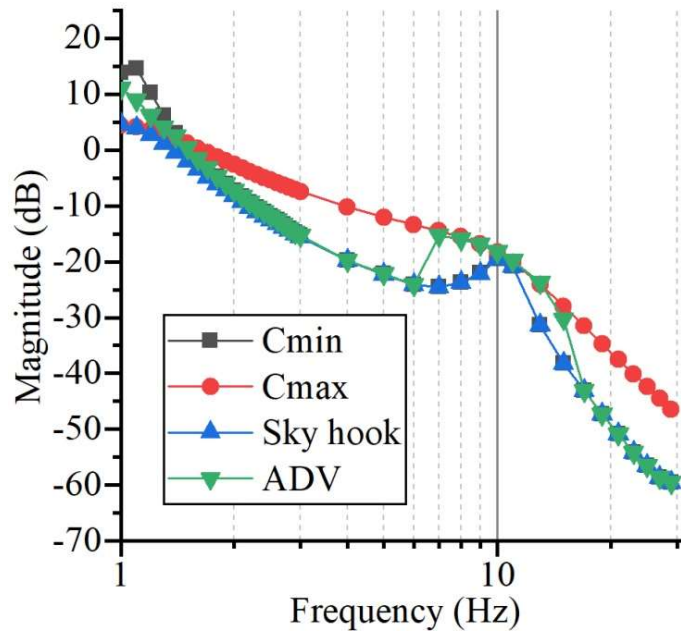
(a)
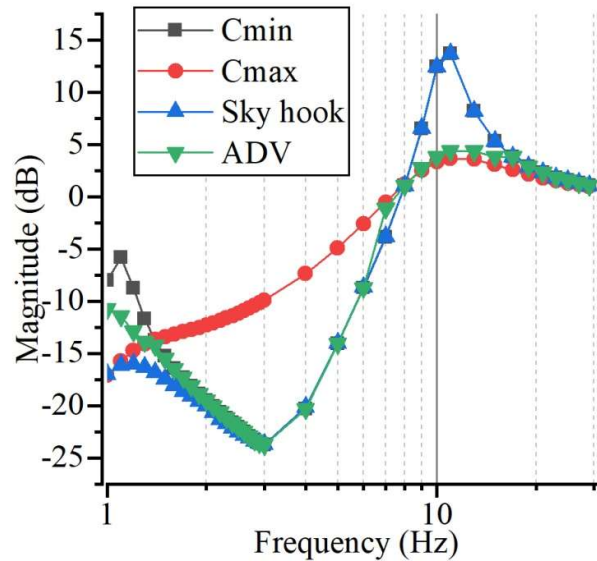
(b)

Figure 5.19 Frequency responses for (a) ride Comfort and (b) road holding

An acceleration threshold of 0.35 m/s² has been used to demonstrate the effect of the control algorithm. Additionally, the skyhook control algorithm has also been implemented.

As shown in the figure 5.19, for low frequencies [1 1.4], best filtering is obtained by stiff damping whereas, soft damping results in large attenuation and thus results in less comfort. The skyhook controller has better ride comfort for higher and lower frequency components as well. The proposed ADV controller has an intermediate response in low frequency range and a response similar to skyhook controller in high frequency range.

Based on frequency plots for road holding, for higher frequencies [8 17], soft damping results in degrading road holding whereas stiff suspension results in better filtering. Further, as expected the skyhook controller results in worse road holding similar to soft damping in higher frequency ranges. On the other hand, the proposed controller has an almost similar performance to that of stiff damper and thus results in better road holding characteristics. Thus the controller works better for improving both road holding and ride comfort.

The experimental results for nonlinear ride comfort at various frequencies are shown in figure 5.20. The controller 'C1' has been set with an acceleration threshold of 0.25 m/s^2 whereas the controller 'C2' has been set with a threshold of 0.35 m/s^2. As seen from the figure 5.20, the controller is able to switch from off state to on state at a frequency of 4.4 Hz.
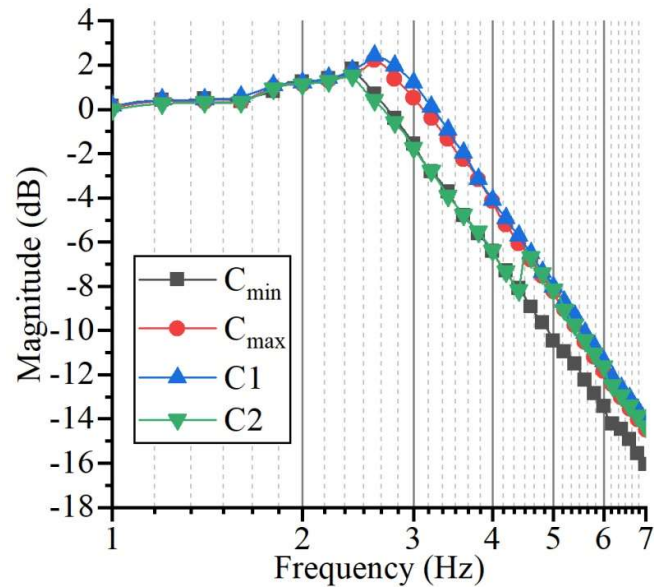
Figure 5.20 Experimental nonlinear frequency ride comfort characteristics

The RMS accelerations of sprung mass crosses the limit of 0.35 m/s^2 after this frequency and thus the suspension adapts from soft to stiff damping. Due to experimental limitations, road holding and also responses for random inputs could not be performed. However, the experimental results for rider comfort show a similar trend as that of simulation results.

5.14 SUMMARY

This chapter presents simulation as well as experimental analysis of the suspension with MR damper in a quarter car system. Initially, a quarter car model was built using MATLAB/Simulink where the tire and the spring properties were substituted based on the characterization result. To imitate the MR damper semi-active nature, the Kwok model was used in the quarter car model. The quarter car was excited using the sinusoidal road profile and at currents of 0A, 1A and through skyhook controller. The

excitation was provided at 1Hz, 2Hz and 3Hz operational frequencies. The performance of MR damper with skyhook controller was found at least 10% better when compared to the off-state condition.

The MR damper was then implemented in quarter car experimental set up to validate the simulation results. To excite the quarter car, similar input conditions were provided in terms of dynamic input or current input. A skyhook controller was developed and implemented during the experimentation. Again, MR damper with skyhook controller performed significantly well when compared to off-state condition. The error plots between the experimental and the simulation results showed that the errors were within 20% except for one case. The inconsistent variation in the error may be due to the non-linearity of MR damper. As an extended part of the work, the suspension with MR damper was excited through trapezoidal road profile. The improvement in performance was again observed with skyhook controller when compared to off-state condition.

This chapter also narrates the single sensor method in the control logic for the quarter car system with the MR damper. This study has been the extended portion for the previous work. Initially, MR fluid sample was prepared in-house for this study using carbonyl iron particle (CIP) and polyalpha olefin as the carrier fluid. The rheological studies revealed a clear distinguish between the shear stress at different current inputs. Maximum shear stress of 49,175mPa was recorded at magnetic field corresponding to 3A current input. With this MR fluid, the MR damper was characterized at 2Hz operational frequency with sinusoidal input.

To reduce the cost incurring due to usage of multiple number of sensors, an acceleration driven velocity (ADV) controller was derived and used in quarter car simulation as well as experimental set up. The quarter car testing was carried out in the range of 1 to 7 Hz for better analysis. The proposed controlled proved to be a better controller in providing better ride comfort as well as road holding when compared to skyhook controller.

CHAPTER 6

ON ROAD TESTING OF CAR WITH MR DAMPER

6.1 INTRODUCTION

An important objective of this study is to implement magneto-rheological damper into a four wheeler vehicle. This chapter elaborates the MR damper execution in the suspension of a four wheeler test vehicle and its on-road testing. This chapter illustrates the response of the vehicle when tested with two different velocities and run over a road bump. Also, the response of the sprung mass when the MR damper is tested with three different current inputs is discussed. Finally the assessment of the comfort quantification is provided on the basis of ISO 2631 standard.

6.2 IMPLEMENTATION OF MR DAMPER INTO VEHICLE

One of the salient features of this study lies in implementation of developed mono-tube MR damper in the front suspension of a four wheeler vehicle and more importantly, its on-road testing.

Characterized mono-tube MR damper was fitted into the McPherson suspension system at the front half of the four wheeler vehicle (vehicle model: Maruti 800). During the fabrication of the damper, a care was taken about the outer dimensions of the damper so that it can fit into the suspension system of the vehicle.

The passive damper existing in McPherson suspension system was replaced by the developed MR damper as shown in figure 6.1. The MR damper was implemented in both sides of the front half of the vehicle in the McPherson system. This was done to provide a balancing effect on both sides.

(a)

(b)

Figure 6.1 (a) Test vehicle used for on-road testing, (b) McPherson strut with passive damper in the vehicle

6.3 ON-ROAD TESTING OF THE VEHICLE

The four wheeler vehicle was run on road after implementing the mono-tube MR damper into its McPherson suspension system.

Figure 6.2 MR damper in the McPherson strut system in the vehicle
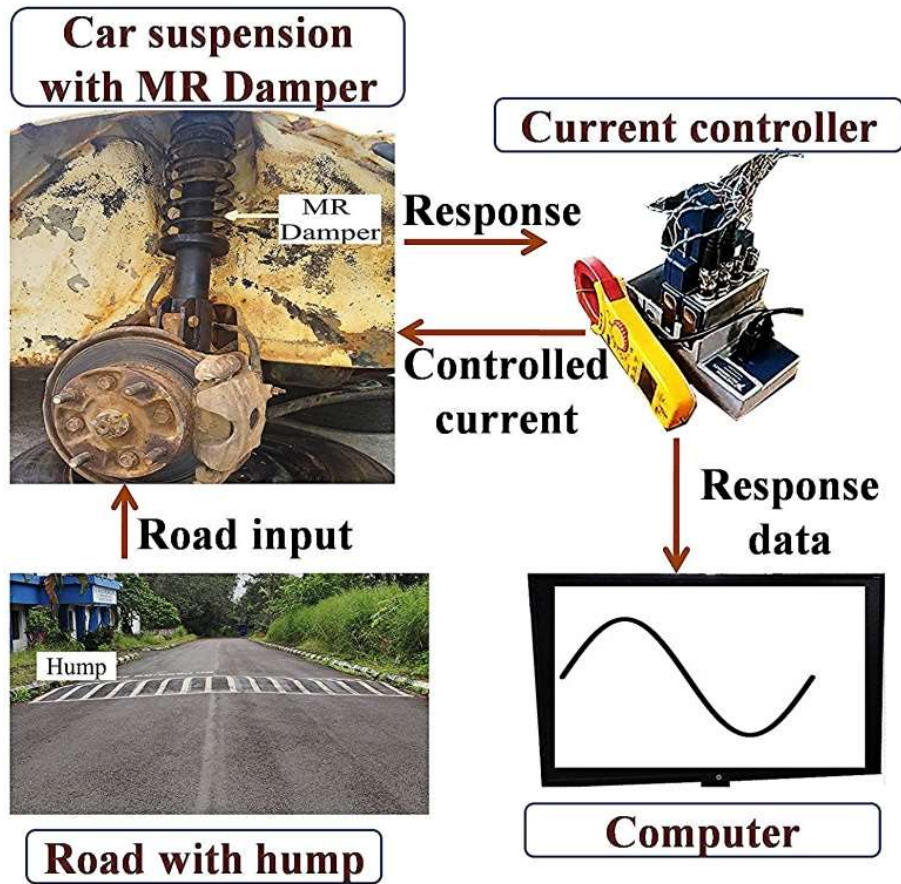
Figure 6.3 On road testing scheme
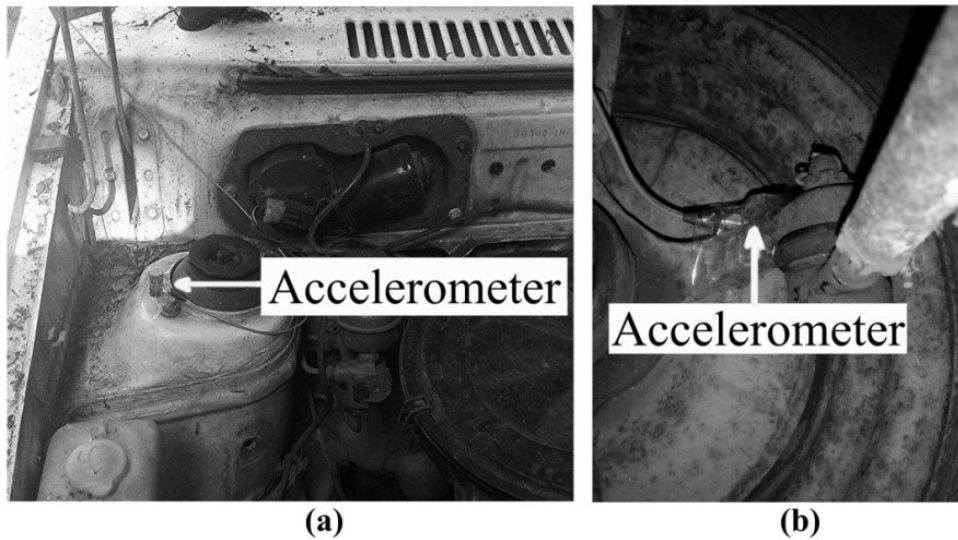
Figure 6.4 Mounting accelerometers on (a) sprung and (b) unsprung mass

For on-road testing of the vehicle, a road surface was selected such that the vehicle encounters at least one hump during its run time. Since the study concentrates only on the vertical vibration of the vehicle, a straight road was selected for test runs.

The road on which the vehicle run was performed is shown in figure 6.3. During on-road testing of the vehicle with MR damper, certain distance was utilized to reach the required velocity of the vehicle. Hence, on an average of 50 meters of road length was used for test run (including the hump). The same profile and path were maintained for all test runs for every condition. To ensure good accuracy and minimum experimentation errors, the vehicle was run twice for every test condition. The results showed repeatability in every test condition with negligible difference.

For the purpose of data acquisition during vehicle test run, accelerometers were attached on sprung and unsprung masses as shown in figure 6.4. Accelerometers were mounted in a vertical position on both sprung and unsprung masses for acquiring vertical acceleration data. The accelerometer was mounted on sprung mass near the top end of the McPherson suspension system as shown in figure 6.4(a).

The performance of MR damper in the four wheeler vehicle was tested with two different velocities: 20 kmph and 30 kmph. It was ensured that data acquirement starts only after the vehicle attains desired velocity. During each velocity condition, the MR

damper was tested without supply of current, with 1A current supply and supply of current through sky-hook and ground-hook controllers separately. During these test runs, the acceleration was recorded using data acquisition system (DAQ) from National Instruments. These acceleration data are helpful in deciding the ride comfort provided by semi-active suspension system with MR damper.

6.4 RESULTS OF ON-ROAD VEHICLE TESTING

This study focuses on the performance of monotube MR damper when fitted into the suspension system of four wheeler vehicle. The acceleration data acquired during the test run is the key factor in understanding the ride comfort level. The vehicle with MR damper was experimented at 20 kmph and 30 kmph respectively, for every current supply condition. Figure 6.5 (a) and figure 6.5 (b) provide sprung mass accelerations at 20kmph and 30kmph respectively.
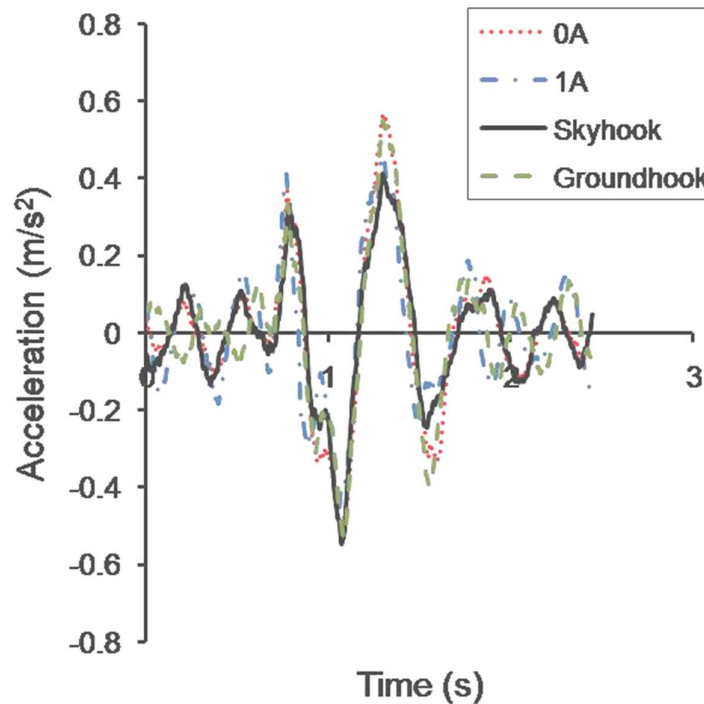
(a)
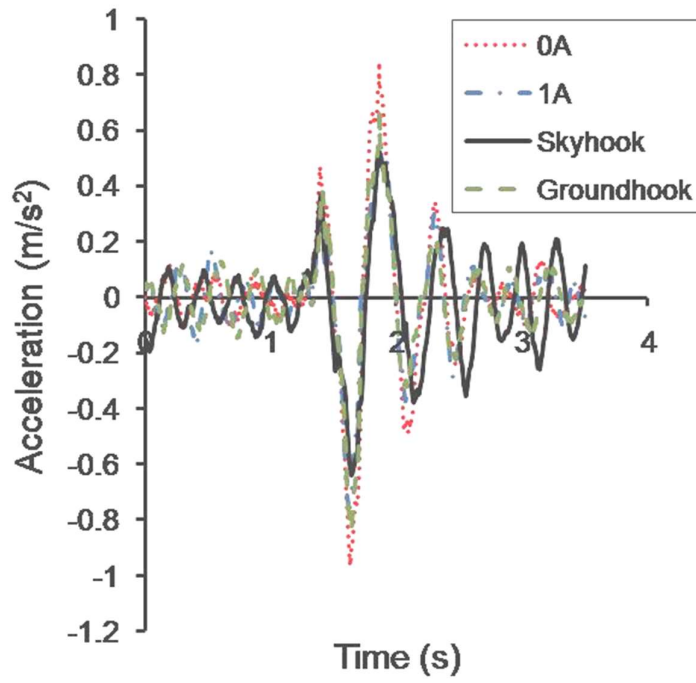
(b)

Figure 6.5 Sprung mass acceleration in time domain at (a) 20 kmph and (b) 30 kmph
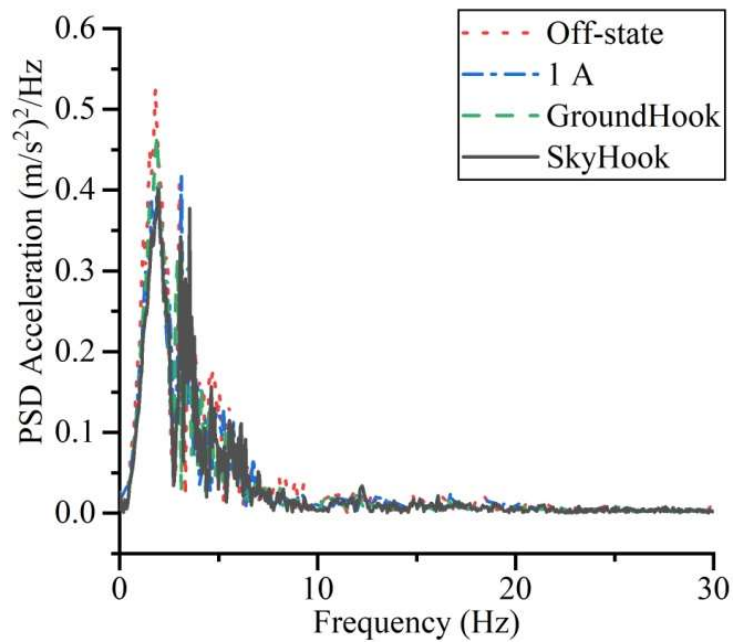
(a)
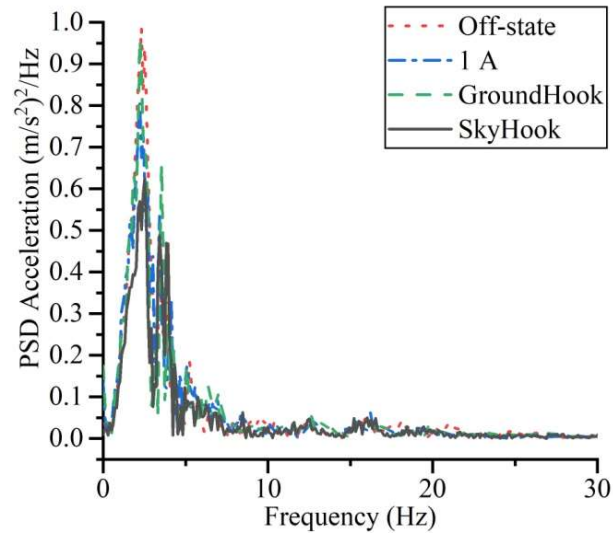
(b)

Figure 6.6 Acceleration data for different current supply condition at (a) 20 kmph and (b)30 kmph.

The time domain acceleration data could not provide a clear idea on comparative performance at different conditions. Hence these data were converted into frequency domain data for better understanding. The sprung mass acceleration data at 20kmph and 30 kmph velocity are shown in figure 6.6.

From the figure 6.6, it can be observed that all acceleration peaks were identified at frequency of about 2Hz. In both cases (20 kmph and 30 kmph), the peak acceleration recorded was less than 1 m/s^2 and maximum peak value was recorded when there was no supply of current to MR damper (off-state condition).

Obtained vehicle data can be utilized to understand the comfort level provided by MR damper in the suspension system when evaluated according to ISO 2631 standard. This work utilizes ISO 2631-1:1997 standard which relates human exposure to whole body vibration. This standard uses weighted frequency accelerations for ride comfort assessment. Frequency weighting curve in the scale 1 to 80 Hz according to this standard is shown in figure 6.7.
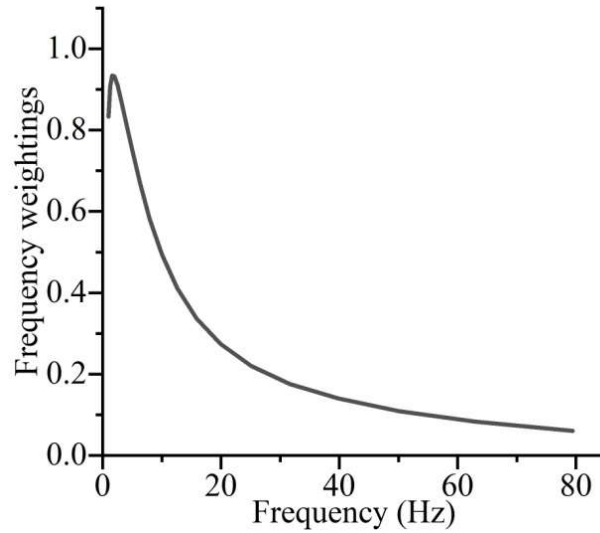
Figure 6.7 Frequency weighting curve based on ISO 2631 standard (1-80 Hz)

Using the curve as shown in figure 6.7, frequency weightings are applied to acceleration data according to the frequency. The root mean square (RMS) of these weighted accelerations (equation 6.1) is the key to decide ride comfort level.

$$a_w = \left[\frac{1}{T} \int_0^T (a_w(t))^2 dt \right] \tag{6.1}$$

Where, a_w is the weighted RMS acceleration, $a_w(t)$ represents weighted acceleration in time domain, T is the time duration of the data measurement.

The peak point of the acceleration can be calculated using maximum transient vibration value (MTVV) which is expressed in equation 6.2.

$$MTVV = \max|a_w(t)| \tag{6.2}$$

The ride comfort of a passenger can be categorized based on range weighted RMS acceleration as per ISO 2631. Table 6.1 provides categories of comfort level.

Table 6.1 Comfort level based on range of weighted RMS acceleration

Magnitude of Weighted RMS acceleration, a_w (m/s^2)	Comfort feeling
Less than 0.315	Not uncomfortable
0.315- 0.630	A little uncomfortable
0.5- 1	Fairly uncomfortable
0.80- 1.60	Uncomfortable
1.25- 2.50	Very uncomfortable
Greater than 2	Extremely uncomfortable

The weighted RMS accelerations (a_w) and maximum transient vibration value (MTVV) for all the test runs were calculated using equations 6.1 and 6.2. The frequency weighting factor has been considered using frequency weighting curve. Table 6.2 provides weighted RMS acceleration and MTVV for all the test conditions.

Table 6.2 provides performance comparison of MR damper subjected to different test run conditions at different velocities. It is clear from the table 6.2 that ride experience in all the test conditions are showing good comfort level by falling in category of 'Not uncomfortable' zone. Thus, the designed and developed MR dampers are serving the purpose well enough to provide good ride comfort. At 20 kmph velocity, 20.1% of reduction in the weighted RMS acceleration is identified with usage of sky-hook controller when compared alongside off-state situation. Similarly, 26.12% improvement in ride comfort is observed at 30 kmph velocity with sky-hook controller in comparison with off-state mode. It can be seen that the ride comfort is better with usage of sky-hook controller when compared to constant current supply of 1A at both velocities. But, ride comfort with 1 A current supply was comparatively better than current supply using ground-hook controller.

Table 6.2 Performance comparison in different conditions

Velocity (kmph)	Current supply criteria	a_w (m/s^2)	MTVV (m/s^2)	Remarks
20	0 A	0.12	0.501	Not uncomfortable
20	1 A	0.098	0.512	Not uncomfortable
20	Sky-hook	**0.092**	0.375	Not uncomfortable
20	Ground-hook	0.102	0.502	Not uncomfortable
30	0 A	0.181	0.930	Not uncomfortable
30	1 A	0.14	0.520	Not uncomfortable
30	Sky-hook	**0.133**	0.53	Not uncomfortable
30	Ground-hook	0.147	0.585	Not uncomfortable

Maximum transient vibration value (MTVV) has also followed similar trend as that of weighted RMS acceleration. Magnitude of MTVV is showing reducing nature with usage of sky-hook control logic. With supply of current, weighted RMS acceleration and MTVV have reduced when compared to off-state condition serving the purpose of magneto-rheology in a significant way. The control logics used in this study enhanced the performance of MR damper, even being conventional control algorithms.

The acceleration experienced at the unsprung mass was also obtained for different category of current supply as shown in figure 6.8.

(a)

(b)
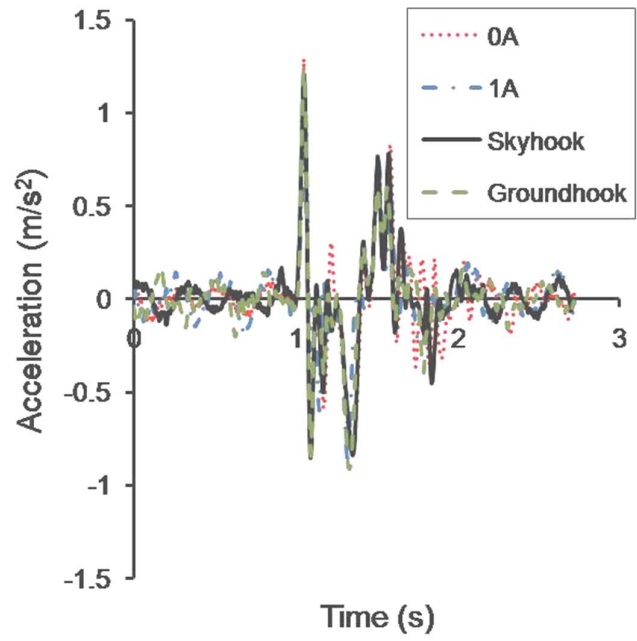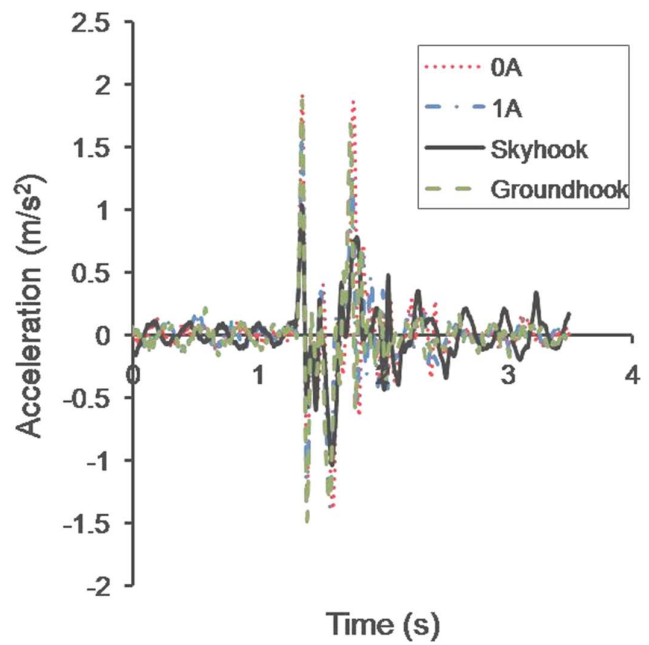
Figure 6.8 Unsprung mass acceleration in time domain at (a) 20 kmph and (b) 30 kmph
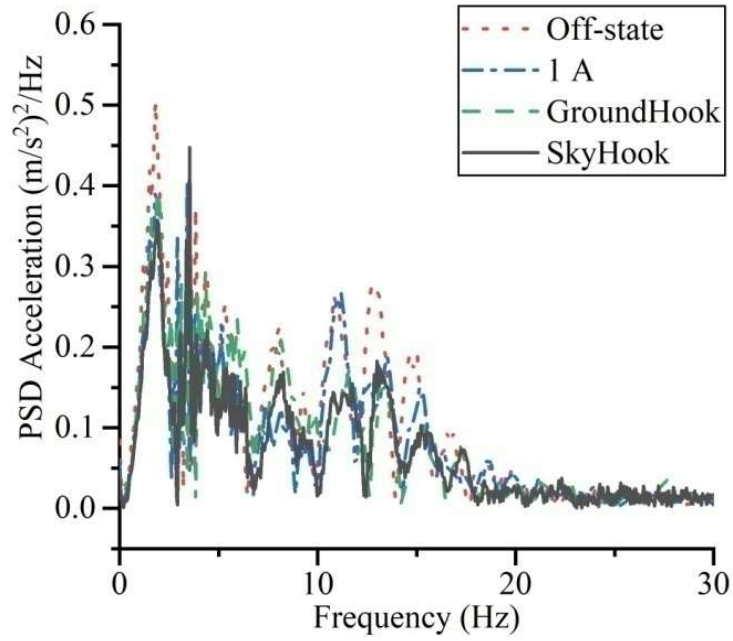
(a)
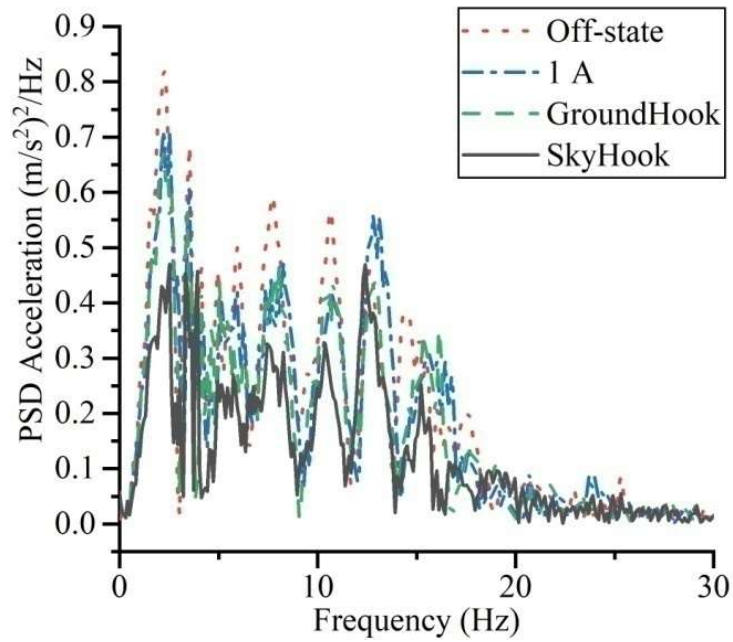
(b)

Figure 6.9 Unsprung mass acceleration at (a) 20kmph and (b) 30 kmph velocity

The figure 6.9 also reveals the vibration nature experienced by the unsprung mass at different frequencies due to several noisy components. The nature of acceleration reveals that the control logics were useful in significant reduction of vibration at unsprung mass too, at both velocity conditions. At 20kmph, the RMS accelerations observed were 0.1455 m/s^2 without current supply and 0.1296 m/s^2 with skyhook control system showing 11% reduction in acceleration. Similarly, 20.24% reduced RMS acceleration was observed with control system upon off-state condition at 30 kmph.

6.5 SUMMARY

This chapter discusses one of the important phases of this research namely MR damper implementation in vehicle and on-road testing. The passive damper in the McPherson suspension of the test vehicle was replaced by the developed MR damper. The on-road testing of the vehicle was performed over a road with bump at two different velocities. Accelerometers were attached at sprung as well as unsprung masses for the vertical vibration measurement. The on-road testing was performed at three current input conditions: off-state, 1A and current through skyhook controller and through groundhook controller.

The ride comfort assessment for the on-road testing was carried out on the basis of ISO 2631 standard. Along with ride comfort assessment, the MTVV was also calculated for every running condition. The ride comfort was improved by 20.1% and 26.12% with the usage of skyhook controller against off-state mode at 20 kmph and 30 kmph speed respectively.

CHAPTER 7

SUMMARY AND CONCLUSIONS

7.1 SUMMARY

The research work reported in this work is summarized under different sections and the conclusions are stated based on the results obtained.

7.1.1 Development of MR damper for vehicular application and characterization

Initially, magneto-rheological (MR) fluid was prepared using electrolytic iron particles (EIP) and paraffin oil. The rheological nature of the in-house prepared fluid was tested using the rheometer and the shear stress variation with the current input was analyzed. An MR fluid damper was initially designed based on the Bingham theory for different forces due to fluid resistance. The damper was of monotube and shear mode type and with spring accumulator. The dimensions of this shear mode damper piston were determined by optimizing the geometric dimensions according to the Bingham criteria and dynamic range considerations. The piston with optimized dimension was analyzed for magnetic flux density in the fluid flow gap using FEMM software. The MR damper as well as the piston were developed by considering the optimized dimensions. The developed MR damper was characterized in the dynamic testing machine (DTM) under different amplitude, frequency and current conditions. The characterization results showed a significant improvement in the damping force with increase in current input to the electromagnetic piston.

7.1.2 Mathematical modeling and quarter car implementation of the MR damper

The damping force variation of MR damper after characterization was mathematically modeled by using a parametric modeling technique known as Kwok modeling technique. The parameters of this mathematical model were determined for every characterization case. The parameters were identified using genetic algorithm (GA) optimization technique by minimizing the error between experimental and theoretical results. Later, these parameters were converted into current dependent parameters by establishing the correlation between model parameters and the input current. A

quarter car model was built with the help of MATLAB/Simulink where the MR damper was represented in terms of Kwok model. The quarter car model was excited with sinusoidal road profile at different amplitude and current conditions. The current input to the MR damper was with three cases: off-state, 1A current and current through skyhook control. The results of this analysis were validated by testing the MR damper in the quarter car setup of a definite vehicle. The performance with MR damper with skyhook control showed considerable improvement when compared to off-state condition.

7.1.3 On-road testing of vehicle with MR damper

After testing in the quarter car test set up and analyzing the results, the MR damper was then implemented in the front suspension of the desired test vehicle. For this purpose, the passive damper in the McPherson suspension was replaced by MR damper in the front suspension of the vehicle. The vehicle was run over the road with bump and the test run was conducted at two velocities: 20kmph and 30kmph. The test run was conducted using skyhook controller too. The comfort level at the sprung mass was quantified with the help of ISO 2631 standard. The MR damper with skyhook controller performed considerable well when compared to off-state condition at both velocities.

7.1.4 Single sensor controller in quarter car

As an extended part of this research an attempt was made to develop a cost effective sensor for vehicular application. The higher cost incurring due to multiple sensor in a control system was reduced by using an acceleration driven velocity (ADV) controller. This controller was derived and implemented in the quarter car system analytically as well as experimentally. The testing with quarter car was conducted from 1 to 7 Hz in the interval of 0.1 Hz to see the effectiveness of derived controller to achieve ride comfort and road holding. The results revealed a significant improved performance of the suspension with derived controller against the conventional skyhook controller towards better ride comfort as well as vehicle stability.

7.2 CONCLUSIONS

Following were the conclusions drawn from the study on development of MR damper and its implementation in the quarter car and the on-road testing.

- Passive damper characterization results revealed an obvious increase in the total damping force with increase in operational velocity and the damping coefficients increased due to higher hysteresis. Maximum damping force was observed for 20 mm amplitude and 1.5 Hz condition and was about 480 N at rebound stroke.

- The small stroke MR damper (prototype-1) was designed on the aim of developing 3kN maximum damping force and with a dynamic range 3. But the results indicated the other way. This may be due to less accuracy during the manufacturing of damper. The piston was covered with a non-magnetic metal sheet to avoid leakage of MR fluid into the piston and piston rod. This may also be the reason behind not getting the desired force.

- Also, at higher operational frequencies, the dynamic range was observed narrowing for small stroke damper. It suggests its suitability at lower operational velocities than higher ones. Maximum damping force observed was 1.25 kN at 15 mm amplitude, 2.5 Hz operational frequency and 1.25 A current.

- The slope in the correlation between the damping coefficient of prototype-1 damper and the current became narrower and narrower as the operational amplitude increased. Again it suggests its preferable use in low stroke applications.

- The in-house prepared MR fluid showed a reasonable rheological result in terms of shear stress variation with varying current. When overlapped with commercially available MR fluid, the rheological properties of the in-house prepared MR fluid were very much comparable in terms of shear stress magnitude and viscosity variation. Therefore, the in-house prepared MR fluid can be effectively used in the semi-active damper applications.

- The electromagnetic piston was designed for dynamic range of 3 and the characterization results revealed the achievement of dynamic range of about 2.5. This denotes the satisfactory working of in-house prepared MR fluid inside the damper. Further closeness of the dynamic range may be possible by using still better magnetic permeable material for the piston development.

- The occurrence of lateral shift observed in case of small stroke MR damper was seen minimized in the actual scale prototype. This suggests acceptable performance of spring accumulator used in the MR damper. The proper usage of spring accumulator may reduce a reasonable cost when compared to a gas charged accumulator.

- The Kwok theory used in modeling the hysteresis of the MR damper was effective in achieving very close match against experimental results. As described in the literature, this modeling technique can be a helpful tool when compared to a well established Bouc-Wen model in terms of model efficiency as well as computational time due to less number of shape deciding parameters.

- Experiments through the quarter car set up revealed atleast 10% improvement in terms of sprung mass acceleration reduction when used with skyhook controller against off-state condition. Even though the skyhook controller is considered to be one of the traditional or oldest semi-active controllers, the effectiveness of the control logic is unquestionable. The simplicity of the skyhook logic makes it one of the economic controllers and hence can be effectively used to achieve semi-active working nature in a reduced cost.

- The quarter car simulation used the value of spring and tire from the characterization results. The error plot of the quarter car analysis showed irregular deviations for some of the operational conditions. This deviation may be due to non-linearity in the tire element and variation between the theoretical Kwok model and the experimental results.

- Implementation of MR damper was done into the McPherson suspension of the four wheeler vehicle for the front side of the vehicle. The suspension performance was analyzed at two different velocities: 20kmph and 30kmph. The ride comfort quantification showed most of the experimental conditions into 'not uncomfortable' zone. But quantitatively MR damper with skyhook controller registered 20.1% as well as 26.1% improved performance when compared to off-state mode at 20kmph and 30kmph velocity respectively.

- An extended part of the study showed effective implementation of control strategy to the MR damper by using single sensor in the scheme. The quarter car analysis with MR damper by using single sensor control scheme showed its effectiveness in achieving better ride comfort and the road holding with much reduced cost. Here, the proposed controller worked really well in improving the road holding when compared to skyhook controller. The proposed ADV controller found working really well at higher frequency range than lower frequency ranges.

7.3 CONTRIBUTIONS

- The methodology proposed here can be effectively used to utilize the iron particles to prepare the MR fluid in-house and to use it as the damping media in MR dampers.

- The literature related to MR dampers lacks the utilization of spring accumulator for MR dampers. The force versus displacement nature of the MR damper reveals the effective utilization of spring accumulator in the damper and this may reduce the cost of the damper further.

- This study implemented Kwok theory to model the hysteresis of MR damper which contain less number of shape deciding parameters when compared to well known Bouc-Wen model. Even though, the Kwok theory is very much efficient and time saving tool, literature lacks its usage in the MR damper study.

- This study used two hardware control schemes: skyhook and single sensor control scheme (ADV). The methodology can be effectively used or referred in the development of control schemes to MR damper or any other MR fluid related engineering applications.

7.4 SCOPE FOR FUTURE WORK

- The study used McPherson system for implementation of MR damper in the suspension scheme. The study may be extended for other types of suspension systems also and the analysis can be extended with other types of test vehicles too.

- The hysteresis behavior of the MR damper was mathematically modeled using a parametric modeling technique known as Kwok model. Literature narrates the superiority of non-parametric techniques also (eg: neural networks) and the study may be extended with those modeling techniques.

- The study considered vertical vibration of sprung and unsprung masses over a straight road for the analysis purpose. Other translatory and rotary motions may also be considered over the straight as well as curved paths in the extended part of the study.

- The single sensor control strategy used in the work found to be efficient to improve the ride comfort and the road holding when compared to skyhook strategy. The study may be extended to analyze its performance against other control strategies and further possibilities may be seen to reduce the cost of the control scheme further.

REFERENCES

Abdelhafez, H. M., and Omara, O. (2017). "Controlling quarter car suspension system by proportional derivative and positive position feedback controllers with time delay". *J. Vibroeng.*, 19(7), 5374-5387.

Acharya, S., Saini, T. R. S., and Kumar, H. (2019). "Determination of optimal magnetorheological fluid particle loading and size for shear mode monotube damper". *J. Braz. Society Mech. Sci. Eng.*, 41(10), 1-15.

Acharya, S., Saini, T. R. S., Sundaram, V., and Kumar, H. (2021). "Selection of optimal composition of MR fluid for a brake designed using MOGA optimization coupled with magnetic FEA analysis". *J. Intell. Mater. Syst. Struct.*, 32(16), 1831-1854.

Ahn, K. K., Truong, D. Q., and Islam, M. A. (2009). "Modeling of a magneto-rheological (MR) fluid damper using a self tuning fuzzy mechanism". *J. Mech. Sci. Tech.*, 23, 1485- 1499.

Akutain, X. C., Vinolas, J., Savall, J., and Castro, M. (2007). "Comparing the performance and limitations of semi-active suspensions". *Int. J. Veh. Syst. Model. Test.*, 2(3), 296-314.

Alghamdi, A. A., Lostado, R., and Olabi, A. G. (2014). "Magneto-rheological fluid technology". In *Modern Mech. Eng.* (pp. 43-62). Springer, Berlin, Heidelberg.

Ashtiani, M., Hashemabadi, S. H., and Ghaffari, A. (2015). "A review on the magnetorheological fluid preparation and stabilization". *J. Magn. Magn. Mater.*, 374, 716-730.

Babawuro, A. Y., Tahir, N. M., Muhammed, M., and Sambo, A. U. (2020, March). "Optimized state feedback control of quarter car active suspension system based on LMI algorithm". In *J. Physics: Conference Series* (Vol. 1502, No. 1, p. 012019). IOP Publishing.

Balamurugan, L., Jancirani, J., and Eltantawie, M. A. (2014). "Generalized magnetorheological (MR) damper model and its application in semi-active control of vehicle suspension system". *Int .J. Automot. Technol.*, 15(3), 419-427.

Balamurugan, L., and Jeyaraj, J. (2014). "Characterisation of magneto-rheological damper and its use in semi-active control of quarter car model". *Int. J. Veh. Noise Vib.*, 10(1-2), 108-128.

Budiwantoro, B., Masyhur, A. H., and Suganda, I. (2018, June). "Testing of dynamic characteristic and comfort of Indonesia automated people mover from Bandung". In *AIP Conf. Proc.* (Vol. 1977, No. 1, p. 040015). AIP Publishing LLC.

Chen, C., Peng, C., Hou, H., and Liang, J. (2021). "Comparison of magnetorheological damper models through parametric uncertainty analysis using generalized likelihood uncertainty estimation". *J. Eng. Mech.*, 147(2), 04020146.

Chindamo, D., Gadola, M., and Marchesin, F. P. (2017). "Reproduction of real-world road profiles on a four-poster rig for indoor vehicle chassis and suspension durability testing". *Adv. Mech. Eng.*, 9(8), 1687814017726004.

Cho, Y., Song, B. S., and Yi, K. (1999). "A road-adaptive control law for semi-active suspensions". *KSME Int. J.*, 13(10), 667-676.

Choi, S. B., Li, W., Yu, M., Du, H., Fu, J., and Do, P. X. (2016). "State of the art of control schemes for smart systems featuring magneto-rheological materials". *Smart Mater. Struct.*, 25(4), 043001.

Chooi, W. W., and Oyadiji, S. O. (2009). "Mathematical modeling, analysis, and design of magnetorheological (MR) dampers". *J. Vib. Acoust.*, 131(6).

Cieslak, M., Kanarachos, S., Blundell, M., Diels, C., Burnett, M., and Baxendale, A. (2020). "Accurate ride comfort estimation combining accelerometer measurements, anthropometric data and neural networks". *Neural. Comput. Appl.,* 32(12), 8747-8762.

Cortés-Ramirez, J. A., Villarreal-González, L. S., and Martinez-Martinez, M. (2007). "Characterization, modeling and simulation of magnetorheological damper behavior under triangular excitation". In *Mechatronics for safety, security and dependability in a new era* (pp. 353-358). Elsevier.

de Jesus Lozoya-Santos, J., Morales-Menendez, R., Tudón-Martínez, J. C., Sename, O., Dugard, L., and Ramirez-Mendoza, R. (2011). "Control strategies for an automotive suspension with a MR damper". *IFAC Proceedings Volumes*, 44(1), 1820-1825.

Desai, R. M., Jamadar, M. E. H., Kumar, H., and Joladarashi, S. (2021). "Performance Evaluation of a Single Sensor Control Scheme Using a Twin-Tube MR Damper Based Semi-active Suspension". *J. Vib. Eng. Tech.*, 9(6), 1193-1210.

Desai, R. M., Jamadar, M. E. H., Kumar, H., Joladarashi, S., and Raja Sekaran, S. C. (2019). "Design and experimental characterization of a twin-tube MR damper for a passenger van". *J. Braz. Society Mech. Sci. Eng.*, 41(8), 1-21.

Devikiran, P., Puneet, N. P., Hegale, A., and Kumar, H. (2022) "Design and development of MR damper for two wheeler application and Kwok model parameters tuning for designed damper". *Proc. Inst. Mech. Eng. Pt. D. J. Auto. Eng.*, 236(7), 1595-1606.

Do, A. L., Sename, O., Dugard, L., Savaresi, S., Spelta, C., and Delvecchio, D. (2010). "An extension of mixed sky-hook and add to magneto-rheological dampers". *IFAC Proceedings Volumes*, 43(21), 25-31.

Ehteshum, M. (2018). "Development of a control scheme for a quarter car test rig" (Doctoral dissertation, Memorial University of Newfoundland).

El-Kafafy, M., El-Demerdash, S. M., and Rabeih, A. A. M. (2012). "Automotive ride comfort control using MR fluid damper". *Eng.,* 4(4), 179-187.

El Majdoub, K., Giri, F., and Chaoui, F. Z. (2013). "Backstepping adaptive control of quarter-vehicle semi-active suspension with Dahl MR damper model". *IFAC Proceedings Volumes*, 46(11), 558-563.

Els, P. S., Theron, N. J., Uys, P. E., and Thoresson, M. J. (2007). "The ride comfort vs. handling compromise for off-road vehicles". *J. Terramechanics*, 44(4), 303-317.

Eshkabilov, S. (2016). "Modeling and simulation of non-linear and hysteresis behavior of magneto-rheological dampers in the example of quarter-car model". *arXiv preprint* arXiv:1609.07588.

Faisal, A.M.M., Muafag, T.S. (2005). "Friction Forces in O-ring Sealing". *American J. Appl. Sci.,* 2(3), 626-632.

Fallah, M.S., Bhat, R. and Xie W.F. (2009). "New model and simulation of Macpherson suspension system for ride control applications". *Veh. Syst. Dyn.* 47(2), 195-220.

Faris, W. F., BenLahcene, Z., and Hasbullah, F. (2012). "Ride quality of passenger cars: an overview on the research trends". *Int. J. Veh. Noise Vib.*, 8(3), 185-199.

Fischer, D., and Isermann, R. (2004). "Mechatronic semi-active and active vehicle suspensions". *Control Eng. Pract.*, 12(11), 1353-1367.

Floreán-Aquino, K. H., Arias-Montiel, M., Linares-Flores, J., Mendoza-Larios, J. G., and Cabrera-Amado, Á. (2021, January). "Modern semi-active control schemes for a suspension with MR actuator for vibration attenuation". In *Actuators* (Vol. 10, No. 2, p. 22). MDPI.

Fu, Q., Wang, D-H., Xu, L. and Yuan, G. (2017). "A magnetorheological damper-based prosthetic knee (MRPK) and sliding mode tracking control method for an MRPK-based lower limb prosthesis". *Smart Mater. Struct.*, 26 (4), 1-14.

Gołdasz, J. (2015). "Theoretical study of a twin-tube magnetorheological damper concept". *J. Theor. Appl. Mech.*, 53(4), 885-894.

Gołdasz, J., and Sapiński, B. (2015). "Insight into magnetorheological shock absorbers". Cham: Springer International Publishing.

Graczykowski, C., and Pawłowski, P. (2017). "Exact physical model of magnetorheological damper". *Appl. Math. Model.*, 47, 400-424.

Gravatt, J. W. (2003). "Magneto-rheological dampers for super-sport motorcycle applications" (Doctoral dissertation, Virginia Tech).

Guan, X., Huang, Y., Hu, S., and Ou, J. (2009, October). "Design method of spring accumulator of single-ended MR dampers". In *Second International Conference on Smart Materials and Nanotechnology in Engineering* (Vol. 7493, pp. 267-273). SPIE.

Gurubasavaraju, T. M., Kumar, H., and Arun, M. (2017). "Evaluation of optimal parameters of MR fluids for damper application using particle swarm and response surface optimization". *J. Braz. Society Mech. Sci. Eng.*, 39(9), 3683-3694.

Gurubasavaraju, T. M., Kumar, H., and Arun, M. (2017). "Optimisation of monotube magnetorheological damper under shear mode". *J. Braz. Society Mech. Sci. Eng.*, 39(6), 2225-2240.

Gurubasavaraju, T. M., Kumar, H., and Mahalingam, A. (2018). "An approach for characterizing twin-tube shear-mode magnetorheological damper through coupled FE and CFD analysis". *J. Braz. Society Mech. Sci. Eng.*, 40(3), 1-14.

Hemanth, K., Kumar, H., and Gangadharan, K. V. (2017). "Vertical dynamic analysis of a quarter car suspension system with MR damper". *J. Braz. Society Mech. Sci. Eng.*, 39(1), 41-51.

Hiemenz, G. J., Hu, W., and Wereley, N. M. (2008). "Semi-active magnetorheological helicopter crew seat suspension for vibration isolation". *J. Aircraft*, 45(3), 945-953.

Hong, S. R., Choi, S. B., Choi, Y. T., and Wereley, N. M. (2005). "Non-dimensional analysis and design of a magnetorheological damper". *J.Sound Vib.*, 288(4-5), 847-863.

Hyniova, K. (2016). "On testing of vehicle active suspension robust control on an one-quarter-car test stand". *Int. J. of Mech. Eng.*, 1, 1-7.

Jamadar, M. E. H., Desai, R. M., Saini, R. S. T., Kumar, H., and Joladarashi, S. (2021). "Dynamic analysis of a quarter car model with semi-active seat suspension

using a novel model for magneto-rheological (MR) damper". *J. Vib. Eng. Tech.*, 9(1), 161-176.

Jeyasenthil, R., and Choi, S. B. (2018). "A novel semi-active control strategy based on the quantitative feedback theory for a vehicle suspension system with magneto-rheological damper saturation". *Mechatronics,* 54, 36-51.

Jiang, X. Z., Wang, J., and Hu, H. S. (2012). "Semi-active control of a vehicle suspension using magneto-rheological damper". *J. Central South University*, 19(7), 1839-1845.

Kasemi, B., Muthalif, A. G., Rashid, M. M., and Fathima, S. (2012). "Fuzzy-PID controller for semi-active vibration control using magnetorheological fluid damper". *Proc. Eng.*, 41, 1221-1227.

Kazakov, Y. B., Morozov, N. A., and Nesterov, S. A. (2017). "Development of models of the magnetorheological fluid damper". *J. Magn. Magn. Mater.*, 431, 269-272.

Kim, W. H., Park, J. H., Kaluvan, S., Lee, Y. S., and Choi, S. B. (2017). "A novel type of tunable magnetorheological dampers operated by permanent magnets". *Sensors and Actuators A: Physical*, 255, 104-117.

Koch, G., Pellegrini, E., Spirk, S., and Lohmann, B. (2010). "Design and modeling of a quarter-vehicle test rig for active suspension control". *Lehrstuhl für Regelungstechnik*, 1-28.

Kumbhar, B. K., Patil, S. R., and Sawant, S. M. (2015). "Synthesis and characterization of magneto-rheological (MR) fluids for MR brake application". *Eng. Sci. Tech., Int. J.*, 18(3), 432-438.

Kwok, N. M., Ha, Q. P., Nguyen, T. H., Li, J., and Samali, B. (2006). "A novel hysteretic model for magnetorheological fluid dampers and parameter identification using particle swarm optimization". *Sensors and Actuators A: Physical*, 132(2), 441-451.

Lam, H. F., and Liao, W. H. (2001, August). "Semi-active control of automotive suspension systems with magnetorheological dampers". In *Smart structures and materials* 2001: smart structures and integrated systems (Vol. 4327, pp. 125-136). SPIE.

Li, W. H., Ujszaszi, R. S., Liu, B., Zhang, X. Z., Kosasih, P. B., and Gong, X. L. (2007). "MATLAB simulation of semi-active skyhook control of a quarter car incorporating an MR damper and a fuzzy logic controller". In *Nonlinear Science And Complexity* (pp. 405-411).

Liu, Y., Yang, S., and Liao, Y. (2011). "A quantizing method for determination of controlled damping parameters of magnetorheological damper models". *J. Intell. Mater. Syst. Struct.*, 22(18), 2127-2136.

Lv, H., Zhang, S., Sun, Q., Chen, R., and Zhang, W. J. (2021). "The dynamic models, control strategies and applications for magnetorheological damping systems: a systematic review". *J. Vib. Eng. Tech.*, 9(1), 131-147.

Madhavrao Desai, R., Acharya, S., Jamadar, M. E. H., Kumar, H., Joladarashi, S., and Sekaran, S. R. (2020). "Synthesis of magnetorheological fluid and its application in a twin-tube valve mode automotive damper". *Proc. Inst. Mech. Eng. Pt. L J. Mater. Des. Appl.*, 234(7), 1001-1016.

Marjanen, Y. (2010). "Validation and improvement of the ISO 2631-1 (1997) standard method for evaluating discomfort from whole-body vibration in a multi-axis environment" (Doctoral dissertation, © Yka Marjanen).

Meeser, R. F. (2015). "Magneto-rheological (MR) Damper design for off-road vehicle suspensions with flow blocking ability" (Doctoral dissertation, University of Pretoria).

Meng, F., and Zhou, J. (2019). "Modeling and control of a shear-valve mode MR damper for semiactive vehicle suspension". *Math. Prob. Eng.*, 2019, 1-8.

Metered, H., Bonello, P., and Oyadiji, S. O. (2010). "The experimental identification of magnetorheological dampers and evaluation of their controllers". *Mech. Syst. signal process.*, 24(4), 976-994.

Mitra, A. C., Kiranchand, G. R., Soni, T., and Banerjee, N. (2016). "Design of experiments for optimization of automotive suspension system using quarter car test rig". *Proc. Eng.*, 144, 1102-1109.

Mitra, A. C., Patil, M. V., and Banerjee, N. (2015). "Optimization of vehicle suspension parameters for ride comfort based on RSM". *J. Inst. Eng. (India) C.*, 96(2), 165-173.

Mitra, A. C., Soni, T., Kiranchand, G. R., Khan, S., and Banerjee, N. (2015). "Experimental design and optimization of vehicle suspension system". *Mater. Today: Proc.*, 2(4-5), 2453-2462.

Nagarkar, M. P., Patil, G. J. V., and Patil, R. N. Z. (2016). "Optimization of nonlinear quarter car suspension–seat–driver model". *J. Adv. Research*, 7(6), 991-1007.

Nahvi, H., Fouladi, M. H., and Nor, M. M. (2009). "Evaluation of whole-body vibration and ride comfort in a passenger car". *Int. J. Acoust. Vib.*, 14(3), 143-149.

Naudé, A. F., and Snyman, J. A. (2003). "Optimisation of road vehicle passive suspension systems. Part 2. Qualification and case study". *Appl. Math. Model.,* 27(4), 263-274.

Negash, B. A., You, W., Lee, J., Lee, C., and Lee, K. (2021). "Semi-active control of a nonlinear quarter-car model of hyperloop capsule vehicle with Skyhook and Mixed Skyhook-Acceleration Driven Damper controller". *Adv. Mech. Eng.*, 13(2), 1687814021999528.

Nguyen, Q. H., and Choi, S. B. (2008). "Optimal design of a vehicle magnetorheological damper considering the damping force and dynamic range". *Smart Mater. Struct.*, 18(1), 015013.

Nguyen, Q. H., and Choi, S. B. (2009). "Optimal design of MR shock absorber and application to vehicle suspension". *Smart Mater. Struct.*, 18(3), 035012.

Nguyen, S. D., Choi, S. B., and Nguyen, Q. H. (2018). "A new fuzzy-disturbance observer-enhanced sliding controller for vibration control of a train-car suspension with magneto-rheological dampers". *Mech. Syst. Signal Process.*, 105, 447-466.

Nie, S., Zhuang, Y., Liu, W., and Chen, F. (2017). "A semi-active suspension control algorithm for vehicle comprehensive vertical dynamics performance". *Veh. Syst. Dyn.*, 55(8), 1099-1122.

Omar, M., El-Kassaby, M. M., and Abdelghaffar, W. (2017). "A universal suspension test rig for electrohydraulic active and passive automotive suspension system". *Alexandria Eng. J.*, 56(4), 359-370.

Orečný, M., Segľa, Š., Huňady, R., and Ferková, Ž. (2014). "Application of a magneto-rheological damper and a dynamic absorber for a suspension of a working machine seat". *Proc. Eng.*, 96, 338-344.

Paddan, G. S., and Griffin, M. J. (2002). "Evaluation of whole-body vibration in vehicles". *J. Sound. Vib.*, 253(1), 195-213.

Park, E. J., Stoikov, D., da Luz, L. F., and Suleman, A. (2006). "A performance evaluation of an automotive magnetorheological brake design with a sliding mode controller". *Mechatronics*, 16(7), 405-416.

Park, J. H., Kim, W. H., Shin, C. S., and Choi, S. B. (2016). "A comparative work on vibration control of a quarter car suspension system with two different magneto-rheological dampers". *Smart. Mater. Struct.*, 26(1), 015009.

Park, S. J., and Subramaniyam, M. (2013). "Evaluating methods of vibration exposure and ride comfort in car". *J. Ergon. Soc. Korea*, 32(4), 381-387.

Parlak, Z., and Engin, T. (2012). "Time-dependent CFD and quasi-static analysis of magnetorheological fluid dampers with experimental validation". *Int. J. Mech. Sci.*, 64(1), 22-31.

Patil, S. A., and More, I. D. (2016). "On-Road Ride Comfort Test and Simulation Analysis of Passenger Cars with Emphasis on Indian Suburban and Rural Road Conditions" (No. 2016-01-1680). SAE Technical Paper.

Pepe, G., Roveri, N., and Carcaterra, A. (2019). "Experimenting sensors network for innovative optimal control of car suspensions". *Sensors*, 19(14), 3062.

Phalke, T. P., and Mitra, A. C. (2017). "Analysis of ride comfort and road holding of quarter car model by Simulink". *Mater. Today. Proc.*, 4(2), 2425-2430.

Poussot-Vassal, C., Sename, O., Dugard, L., Ramirez-Mendoza, R., and Flores, L. (2006). "Optimal skyhook control for semi-active suspensions". *IFAC Proceedings Volumes*, 39(16), 608-613.

Prabakar, R. S., Sujatha, C., and Narayanan, S. (2009). "Optimal semi-active preview control response of a half car vehicle model with magnetorheological damper". *J. Sound Vib.*, 326(3-5), 400-420.

Prabakar, R. S., Sujatha, C., and Narayanan, S. (2013). "Response of a quarter car model with optimal magnetorheological damper parameters". *J. Sound Vib.*, 332(9), 2191-2206.

Rabinow, J. (1948). "The magnetic fluid clutch". *Electr. Eng.*, 67(12), 1167-1167.

Rahman, M., Ong, Z. C., Julai, S., Ferdaus, M. M., and Ahamed, R. (2017). "A review of advances in magnetorheological dampers: their design optimization and applications". *J. Zhejiang University-Science A*, 18(12), 991-1010.

Rashid, M. M., Hussain, M. A., and Rahim, N. A. (2006). "Application of magneto-rheological damper for car suspension control". *J. Appl. Sci.*, 6(4), 933-938.

Reddy, M. S., Vigneshwar, P., Ram, M. S., Sekhar, D. R., and Harish, Y. S. (2017). "Comparative optimization study on vehicle suspension parameters for rider comfort based on RSM and GA". *Mater. Today. Proc.*, 4(2), 1794-1803.

Rewabhai, S. H. (2017). "Design and development of magneto rheological fluid base damper" (oral dissertation, Gujarat Technological University).

Roumy, J. G., Boulet, B., Dionne, D. (2003). "Active control of vibrations transmitted through a car suspension". *Int. J. Veh. Auton. Syst.*, 2(3/4), 236-254.

Ryabov, I. V., Novikov, V. V., and Pozdeev, A. V. (2016). "Efficiency of Shock Absorber in Vehicle Suspension". *Proc. Eng.*, 150, 354-362.

Şahin, İ., Engin, T., and Çeşmeci, Ş. (2010). "Comparison of some existing parametric models for magnetorheological fluid dampers". *Smart Mater. Struct.*, 19(3), 035012.

Sassi, S., Cherif, K., Mezghani, L., Thomas, M., and Kotrane, A. (2005). "An innovative magnetorheological damper for automotive suspension: from design to experimental characterization". *Smart Mater. Struct.*, 14(4), 811.

Savaresi, S. M., and Spelta, C. (2008). "A single-sensor control strategy for semi-active suspensions". *IEEE Transact. Control Syst. Technol.*, 17(1), 143-152.

Savaresi, S. M., Bittanti, S., and Montiglio, M. (2004). "Non-linear models of magneto-rheological dampers for semiactive control of vehicle dynamics". *IFAC Proceedings Volumes*, 37(13), 811-816.

Schiehlen, W., and Iroz, I. (2015). "Uncertainties in road vehicle suspensions". *Procedia IUTAM*, 13, 151-159.

Sefidkar-Dezfouli, S. (2014). "Design, Simulation, and Fabrication of a Lightweight Magneto Rheological Damper" (Doctoral dissertation, Applied Sciences: School of Mechatronic Systems Engineering).

Sherje, N. P., Deshmukh, S.V. (2019) "Design, Development of Magneto-Rheological Damper for Commercial Vehicles". *Int. J. Control. Autom.*, 12(4), 56-69.

Shiao, Y. J., Nguyen, Q. A., and Lai, C. C. (2013). "Application of Magneto Rheological Damper on Semi-Active Suspension System". In *Applied Mechanics and Materials* (Vol. 284, pp. 1754-1758). Trans Tech Publications Ltd.

Shirahatti, A., Prasad, P. S. S., Panzade, P., and Kulkarni, M. M. (2008). "Optimal design of passenger car suspension for ride and road holding". *J. Braz. Society Mech. Sci. Eng.*, 30, 66-76.

Shivaram, A. C., and Gangadharan, K. V. (2007). "Statistical modeling of a magnetorheological fluid damper using the design of experiments approach". *Smart Mater. Struct.*, 16(4), 1310.

Shixing, Z., Peng, W., and Jing, T. (2011). "Experimental research on aircraft landing gear drop test based on MRF damper". *Proc. Eng.*, 15, 4712-4717.

Song, X. (2009). "Cost-effective skyhook control for semiactive vehicle suspension applications". *The Open Mech. Eng. J.*, 3(1).

Spelta, C., Delvecchio, D., Savaresi, S. M., Bonaccorso, G., and Ghirardo, F. (2010, January). "Analysis of a Sensor Reduction in a Semi-Active Suspension System for a 4-Wheel Vehicle". In *Dynamic Systems and Control Conference* (Vol. 44182, pp. 757-763).

Spelta, C., Previdi, F., Savaresi, S. M., Fraternale, G., and Gaudiano, N. (2009). "Control of magnetorheological dampers for vibration reduction in a washing machine". *Mechatronics*, 19(3), 410-421.

Sreekar Reddy, M. B. S., Rao, S. S., Vigneshwar, P., Akhil, K., and RajaSekhar, D. (2016). "An intelligent optimization approach to quarter car suspension system through RSM modeled equation". In *Proceedings of First International Conference on Information and Communication Technology for Intelligent Systems*: Vol. 2 (pp. 97-108). Springer, Cham.

Sreekar Reddy, M. B. S., Vigneshwar, P., RajaSekhar, D., Akhil, K., and Lakshmi Narayana Reddy, P. (2016). "Optimization study on quarter car suspension system by RSM and Taguchi". In Proceedings of the *International Conference on Signal, Networks, Computing, and Systems* (pp. 261-271). Springer, New Delhi.

Steišūnas, S., Dižo, J., Bureika, G., and Žuraulis, V. (2017). "Examination of vertical dynamics of passenger car with wheel flat considering suspension parameters". *Proc. Eng.*, 187, 235-241.

Sternberg, A., Zemp, R., and de la Llera, J. C. (2014). "Multiphysics behavior of a magneto-rheological damper and experimental validation". *Eng. Struct.*, 69, 194-205.

Stutz, L. T., and Rochinha, F. A. (2011). "Synthesis of a magneto-rheological vehicle suspension system built on the variable structure control approach". *J. Braz. Society Mech. Sci. Eng.*, 33, 445-458.

Sung, K. G., and Choi, S. B. (2008). "Effect of an electromagnetically optimized magnetorheological damper on vehicle suspension control performance". *Proc. Inst. Mech. Eng. Pt. D. J. Auto. Eng.*, 222(12), 2307-2319.

Suresh, A. (2016). "Semi-active suspension system using a Magnetorheological Damper" (Master of Science thesis, The University of Texas at Arlington).

Terasawa, T., and Sano, A. (2005)."Fully Adaptive Semi-active Control of Vibration Isolation by MR Damper". *IFAC Proceedings Volumes*, 38(1), 199-204.

Tharehalli Mata, G., Kumar, H., and Mahalingam, A. (2019). "Performance analysis of a semi-active suspension system using coupled CFD-FEA based non-parametric modeling of low capacity shear mode monotube MR damper". *Proc. Inst. Mech. Eng. Pt. D. J. Auto. Eng.*, 233(5), 1214-1231.

Truong, D. Q., and Ahn, K. K. (2012). "MR fluid damper and its application to force sensorless damping control system". *Smart Actuation and Sensing Systems-Recent Advances and Future Challenges*, 383-425.

Tu, F., Yang, Q., He, C., and Wang, L. (2012). "Experimental study and design on automobile suspension made of magneto-rheological damper". *Energy Proc.*, 16, 417-425.

Unni, R. K., and Tamilarasan, N. (2018, February). "Design and analysis of a magneto-rheological damper for an all terrain vehicle". In *IOP Conference Series: Materials Science and Engineering*, 310(1), 012128). IOP Publishing.

Vaes, D., Smolders, K., Swevers, J., and Sas, P. (2005, December). "Multivariable control for reference tracking on half car test rig". In *Proc. 44th IEEE Conference on Decision and Control*, 6498-6503, IEEE.

Vivas-Lopez, C. A., Tudon-Martinez, J. C., Estrada-Vela, A., de Jesus Lozoya-Santos, J., and Morales-Menendez, R. (2021). "Damping Variation Effects in Vehicle Semi-active MR Suspensions: A Stress Concentration Analysis". *Frontiers in Mater.*, 8, 590390.

Wahid, S. A., Ismail, I., Aid, S., and Rahim, M. S. A. (2016, February). "Magneto-rheological defects and failures: A review". In *IOP Conference Series: Materials Science and Engineering* (Vol. 114, No. 1, p. 012101). IOP Publishing.

Xu, Z. D., Sha, L. F., Zhang, X. C., and Ye, H. H. (2013). "Design, performance test and analysis on magnetorheological damper for earthquake mitigation". *Struct. Control Health Monitor.*, 20(6), 956-970.

Yang, G., Spencer Jr, B. F., Carlson, J. D., and Sain, M. K. (2002). "Large-scale MR fluid dampers: modeling and dynamic performance considerations". *Eng. Struct.*, 24(3), 309-323.

Yang, Z., Yong, C., Li, Z., and Kangsheng, Y. (2018). "Simulation analysis and optimization of ride quality of in-wheel motor electric vehicle". *Adv. Mech. Eng.*, 10(5), 1687814018776543.

Yao, G. Z., Yap, F. F., Chen, G., Li, W., and Yeo, S. H. (2002). "MR damper and its application for semi-active control of vehicle suspension system". *Mechatronics*, 12(7), 963-973.

Yao, G. Z., Yap, F. F., Chen, G., Li, W., and Yeo, S. H. (2002). "MR damper and its application for semi-active control of vehicle suspension system". *Mechatronics*, 12(7), 963-973.

Yazid, I. I. M., Mazlan, S. A., Kikuchi, T., Zamzuri, H., and Imaduddin, F. (2014). "Design of magnetorheological damper with a combination of shear and squeeze modes". *Mater. Design.* (1980-2015), 54, 87-95.

Yerrawar, R. N., and Arakerimath, R. R. (2017). "Development of methodology for semi active suspension system using MR damper". *Mater. Today. Proc.*, 4(8), 9294-9303.

Yildiz, A. S., and Sivrioglu, S. (2016). "Semi-active vibration control of lateral and rolling motions for a straddle type monorail vehicle". *IFAC-PapersOnLine*, 49(3), 279-284.

Zhao, L., Zhou, C., Yu, Y., and Yang, F. (2017). "An analytical formula of driver RMS acceleration response for quarter-car considering cushion effects". *Veh. Syst. Dyn.*, 55(9), 1283-1296.

Zhu, X., Jing, X., and Cheng, L. (2012). "Magnetorheological fluid dampers: a review on structure design and analysis". *J. Intell. Mater. Syst. Struct.*, 23(8), 839-873.

Appendix I

Specifications of instruments used

1. Electronic Weighing Balance

Parameter	Specification
Maximum capacity	1 Kg
Accuracy	0.1 gram
Power supply	230V AC, 50Hz

2. Mechanical Stirrer

Parameter	Specification
Max. stirring Capacity	5 litres
Speed range	50-1500 rpm
Power	10 watt
Supply voltage	220-240 V
Line frequency	50 Hz, single phase

3. Damper testing machine (Make: Heico)

- **Hydraulic power pack**

Parameter	Specification
Flow of the pump	64 LPM
Max. Operating Pressure	210 bar
Oil tank capacity	200 ltr.
Power rating of motor	40 HP
Length of hoses	5 m. (each)
Electric power supply	440V, 3 phase (AC supply)

- **Force transducer**

Parameter	Specification
Capacity	+/- 30 kN
Resolution	0.001 kN
Full scale output	2 mV/V
Excitation Voltage	10 Volts DC
Non-linearity	< +/- 0.15 % FSO
Safe overload	150 %
Operating temperature	0 to +60 deg. C
Accuracy	0.5% of indicated value as per ISO7500-1

- **Hydraulic actuator**

Parameter	Specification
Type	Double acting double ended
Capacity	+/- 20 kN
Stroke	150 mm (+/- 75 mm)
Max. working pressure	210 bar

Max. sustained velocity	0.8 m/s
Peak velocity	1.2 m/s
Servo valve	63 LPM
Pressure line filter	180 LPM with 3 microns filtration
Accumulator (2 No.)	0.36 ltr. capacity

- **Position sensor/ Displacement transducer**

Parameter	Specification
Range	200 mm
Make	Gefran/Balluff
Full scale output	10 volts
Repeatability	<0.01 mm
Pressure withstand	Upto 600 bar
Excitation voltage	24 volts DC
Sampling rate	2 kHz
Operating temperature	-30 to +75 deg. C

- **Signal conditioning and controlling unit**
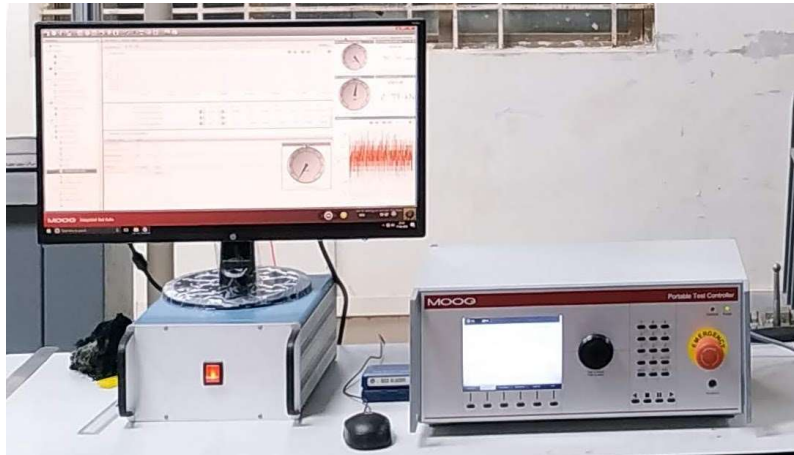
Specifications of controller

- Auto PID operation with auto zeroing, auto tuning and auto-adjustment feature servo operation.

- Digital signal processing (DSP) based closed loop servo controller with closed loop update rate of 10 kHz.

- Number of control channels - 4 (Load/Displacement/External channel strain 1 and strain2).

- Demand wave generation - Sine, Triangular, Square and ramp signal.

- High speed 32 bit data acquisition with 6 kHz sampling rate on all primary channels.

- Auto calibration and digital auto zero capability.

4. **Suspension test rig**

- **Base frame**

Parameter	Specification
Length of the frame	1500 mm
Width of the frame	1000 mm
Working height of the frame	500 mm
T slots size	M16
Vertical loading capacity	30 kN
Number of T slots	4

- **Vertical frame**

Parameter	Specification
Base of the frame	600 mm
Length of the frame	400 mm
Height of the frame	3000 mm
Main carriage adjustment	1500 mm
Front plate of the carriage	Matrix of 100x100xM12
Travel of slide carriage (linear bearing)	100 mm

- **Frame for mounting shock absorbers or dampers**

Parameter	Specification
Capacity	20 kN
Horizontal clearance	400 mm
Vertical clearance (adjustable)	200-1000 mm

5. Rheometer
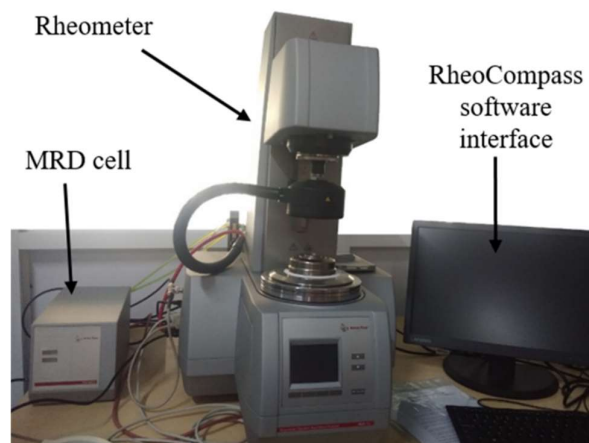
Parameter	Specification
Minimum torque, rotation	1 nNm
Maximum torque, rotation	230 mNm
Minimum torque, oscillation	0.5 nNm
Maximum angular frequency	628 rad/s
Normal force range	0.005 to 50 N
Maximum temperature range	160 to +1000 °C
Pressure range	up to 1000 bar
Rheometer Software RheoCompass™ Professional	Running under Microsoft Windows 7/8/8.1/10 (64bit versions only)
Magnetorheological Device Cell	Magnetic Flux density upto 1Tesla Temperature range -10 to 170°C
Hood With Peltier Heating/Cooling	Temperature range: -40 to 200 °C
Compressor	230/50 V/Hz, 55 l/min, OILFREE Motor Power: 0.55 kW Output (5 bar): 55 l/min max. Pressure: 8 bar Tank Volume: 10 l Weight: 59 kg Dimensions: 510x530x515 mm
Peltier Temperature Control Device	Temperature range: -5 to 200 °C
Power Supply Magneto Cell	230V HCP 14-12500,12.5,1 mA

6. Commercial MR Fluid, MRF 132 DG (Lord Corporation, USA)

Parameter	Specification
Appearance	Dark Gray Liquid
Viscosity, Calculated as slope 800-1200 sec-1 , Pa-s @ 40°C (104°F)	0.112 ± 0.02
Density, g/cm^3 (lb/gal)	2.95-3.15 (24.6-26.3)
Solids Content by Weight, %	80.98
Flash Point, °C (°F)	>150 (>302)
Operating Temperature, °C (°F)	-40 to +130 (-40 to +266)

7. DC Power supply (Make: Scientific Instruments, PSD3005 30V**)**

Parameter	Specification
DC output	0 to 30V / 5A
Settling resolution	V: 10 mV, I : 5 mA
Load Regulation	<= +/-(0.05% + 10 mV)
Input Supply	230 AC +/- 10% / 50-60 Hz
Internal resistance	<=10 milliOhms

8. NI 9234 C- series sound and vibration Input module IEPE

Parameter	Specification
IEPE channels	4 channel sound and
Resolution	24-bit resolution
Operational	±5 V, 0 to 20mA Input
Connectivity	BNC connectivity only
Sampling rate	51.2 kS/s

LIST OF PUBLICATIONS

INTERNATIONAL JOURNALS

1. Puneet, N. P., Devikiran, P., Kumar, H., and Gangadharan, K. V. (2022). Performance Evaluation of Magneto-Rheological Damper Through Characterization Testing, Modeling and its Implementation in Quarter Car. *Journal of Vibration Engineering and Technologies*, 10, 967-983. https://doi.org/10.1007/s42417-021-00422-7 (SCIE and Scopus indexed, IF-1.889, Q3)

2. Puneet, N. P., Pinjala Devikiran., Hemantha Kumar and Gangadharan, K. V., Performance Evaluation of Magneto-rheological Damper with Spring Accumulator and On-Road Testing with Implementation in a Four Wheeler Vehicle (*Communicated to Sadhana, SCIE and Scopus indexed*).

3. N. P. Puneet, Radhe Shyam Tak Saini, Hemantha Kumar and Gangadharan, K. V., Cost effective Semi-active Vehicular Suspension System: Design, Fabrication and Testing on Full Scale Quarter Car Suspension Rig (*communicated to Journal of the Brazilian Society of Mechanical Sciences and Engineering , Publisher: Springer, SCIE ad Scopus indexed)*

CONFERENCE PROCEEDINGS

1. Puneet, N. P., Hegale, A., Kumar, H., and Gangadharan, K. V. (2019, December). Multi objective optimization of quarter car parameters for better ride comfort and road holding. In *AIP Conference Proceedings* (Vol. 2200, No. 1, p. 020046). AIP Publishing LLC. https://doi.org/10.1063/1.5141216 (Presented in 1st International Conference on Manufacturing, Material Science and Engineering (ICMMSE-2019) at CMRIT, Hyderabad, 16-18 August 2019)

2. Puneet, N. P., Hegale, A., Kumar, H., and Gangadharan, K. V. (2020, January), Design, fabrication and dynamic performance analysis of MR damper suitable for vehicle application, In International Conference on Design, Automation and Control 2020 (ICDAC 2020) at VIT, Vellore, 6-8

January, 2020. (*Under consideration for publication in Journal of Chemical Technology and Metallurgy, a Scopus indexed journal*)

3. N P Puneet, Swagat Kumbhar, Hemantha Kumar, K V Gangadharan (2022), Analysis of magneto-rheological fluid damper and linearization of semi-active quarter car model, In International Conference on Innovations in Mechanical and Materials Engineering (IMME-2022), MNNIT Allahabad, November 4-6. (*Under consideration for publication in Nanoworld Journal, a Scopus indexed journal*)

BOOK CHAPTER

1. Puneet, N. P., Hegale, A., Kumar, H., and Gangadharan, K. V. (2021). Optimal Parameters Identification of Quarter Car Simulink Model for Better Ride Comfort and Road Holding. In *Recent Advances in Computational Mechanics and Simulations* (pp. 623-636). Springer, Singapore., https://doi.org/10.1007/978-981-15-8315-5_53

BIODATA

Name   Puneet N P

Date of birth 01-Jan-1990

Mobile Number +91-9900627912

Email Id   puneetnp12@gmail.com

Address   Pushyaragam, Behind APMC yard, Shreeramanagar, Salmara, Puttur- 574201,   Dakshina Kannada district, Karnataka

Qualification

Degree	Institute/University	Year	Percentage/CGPA
Ph.D.	National Institute of Technology Karnataka, Surathkal	Pursuing	8.00 (Course work)
M. Tech (Machine Design)	NMAMIT, Nitte	2013-2015	9.43
B.E.(Mechanical Engineering)	Vivekananda College of Engg. & Technology, Puttur	2008-2012	72.71%

Experience

Sl.No.	Institution	Designation	Period
1	Vivekananda College of Engg. & Technology, Puttur	Lecturer	2012-2013
2	Srinivas Institute of Technology, Mangaluru	Assistant Professor	2015-2017
3	National Institute of Technology Karnataka, Surathkal	Senior Research Fellow	2017-2022

Journal Publication: 3

International Conferences: 4